Neural oscillations in auditory working memory

Impressum

Max Planck Institute for Human Cognitive and Brain Sciences, 2015



Druck: Sächsisches Druck- und Verlagshaus Direct World, Dresden

Titelbild: © Lee Gingold, 2015

ISBN 978-3-941504-51-6

# Neural oscillations in auditory working memory

Der Fakultät für Biowissenschaften, Pharmazie und Psychologie
der Universität Leipzig
genehmigte

D I S S E R T A T I O N

zur Erlangung des akademischen Grades
doctor rerum naturalium
(Dr. rer. nat.)

vorgelegt von
Diplom-Psychologin Anna Wilsch
geboren am 04. Januar 1984 in Neuss

| | |
|---|---|
| Dekan: | Prof. Dr. Erich Schröger |
| Gutachter: | Prof. Dr. Jonas Obleser |
| | Prof. Dr. Erich Schröger |
| | Prof. Dr. Nathan Weisz |

Tag der Verteidigung: 12.03.2015

Bibliographic details

Anna Wilsch, *Neural oscillations in auditory working memory*

Fakultät für Biowissenschaften, Pharmazie und Psychologie, Universität Leipzig

Dissertation

154 pages, 279 references, 17 figures, 0 tables

The present thesis investigated memory load and memory decay in auditory working memory. Alpha power as a marker for memory load served as the primary indicator for load and decay fluctuations hypothetically reflecting functional inhibition of irrelevant information. Memory load was induced by presenting auditory signals (syllables and pure-tone sequences) in noise because speech-in-noise has been shown before to increase memory load. The aim of the thesis was to assess with magnetoencephalography whether a-priori temporal expectations for the onset-time of a to-be-remembered stimulus reduces memory load. It was reported previously that top-down modulations such as spatial expectations reduce memory load and improve memory performance. However, this effect has neither been investigated with temporal expectations nor in the auditory domain. The present thesis showed that temporal expectations for a syllable in noise reduced memory load. Reduced alpha power during stimulus maintenance as well as improved performance indicated the decrease in memory load. Alpha power effects emerged from the right cingulo-opercular network, presumably reflecting a reduced need for functional inhibition. Critically, symbolic cues induced temporal expectations. This effect could not be replicated for clear speech. However, more implicit temporal expectations based on the passage of time elicited a similar decrease in alpha power for clear speech reflecting reduced memory load. Memory decay was assessed with variable delay phases in an auditory sensory memory task with pure-tone sequences. Similarly to memory performance, alpha power decreased with longer delay phases. Critically, temporal expectations counteracted memory decay and led to more sustained performance as well as alpha power across different delay phases. These alpha-power effects were localized to frontal and parietal attention networks as well as primary auditory and visual sensory areas. This implies the involvement of different brain regions relevant for encoding and maintenance in auditory memory and questions a parsimonious functional inhibition explanation. A correlation of alpha power

and behavioral performance underpinned the importance of alpha power for auditory working memory. Altogether, the results of the present thesis provide evidence for a beneficial effect of a-priori temporal expectations for an auditory signal on working memory. Moreover, alpha dynamics were shown to be a distinct marker for the neural efficiency of managing working memory limitations.

## Acknowledgments

I would like to thank those people who contributed to my PhD-project throughout the past three and a half years.

First and foremost, I would like to thank my supervisor Jonas Obleser for his support throughout all stages of this project. In particular, I am thankful for all the discussions we had, for being challenging and also understanding, and for giving me the opportunity to carry out the present dissertation.

I am thankful to Erich Schröger and Nathan Weisz for reviewing this thesis.

I would like to thank my fellow lab members, past and present, of the *Auditory Cognition* group, Alex Brandmeyer, Julia Erb, Dunja Kunke, Molly Henry, Björn Herrmann, Sung-Joo Lim, Mathias Scharinger, Antje Strauß, and Malte Wöstmann for great scientific and non-scientific discussions; in particular, Molly for her patient and very didactic explanations of complicated methods; Björn for sharing his broad knowledge on MEG analyses; Malte for fruitful discussions about alpha power; and Antje for our PhD-support group and the joint finish.

I also would like to thank those people without whom the acquisition of data would have been impossible: I am thankful to Burkhard Maess for introducing me to MEG, for guiding my first steps of MEG analysis, and for his overall kindness; I am also thankful to Yvonne Wolff for her great job recruiting and testing numerous MEG participants; and to Dunja, Leo, Steven, Christoph, and Mirja for inviting participants and for their support in testing behavioral experiments.

I am thankful to Christian for many discussions, for proof-reading major parts of this thesis, for sharing my ups and downs, and simply for being there for me throughout the past years.

# Contents

# Introduction

Perception and comprehension of auditory information is essential for the interaction with the environment. For example the comprehension of speech signals is important for communication. The clear perception of non-verbal signals is important to direct attention to relevant events. In order to fulfill the goal of comprehending the meaning of an auditory information, it has to be encoded, maintained, and processed in working memory. However, the working memory's resources that are necessary to execute these functions are limited which means that only a limited amount of information can be stored (memory load) over a limited amount of time (memory decay).

Despite these limitations, working memory handles very well the overload of sensations, otherwise communication or other human behavior based on the processing of information would fail. Findings from vision research, for example, provided information about the beneficial effect of focusing attention towards relevant information on working memory. In principle, the knowledge about, for example, when or where in the environment what kind of relevant event will occur guides the focus of attention away from irrelevant events. That in turn renders the interaction with the environment very efficient and prevents working from exceeding its limitations.

In order to provide further insights on the impact of focused attention on auditory working memory, the present thesis investigated the effect of temporal expectations on the limitations of auditory working memory. Specifically, temporal expectations, the knowledge about when events occur, were manipulated for auditory stimuli that were degraded by a noise masker approximating the realistic problem of overlapping auditory information in the environment.

First, the aim was to investigate whether temporal expectations are beneficial for high memory load for speech-in-noise as well as low memory load for clear speech in auditory working memory (*Experiment I, Experiment IIa*). Besides behavioral memory performance, the focus was on neural oscillations in the alpha frequency band, a

sensitive marker of memory load. Next, the underlying neural mechanism of temporal expectations which might explain variance of a beneficial effect of temporal expectations were explored. Here the focus was not only on fluctuations of alpha power but also on slow oscillatory phase concentration (*Experiment IIb*).

Then, the effect of temporal expectations on memory decay was assessed. First of all, I was interested in the modulation of alpha power by memory decay in auditory sensory memory but also on the effect of temporal expectations on memory decay (*Experiment III*). In addition, the aim was to elucidate the functional role of alpha power reflecting memory load and memory decay by means of source localization. Lastly, a purely behavioral experiment was conducted to provide more nuanced informations effects on the beneficial effect of temporal expectations on memory decay (*Experiment IV*). Here, the aim was to fit forgetting curves describing memory decay in auditory sensory memory depending on temporal expectations.

# 1 Working memory

Working memory plays a crucial role in the cognitive system because it serves as an interface between perception, long-term memory, and action (Baddeley, 2003). Every consciously perceived sensory information enters working memory. At this point, despite the physical absence of the sensory input, a representation of the information can be maintained and manipulated over a brief period of time (Baddeley, 2012). The cognitive resources constituting working memory are very limited with regard to the load of information that can be maintained as well as the duration of information maintenance. The constraints are bound to the limited amount of allocatable attention that can be focused on the to-be-remembered information and when limitations are exceeded performance declines due to a lack of attentional resources (Norman and Bobrow, 1975).

## 1.1 Limitations of working memory

The limitations of working memory have been widely discussed and are of great interest in the field of cognitive science. Limitations can be observed at three stages: encoding, maintenance, and retrieval of the information entering memory (Baddeley, 2012). Encoding describes the perceptual processing of information in the focus of attention. Next, once items are successfully encoded, they are maintained in memory. At this stage, the memory representation is protected from disrupting/irrelevant information (Postle, 2006). The last stage, the retrieval of stored information, refers to the process of reactivating stored information. Retrieval has been proposed to correspond to a shift of the attentional focus onto the maintained information (Jonides et al., 2008).

### 1.1.1 Memory load[1]

Traditionally, memory capacity has been defined by the number of items that can be maintained in memory. The amount of items corresponds to the load in memory. Miller (1956) was the first to postulate $7 \pm 2$ items being the limit of of working memory capacity. This number has later been revised to four items by Cowan (2001), because Miller (1956) did not control for rehearsal and chunking, mechanisms that facilitate memory storage (see Waugh and Norman, 1965). So called slot models of working memory are in line with memory capacity limits based on item number. They assume that each item gets a slot in memory until all slots are filled (Zhang and Luck, 2008). All of these items are then maintained with equal precision (for a review see Fukuda et al., 2010; Luck and Vogel, 1997; Alvarez and Cavanagh, 2004). However, recent findings have shown that the acuity of memory performance declines with an increasing number of items implying that, without exceeding the capacity limits, performance deteriorates just because of increasing memory load (Wilken and Ma, 2004). Based on such findings, a different group of working memory models on the use of limited resources has been proposed (for a review see Ma et al., 2014).

The assumptions of so-called resource models is that representations in memory are always noisy and that the noise increases with increasing memory load (Bays and Husain, 2008; Wilken and Ma, 2004). The noise is here treated as inherent to the cognitive system. It is based on random (neuronal) fluctuations that avoid a perfect mapping of the sensory information onto memory. Noise can be reduced by allocating more attentional resources. Resource models agree that the total amount of available resources is limited but the number of items that can be represented in memory is not. However, more items in memory requires partitioning resources among items. That in turn results in less precise memory representations.

Resource models can be discriminated by their way of allocation and distribution of resources among the items stored in memory. The model of equal resources (Wilken and Ma, 2004) proposes that all available resources are distributed equally across all items in memory. Consequently, the precision in memory decreases with increasing item number. Discrete-representation models (Zhang and Luck, 2008) are similar to the slot models (see above) in so far as they assume a fixed number of resource slots. These

[1] "Memory load" and "cognitive load" are both used throughout this thesis and refer to the same concept.

resources are distributed among the items, whereas items that outnumber the slots are discarded and hence not stored in memory. Variable precision models postulate that the distribution of resources and accordingly precision varies among the stored items and vary from trial to trial (Fougnie et al., 2012; van den Berg et al., 2012). Here as well, an increased number of items results in an overall decrease of precision.

The concept of precision is based on the idea that distinct information that is stored in working memory elicits firing of distinct neural populations in sensory cortices (Ester et al., 2013). However, when the distinctiveness of items in memory is reduced, for example due to similarity among the stored items (Awh et al., 2007), neural responses are more unspecific, the neural noise increases (Bays, 2014), and consequently memory acuity decreases.

The noise that reduces the precision of the memory representation can arise throughout the encoding of the sensory information which is determined by the clarity of the stimulus or for example by the time available to fully encode the stimulus (Bays et al., 2011). Noise can also increase throughout the storage of an item, since memory performance has been observed to decrease with longer delay phase duration (Ma et al., 2014). Memory decay over the passage of time as another critical limitation of working memory will be elaborated in the next section.

Memory load and degraded speech So far the limitations of working memory have been summarized with regards to the number of items, as well as to the amount of necessary resources. However, the aim of the present thesis is to assess the storage of auditory speech stimuli because, interestingly, speech has been shown to be very demanding for the cognitive system as soon as it is degraded. For example the degradation of speech signals by adding a noise masker have been shown to increase memory load reflected by a decrease in performance (for a review see Pichora-Fuller and Singh, 2006; Pichora-Fuller et al., 1995; Rudner et al., 2011). Pichora-Fuller and Singh (2006) explain that the processing of degraded speech is very effortful. Therefore, additional cognitive resources need to be allocated which leads to an increase of memory load. The increase of memory load due to degraded speech is in line with the resource models: Due to additional resources needed to process degraded speech, less resources are available to reduce the noise of the memory representation and memory load increases. Additionally, with respect to working memory precision, degraded speech already lacks

precision by nature, preventing a precise representation of the speech signal in working memory.

### 1.1.2 Memory decay

Working memory is not only limited by the amount of information that can be maintained but also by the duration of information maintenance. The longer items are stored in working memory the poorer is the memory acuity reflected by a decreases in memory task performance (for a review see Ricker et al., 2014). The memory trace decay theory (Brown, 1958) is one approach that explains the decline in performance. According to Brown (1958), sensory information leaves a memory trace (cf., memory representation) that fades out over the passage of time (Posner and Keele, 1967). The loss of the memory representation is therefore assumed to be a consequence of the amount of time that has elapsed (Cowan et al., 1997).

A more recent approach supporting the concept of memory decay, the Time-Based Resource-Sharing model (TBRS) has been introduced by Barrouillet et al. (2004). Barrouillet and colleagues claim that time per se is not the factor that causes forgetting. Instead, attentional resources focused on the memory representation are able to counteract decay by means of refreshing the representations (see also Barrouillet et al., 2007). However, if the memory load is high, resources are allocated to process the load and can not be used to prevent decay. Hence, the TBRS assumes that memory load determines the decay and therefore memory decay depends on the balance of decay over time and attentional resources that refresh the memory representations.

The discussion about the decrease in memory performance over time has been controversial. In opposition to the idea of memory decay, findings of different studies have shown that performance decreases due to an increase of interference in memory (Lewandowsky et al., 2009; Oberauer and Lewandowsky, 2013; Oberauer and Lewandowsky, 2014). Interference either describes a process that impairs working memory by interfering representations or operations or it describes the effect of irrelevant stimuli on memory retrieval (Lewandowsky et al., 2009). Fore example, Farrell and Lewandowsky (2002) proposed the Serial-Order-in-a-Box model (SOB) which explains decline in memory over time solely by interference. However, the discussions about decay versus interference are predominantly constraint to the maintenance of verbal information in working memory.

**Memory decay in auditory sensory memory** Despite the inconclusive debate on memory decay and interference, there has been strong evidence that forgetting of non-verbal stimuli in sensory memory indeed underlies memory decay (McKeown and Mercer, 2012; Mercer and McKeown, 2014). Most of the findings arose from the assessment of memory decay in auditory sensory memory. Auditory sensory memory enables integration of auditory information and preservation of information such as sound features over brief periods of time (for a review see Schröger, 2007). Cowan (1984) has distinguished between an early sensory store that lasts between 100 and 300 ms and a longer store where auditory information can be stored up to ten seconds. One of the reasons for stronger decay in sensory memory compared to working memory is that non-verbal or pre-lexical stimuli (Obleser and Eisner, 2009) preclude rehearsal during stimulus maintenance and the representation fades away (Cowan, 1984; Cowan et al., 1997; Cowan and AuBuchon, 2008; Keller et al., 1995; McKeown and Mercer, 2012).

It remains to be shown how the cognitive system, despite its limitations, renders maintenance and manipulation of encoded information possible. This will be the object of the next section.

## 1.2 Neural basis of working memory

In order to understand how maintenance and manipulation in working memory despite its limitations of resources operate, the sources of these operations in the brain have to be taken into account. The question that needs to be answered is what are the underlying mechanisms also often referred to as cognitive or attentional resources that actually conduct active maintenance and manipulation of information in working memory? Therefore, first the neuroanatomy underlying working memory will be elaborated followed by a summary of neural oscillatory markers of working memory processes.

### 1.2.1 Neuroanatomical basis of working memory

The location of information storage has traditionally been associated with the modality or characteristics of the stored information. That is, during the storage of verbal information, activity has found to be increased in left inferior-parietal cortex (BA40) and frontal sites such as BA44 (inferior frontal gyrus) and BA 6 containing supplementary motor and pre-motor areas (Paulesu et al., 1993; Smith and Jonides, 1998). These

areas are relevant for speech processing and were therefore assumed to reflect rehearsal processes during memory maintenance or storage.

The assessment of spatial working memory in monkeys revealed activity in the dorsolateral pre-frontal cortex (DLPFC), showing selective neuronal firing patterns for specific locations (Fuster, 1999). In humans, posterior parietal cortex (BA 40), anterior occipital cortex (BA19), the pre-motor area (BA6), and an inferior prefrontal site (BA47) were found for the storage of spatial information (Smith and Jonides, 1998).

For the storage of object information, Wilson et al. (1993) found pre-frontal ventral regions to be involved. Goldman-Rakic (1995) summarizes the persistent neuronal activations in frontal brain regions to indicate that the pre-frontal cortex (PFC) stores memory representations. The PFC in general has been found to be crucial for the execution of attentional and cognitive processes. Specifically for working memory processes, the PFC has been found to enable the maintenance of memory representations (for a review see Postle, 2006).

More recent findings, however, indicate that the actual memory representations are coded in sensory cortices instead of PFC (for a review see Sreenivasan et al., 2014; Pasternak and Greenlee, 2005). Hence, the (new) role of PFC has to be elaborated. A variety of studies have shown that neurons in the PFC do not code single memory representations selectively, instead they code a variety of different task features at the same time, still being selective for the relevant information (Stokes et al., 2013; Barak et al., 2010). However, the difference between coding of representations in sensory cortices and the role of the PFC is that the latter rather codes categorical and not the sensory pattern of the representation (Chen et al., 2012). PFC has been found to rather influence representations in other regions (Miller and Cohen, 2001). Its connections to sensory areas have been argued to modulate sensory systems in a top-down fashion during working memory. The interaction of PFC and sensory cortices seems to be essential throughout encoding and maintenance (Cohen et al., 2014; Sreenivasan et al., 2014).

### 1.2.2 Neural correlates of memory load

In order to shed light on the underlying mechanisms that enable the processing of high memory load in working memory it is necessary to understand the underlying neural processes. Neural oscillations are a suitable measure (see Section 4.4.2). Their

increase in power reflects synchronized firing of entire neuron populations (Buzsáki, 2006). Neural oscillations in the theta (4–8 Hz), alpha (8–13 Hz), and gamma (30–200 Hz) frequency range during working memory maintenance have been reported to vary in amplitude with working memory load (for a review see Roux and Uhlhaas, 2013; Jensen, 2006; Lisman and Idiart, 1995). Still, these different frequency bands are assumed to represent distinct working memory functions.

Gamma power has been reported to increase during working memory maintenance of visual (Tallon-Baudry et al., 1998; Medendorp et al., 2007; Jokisch and Jensen, 2007; Roux and Uhlhaas, 2013), auditory (Lutzenberger et al., 2002; Kaiser et al., 2007b; Kaiser et al., 2009; Leiberg et al., 2006a), and somatosensory (Haegens et al., 2010) stimuli, presumably reflecting active maintenance of working memory representations.

Theta power, similarly to gamma power, has been found to also increase with working memory load (Raghavachari et al., 2001; Jensen et al., 2002; Moran et al., 2010). Specifically, theta oscillations have been associated with the storage of sequences such as in the Sternberg paradigm (Sternberg, 1966).

In the present thesis the focus will be on alpha power reflecting memory load in working memory. The alpha frequency band is the most prominent frequency band in human neural oscillations (Berger, 1929). Alpha power was shown to be indicative of a variety of cognitive states and functions predominantly related to attentional processes (see Weisz et al., 2011, for a review on alpha power in audition). With regards to working memory, alpha power has been found to reflect modulations of memory load. That is, alpha power increases parametrically with the number of to-be-remembered items during stimulus maintenance. This increase has been found for different sensory modalities (visual: Jensen et al., 2002; Jokisch and Jensen, 2007, auditory: Leiberg et al., 2006b; Kaiser et al., 2007a; Obleser et al., 2012, somatosensory: Haegens et al., 2010). In particular, within the framework of the "functional inhibition" hypothesis, it has been argued that higher alpha power during item retention in working memory reflects the inhibition of task- irrelevant information (for review see Klimesch, 2012) and/or brain regions (for review see Jensen and Mazaheri, 2010).

In contrast to increased memory load due to item number, a previous study observed increased alpha power during the maintenance of degraded speech items in working memory (Obleser et al., 2012). In particular, Obleser et al. noted parametric increases in alpha power both with the number of to be remembered items and with the decline

in acoustic signal quality, suggesting that memory load is increased by task detrimental acoustic factors as well.

In line with the functional inhibition idea, studies on visual working memory reported alpha power to emerge from visual brain regions in order to inhibit sensory processing during memory maintenance (Jensen et al., 2002; Tuladhar et al., 2007). Comparable effects have been found in the auditory modality where alpha power has been found in the right hemisphere inhibiting active pitch processing during a pitch-discrimination task (van Dijk et al., 2010b) as well as for somatosensory working memory where alpha power was shown to be increased over primary somatosensory cortices in the ipsilateral (irrelevant) hemisphere (Haegens et al., 2010; Whitmarsh et al., 2014). Interestingly, an animal study by Haegens et al. (2011b) demonstrated that alpha activity drives neuronal spiking and that alpha power is associated with the rate of spiking during maintenance of a somatosensory stimulus supporting the inhibitory effect of alpha power.

Compatible with the "functional inhibition" framework, a decrease of alpha power can be related to active stimulus processing (e.g., Hanslmayr et al., 2012) and to increased excitability in sensory cortices (e.g., Jensen et al., 2012; Lange, 2013; Müller and Weisz, 2012). Moreover, controlled inhibition (as reflected by alpha power increases) and active processing (as reflected by alpha power decreases) are likely to play a role in improving the signal-to-noise ratio (SNR) of the relevant information stored in memory (for review see Weisz et al., 2011; Klimesch, 2012).

### 1.2.3 Neural correlates of memory decay

There is only little neural evidence of memory decay proper. However, in line with a decline in performance due to memory decay, a few studies have reported a decline in neural activation. For example, single-cell recordings of monkeys' neural activation decreased throughout the delay phase of a short-term memory task (Fuster, 1999). Similarly, Jha and McCarthy (2000) found a decline in the BOLD response of posterior regions during the visual memory delay phase.

More evidence has been accumulated for memory decay in auditory sensory memory. An fMRI study on pitch memory has shown that the bilateral supramarginal gyrus (SMG, BA40) is activated throughout the delay phase reflecting the maintenance of pitch. Especially in left SMG, activation decreased with the passage over time re-

flecting memory decay (Gaab et al., 2003). An even better investigated marker of auditory sensory memory and memory decay is the mismatch negativity (MMN), a negative event-related potential (ERP) measured with EEG or MEG (for a review see Näätänen, 2000). It occurs right after stimulus onset (100-200 ms) and is a measure of the accuracy of central auditory processing (Näätänen et al., 1978). It is sensitive to changes (deviant) in frequency, duration, or intensity in an repetitive auditory stream (standard). The MMN indicates that the standard sounds form a memory trace from which the sound that deviates elicits the MMN. In principle, after the regularities of sounds were extracted, predictions are formed about the upcoming auditory event. A deviance from this prediction elicits an MMN (Schröger, 2007; Schröger et al., 2014)[2]. The MMN serves also as an indicator for memory decay: the longer the delay phase, the interval between standard stimuli and the deviant stimulus, the smaller is the amplitude of the MMN (Mäntysalo and Näätänen, 1987). A decreased MMN can be interpreted as a marker for a fading out of the memory trace over the passage of time. However, the MMN will not be further discussed because the focus of the present thesis is on neural oscillations reflecting the maintenance of information.

After summarizing the neural correlates of working memory, it is to point out that the communication between PFC and sensory areas as well as the concept of functional inhibition describe an efficient utilization of limited resources. However, considering situations in everyday life, working memory is not just overloaded by all present stimuli. Humans are rather able to decide beforehand what is relevant and what is not relevant to process, a pre-selection of stimuli entering working memory based on selective attention (Hillyard et al., 1998; Posner, 1980). The focus of this thesis, is to investigate the effect of temporal expectations, a specific type of selective attention, on working memory. Temporal expectations guide the focus of attention to a point in time when a target stimulus is expected to occur thereby organizing behavior (Coull and Nobre, 1998). In how far temporal expectations might have a facilitating effect on working memory in general, and memory load and memory decay specifically, will be elaborated in the subsequent chapter.

[2]See the Auditory Event Representation System (AERS) by Schröger et al. (2014) for a detailed elaboration of auditory representations as a basis for the MMN

# 2 Temporal expectations

From the reviewed literature above it should have become evident that brain mechanisms, such as top-down control prioritize relevant from irrelevant information in working memory. Although, traditionally, working memory and (selective) attention have been regarded as almost separate cognitive functions, more recent findings have pointed out their commonalities: In brief, selective attention describes the process of focusing either on locations, object features, or points in time while ignoring others (e.g. Posner, 1980). It has been argued that working memory in principle applies this same attentional mechanism to internal memory representations instead of physical stimuli (Awh et al., 2006; Cowan, 2000; Postle, 2006). Based on this conceptual idea, a variety of studies have found selective attention to modulate working memory in a top-down fashion (for a review see Gazzaley and Nobre, 2012). This kind of top-down modulation can take place at different stages of the working memory process: A priori expectations for a to-be-remembered stimulus; prioritizing information during encoding; enhancing or reactivation of representations during maintenance; as well as retrieval have all been shown to benefit working memory performance (Bollinger et al., 2010; Gazzaley, 2011; Kuo et al., 2009; Murray et al., 2011; Stokes, 2011).

In the present thesis I have focused on a priori expectations. Expectations can be generated for the location of a stimulus (i.e., spatial expectation), for certain stimulus features, or for the time of stimulus occurrence (Bollinger et al., 2010; Lange, 2009; Rimmele et al., 2011; Zanto et al., 2011). All of these different kinds of expectations have been shown to benefit behavioral performance at a target stimulus (e.g., Posner, 1980). In this thesis, I was interested in temporal expectations. Specifically, I assessed the effect of temporal expectations on auditory working memory.

## 2.1 Sources of temporal expectations

Temporal expectation are generated on the basis of the temporal structure of the context. Specifically, one sensory event, a cue, is needed that provides information about the onset-time of a subsequent target event. The onset-time is measured with regards to cue-onset or -offset and the interval between cue and target is the so called foreperiod. A 100 years ago, Woodrow (1914) was the first to show that predictable stimulus onset times based on a warning signal (i.e., cue) increase response speed to a target. More recent studies were able to support the findings on improved behavioral performance modulated by temporal expectations (for a review see Niemi and Näätänen, 1981; Correa et al., 2004; Coull and Nobre, 1998; Lange and Röder, 2006; Miniussi et al., 1999)

However, Coull and Nobre (2008) distinguish between exogenous and endogenous temporal expectations which refers to the modality the cue contains information about target-onset times. Exogenous temporal expectations are generated automatically by means of a predictable temporal structure of stimulus presentation such as rhythm. In a rhythmic sequence, the onset times of each stimulus become highly predictable (Lange, 2009; Large and Jones, 1999; Barnes and Jones, 2000; Jones et al., 2002). Endogenous temporal expectations are induced via the presentation of a symbolic temporal cue that may or may not allow the prediction of the onset-time of an expected event (Coull and Nobre, 1998).

A third kind of temporal expectations that rather can be subsumed under the group of exogenous temporal expectations is based on the passage of time: for a situation in which an event is certain to occur, but the exact time of occurrence is not known, temporal expectations follow a "hazard rate function", meaning that expectations for the event's onset increase with passage of time (Janssen and Shadlen, 2005; Luce, 1986; Nobre et al., 2007). In this case, temporal expectations are driven by time itself instead of sensory information. All these types of temporal expectations have been shown to enhance perceptual processing of the expected stimulus (Correa and Nobre, 2008), which is reflected by decreasing response times (Correa et al., 2006; Doherty et al., 2005; Nobre, 2001; Rohenkohl et al., 2011; Rohenkohl et al., 2012; Stefanics et al., 2010; Sanabria and Correa, 2013) and increasing encoding precision (Rohenkohl et al., 2012; Cravo et al., 2013).

Altogether, the findings on the different sources of temporal expectations manifest a great flexibility of focusing attention to relevant point in time. But the question remains: What enables the cognitive system to estimate time so precisely and why does a precise estimation result in improved target processing? To find answers to these questions, the next section elaborates the neural basis of temporal expectations.

## 2.2 Neural basis of temporal expectations

The neural correlates of temporal expectations are reviewed briefly in this section in order to give rise to answers of two questions: First, what brain areas are involved and what are their roles in picking up on temporal regularities, as well as forming and updating temporal expectations? Second, what are neural markers that are modulated by temporal expectations and which eventually enhance perceptual encoding of an expected target?

### 2.2.1 Neuroanatomical basis of temporal expectations

Based on the findings of neuroimaging studies brain regions and their functional role in forming and updating temporal expectations will be briefly summarized in this section (for a review see Coull et al., 2011).

When temporal expectations were induced via temporal cues that indicated precisely the onset time of the target, activations in lateral cerebellum were found (Coull and Nobre, 1998; Beudel et al., 2009). The cerebellum has been traditionally considered a motor structure. Whereas in the context of temporal expectations the cerebellum has been argued to predict the consequences of motor-behavior in a forward-model manner (Coull and Nobre, 2008; O'Reilly et al., 2008; Wolpert et al., 1995). Furthermore, activation in posterior regions, inferior parietal areas, and pre-motor areas were found (Coull et al., 2000; Schubotz et al., 2003). Here, the pre-motor cortex and inferior parietal cortex have been found to implement timing estimation rather than motor preparation (Dreher et al., 2002; Praamstra et al., 2006).

On the other hand, when temporal expectations were induced by longer foreperiods (i.e., hazard rate function), activations in right frontal areas of the pre-frontal cortex (PFC) have been reported (Triviño et al., 2010; Vallesi et al., 2007b). Here, the PFC has been argued to have a monitoring or updating role. The PFC gets feedback from

sensory areas about whether they have received sensory input. If there has been no sensory input, expectations are updated (Vallesi et al., 2007a).

### 2.2.2 Neural oscillations enhance stimulus encoding

In the following section, I will elaborate on neural oscillations and their role in the facilitatory or beneficial effect of temporal expectations. So far, the benefit of temporal expectations has been observed on the behavioral level in terms of improved response times and accuracy on stimulus detection or discrimination (for a review see Niemi and Näätänen, 1981).

However, temporal expectations are also thought to modulate neural oscillatory activity that results in enhanced encoding precision. These mechanisms have already previously been found when manipulating spatial expectations (e.g., Gould et al., 2011).

Neural oscillations constitute a parsimonious neural mechanism for facilitatory effects of temporal expectations (Henry and Herrmann, 2014). By this account, the brain capitalizes on temporal regularities to be in its optimal (i.e., high-excitability) state when the relevant stimulus occurs (Schroeder and Lakatos, 2009). Specifically, temporal expectations increase excitability by means of decreasing alpha power prior to the target stimulus. This mechanism has been found for visual (Lima et al., 2011; Rohenkohl and Nobre, 2011), auditory (Todorovic et al., 2011), and somatosensory tasks (van Ede et al., 2011; van Ede et al., 2012). Simultaneous to alpha power decrease or desynchronization, Lima et al. (2011) observed increased gamma at the earliest stages of visual processing presumably reflecting early perceptual processing activity.

Furthermore, expectations generated by symbolic cues about time-of-occurrence have been shown to reorganize slow neural oscillatory phase (Stefanics et al., 2010). For the most part, however, the relationship between the phase of slow neural oscillations and temporal expectations has been studied using rhythmically presented stimuli. In this case, neural oscillations are entrained by temporal regularities leading to increased neural phase concentration across trials in the frequency range corresponding to the stimulation rate (2.5 Hz: Cravo et al., 2013; 1.5 Hz: Lakatos et al., 2008, 2013; 3.95 Hz: Herrmann et al., 2013; 3 Hz: Henry and Obleser, 2012; 0.67 Hz: Lakatos et al., 2013).

As mentioned in the beginning, expectations for locations and object features have been shown to modulate working memory in a top-down style improving memory performance. Presumably these modulations are based on the improved neural excitability elicited by temporal expectations. To this end, however it is still unknown whether temporal expectations will have similar modulatory effects on working memory, such as that enhanced encoding precision impacts subsequent memory performance.

# 3 The present thesis

After reviewing the literature about working memory and temporal expectations, we are at a point of linking both concepts. The focus of the present thesis is on working memory or more specifically on its limitations. As already elaborated above the most striking characteristic of working memory is its limited cognitive resource which is easily challenged by the magnitude of information to-be-maintained (memory load) and the duration of maintenance (memory decay). The underlying neural mechanisms such as top-down modulation of the sensory areas by the pre-frontal cortex (PFC), as well as functional inhibition by means of neural oscillations in the alpha range, remain likely candidate mechanisms for an efficient way to handle the limitations.

Interestingly, most of the research conducted on working memory has been conducted in the visual domain. Therefore, to us it has been of major interest in how far memory limitations are challenged by auditory stimuli. As stated before, degraded speech has turned out to be a quite suitable object because it has been shown to increase memory load (Pichora-Fuller and Singh, 2006). Moreover, in a study of Obleser et al. (2012) alpha power, a prominent marker for memory load, increased parametrically with increasing speech degradation, proving that alpha power is also sensitive for memory load in the auditory domain.

Based on this finding, I here wanted to assess the impact of temporal expectations on auditory working memory. In everyday life scenarios when processing (degraded) speech, one has prior knowledge about when the speech signal will be produced, based on the temporal structure of speech presentation, as in ongoing conversations. I therefore assumed that the a priori information on when to listen would facilitate the processing of degraded speech in working memory. Specifically, as elaborated before, implications from previous findings on enhanced encoding precision due to temporal expectations allow to expect a load reducing effect of temporal expectations for degraded speech. In brief, the aim of the present thesis is to assess how temporal expectations

modulate memory limitations as reflected in fluctuations of alpha power and behavioral performance with magnetoencephalography (see Fig. 3.1).

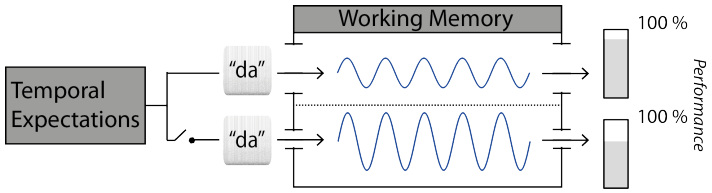


***Figure 3.1.*** **Expected impact of temporal expectations on working memory.** A syllable, "da", presented in noise enters working memory. Either, the syllable is temporally expected (upper stream) or temporally unexpected (lower stream). The amount of cognitive load is illustrated by means of a sinusoidal curve reflecting alpha power. Larger amplitude refers to high alpha power in when there is no temporal expectations (lower stream). Lower amplitude refers to low alpha power when the syllable is expected (lower stream). Bars on the right illustrate expected behavioral performance modulated by temporal expectations: better performance with temporal expectations and lower performance without temporal expectations.

In detail, the study presented in Chapter 5 (*Experiment I*) addressed the question whether temporal expectations reduce memory load of degraded speech. Two spoken syllables (S1, S2) were presented in a delayed matching-to-sample task separated by a two-second delay phase. Syllables were masked with noise in order to increase the memory load. Critically, temporal expectations for S1 was manipulated by means of three different a priori temporal cues that were either informative or not informative about S1-onset time with regard to cue-offset. We expected to observe reduced memory load in trials with temporal expectations reflected by decreased alpha power and increased memory performance.

In a subsequent study with a subset of participants of the previous study we conducted the same experiment with clear speech in order to find out whether the previously observed reduction of memory load due of temporal expectations was specific to the noise masker or whether similar effects could also be observed in clear speech (*Experiment IIa*). Moreover, we also tested whether temporal expectations induced by the hazard rate function had an impact on processing of the target stimulus (S1) as well as on alpha power during the delay phase (*Experiment IIb*). Note that foreperiods between cue and S1 were jittered after each of the three different cues providing enough variability in the foreperiod to observe the effect of longer foreperiods. We expected to find increased phase coherence of slow neural oscillations in the frequency range of

stimulus presentation with longer foreperiods. Here, increased phase coherence would be an indicator for a state of increased excitability due to temporal expectations. At the same time, we expected longer foreperiods to concomitantly reduce alpha power during the delay phase indicating that temporal expectations based on the hazard function have reduce cognitive load, similar to temporal cues.

In order to attain a complete picture on the limitations of auditory working memory and how they are reflected by modulations of alpha power, memory decay was examined in the next study (*Experiment III*). Here, we assessed auditory sensory memory by presenting pure-tone sequences (S1, S2) instead of syllables which allowed for decay in memory indicated by a decline in performance with longer delay phases. As before, S1 and S2 were embedded in noise to increase memory load and memory decay was manipulated parametrically by means of three different delay phase durations. Since there had been no prior evidence on the modulations of alpha power by memory decay we could only assume whether a decline in performance after longer delay phases would be accompanied with a decline in alpha power. In addition, we again manipulated temporal expectations for S1 to investigate whether temporal expectations not just reduce memory load per se but also counteract memory decay on the behavioral level as well as reflected by alpha power modulations. In addition to analyses on the sensor level, we conducted a source localization of alpha power modulations for further insights on the brain regions modulated by the different experimental manipulations such as potential involvement of PFC.

In the last experiment I picked up on the interaction of temporal expectations and memory decay (*Experiment IV*). In principle,the same experiment as in the previous study was conducted. The aim of this experiment, however, was to fit a forgetting curve or exponential decay function onto the performance measure $A_z$ (see below), separately for trials with and without temporal expectations in order to describe more precisely the effect of temporal expectations on memory decay. For that reason, memory decay was operationalized by means of six different delay phase durations instead of three different delay phase durations as in the previous experiment.

More specific theoretical background will be provided in the introduction section of each experimental chapter, as well as detailed descriptions of applied methods and results. The next chapter gives an overview and describes the general methods applied to conduct and analyze the experiments.

# 4 General methods

In this chapter the methods applied in the experiments of this thesis are described in more general form. Configurations of methodological approaches that differ between experiments are specified in the method sections of the respective chapters.

## 4.1 Experimental paradigm

As elaborated in the previous section, the assessment of memory processes is at the heart of this thesis. The experimental paradigm which was applied to investigate short-term memory was a modification of the so called *delayed matching-to-sample task* (DMTS, see Fig. 7.1A). In a DMTS task, a standard stimulus is presented which has to be retained in memory for a certain delay phase. Then, a set of at least two stimuli is presented and participants have to indicate which stimulus within the set was the same as the stimulus presented first (Herremans and Hijzen, 1997). In our modified version, only two stimuli were presented, the standard (S1) and a second stimulus (S2) after the delay phase. Here, participants had to indicate whether S2 was identical to or different from S1.

The principle of these delayed response task was first reported by Hunter (1913) who tested short-term memory in children and pigeons. The classic DMTS as well as the modified version have been widely applied to study short-term memory in humans (e.g., Haegens et al., 2010; Jokisch and Jensen, 2007; Kaiser et al., 2007a; Kaiser et al., 2009; van Dijk et al., 2010b; Pinal et al., 2014) as well as in animals (e.g., Blough, 1959; Herman and Gordon, 1974; Herremans and Hijzen, 1997; van Hest and Steckler, 1996) in different sensory modalities.

One of the advantages of the DMTS is that all stages of short-term memory (encoding, maintenance, retrieval; Jonides et al., 2008) occur one after another and do not overlap. First, the encoding of the to-be-remembered stimulus can be observed during the presentation of S1. The maintenance of S1 takes place during the delay

phase and the memorized stimulus is retrieved when S2 is presented (see also Pinal et al., 2014). Other than for example in an n-back task (Owen et al., 2005), stages of stimulus perception and stimulus maintenance are almost distinct.

Moreover, the sequence of the DMTS task is very flexible in terms of temporal variability. That is, stimuli can be presented prior to S1 and could serve as a cue providing information about the time of S1-occurrence. Then, the duration of the delay phase can be changed gradually for example to modulate memory decay over the passage of time (*Experiment III*). Moreover, the task-response can be prompted arbitrarily some time after the presentation of S2 to for example avoid S2 encoding and button presses to overlap (important when measuring brain data).

In the experiments presented in this thesis, S1-onset times varied in reference to a visual cue, presented prior to the actual DMTS task. The controlled manipulation of the interval between cue and S1 (i.e., foreperiod) either induced or avoided the generation of temporal expectations for S1-onset. The specific temporal and probabilistic characteristics of the foreperiods are described in each experimental chapter separately.

Thus, in order to analyze all the stages of short-term memory in a DMTS task temporally independently from each other, it is useful to measure brain activity with high temporal resolution (cf. see Section: 4.4).

## 4.2 Auditory stimuli

In this section, the generation and the characteristics of the auditory stimuli presented in the following experiments are described.

### 4.2.1 Spoken syllables

In experiments I, IIa, and IIb the aim was to assess auditory (verbal) working memory with syllables. Therefore, we presented four different syllables during the previously described DMTS task: “da”, “de”, “ga”, and “ge”. These syllables were edited from full words beginning with the respective syllable. Two different words and two recordings per word were used to create a pool of four naturally varying tokens for each syllable (e.g., Obleser et al., 2003). Speech stimuli were recorded by a trained female speaker of German in a sound proof chamber. Recordings were digitized at 44100 Hz. All syllables

were edited to be of 200 ms final length, including 3-ms onset and 30-ms offset ramps. Sound files were peak normalized to equal decibel full scale amplitude.

### 4.2.2 Pure-tone sequences

In experiments IIIa and IIIb, pure-tone sequences were presented instead of syllables because the focus in this experiment was to investigate memory decay in auditory sensory memory (e.g. Cowan, 1984). Sound pairs, a standard and a deviant, were created for the S1-S2 "same"/"different" task. The deviant was higher in pitch than the standard. All sounds were sequences consisting of five pure tones, each pure tone had a duration of 40 ms resulting in a total sound duration of 200 ms (Watson et al., 1975). The pitch, or frequency of each pure tone in a sound sequence was derived from a varying starting frequency. This starting frequency was randomly selected from a range between 450 and 600 Hz. In the standard sound sequence, this frequency corresponded to the frequency of the third pure tone, the pure tone in the center of the sequence. The adjacent pure tones, number two and number four, had a frequency ranging from 1 to 4 semitones below the third pure tone. Pure tone one and five in a sequences were between four and seven semitones higher in pitch compared to the third pure tone. The exact number of semitones deviating from the third pure tone was randomly selected for each pure tone individually.

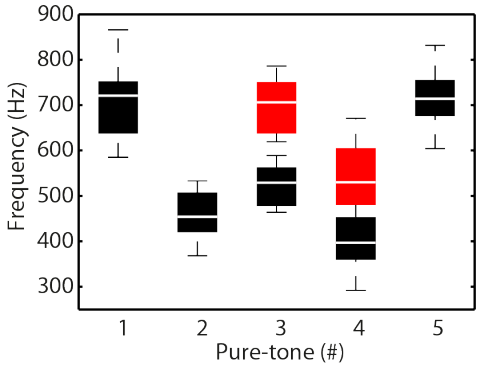


***Figure 4.1.*** **Frequency range of pure-tone sequences.** Example frequencies of all pure-tones presented to one participant of Experiment III, across 33 sequences in total. Red boxes indicate median frequencies of all deviating pure-tone sequences and error bars represent the standard deviation.

At the deviant sound, the third and the fourth pure tone in the sequence were higher in pitch compared to the standard. The difference between tone 3 in the standard compared to the deviant was the same as the differences in tone 4 between standard and deviant. The exact difference, though, was adjusted for each subject individually.

Each pure tone had an onset- and offset-ramp of 10 ms to avoid clicking sounds. The order of the standard or the deviant being the first sound was counterbalanced across the experiment as was the number of same and different trials. See figure 4.1 for the frequency distributions of each pure-tone in the sequence.

### 4.2.3 Noise masker

In experiments I, IIIa, and IIIb we investigated the impact of noise on auditory perception and cognitive processes. For that reason, syllables and pure tone sequences were embedded in noise which has been shown to increase the load in short-term memory (Pichora-Fuller and Singh, 2006; Surprenant, 1999). Syllables described above were masked with speech-shaped noise in Experiment I. Speech-shaped noise was generated by filtering white noise to approximate the long-term average spectrum of speech (e.g., Peters et al., 1998). Power per frequency band from a concatenated set of 60 German nouns (female speaker) was convoluted with the white noise signal. This resulted in noise with an approximately speech-shaped spectral envelope and an approximately flat amplitude envelope (i.e., a non fluctuating noise masker). In contrast, pure-tone sequences in experiments IIIa and IIIb were masked with non-modulated white noise to guarantee masking of all frequencies of the pure tone sequences.

## 4.3 Psychophysics

### 4.3.1 Adaptive tracking

In order to obtain equal task performance across participants and also to avoid ceiling and floor effects of behavioral and brain responses we controlled for task difficulty by adjusting task difficulty for each participant individually. The task difficulty can be changed by manipulating the characteristics of the presented stimuli. For example in Experiment I, the SNR of syllables and noise was determined in a way that a task difficulty of 70.9 % correct trials was attained. In Experiment IIIa and IIIb, the pitch difference between the first and second sound was manipulated, where a smaller difference is more difficult to discriminate. For each individual, a certain manipulation of a characteristic results in a certain task difficulty or task performance. That is that a target sound masked with a certain SNR is perceived more clearly for one individual than for another. Thus, in order to attain approximately the same task difficulty across

all participants, their individual threshold (i.e., manipulation of stimulus characteristic) for this level of difficulty has to be estimated.

The basic principle of threshold estimation is that changing a physical characteristic of a stimulus (increase of stimulus level) in one direction leads to an increase in performance. Changing the physical characteristic in the other direction (decrease of stimulus level) results in a performance decrease (Macmillan and Creelman, 2004). The (individual) relationship between stimulus level and performance is described by the psychometric function (Wichmann and Hill, 2001). In order to fit a psychometric function, participants have to respond to a large number of tasks across a wide range of variant stimulus characteristics. Adaptive methods for threshold estimation, on the other hand, aim to find the targeted stimulus level by limiting presented stimulus characteristics to be close to the targeted threshold. The specificity of adaptive methods is that the stimulus level in one trial is determined by the stimulus levels and behavioral performance of the previous trials (Levitt, 1971). Two classic adaptive methods are the Békésy technique (Békésy, 1947) and the method of limits. In both methods the stimulus level is reduced from one trial to the other until the response to the stimulus could not be detected anymore. Then the stimulus level is increased again. The threshold is then at the stimulus level where the stimulus was barely detectable (Leek, 2001).

Staircase procedures were derived from these methods with the difference that they tested multiple of ascending and descending stimulus-level tracks collecting a number of threshold values (Anderson et al., 1946). These are so-called up–down procedures that result in a threshold of 50 % correct. In the present thesis a transformed up–down procedure was applied (Levitt, 1971). That is, the 2-down–one-up adaptive staircase tracking which estimates the threshold of 70.7 % proportion correct performance. The difference to the classic up–down tracking is that the stimulus level is decreased just after two correct responses to the same stimulus level (i.e., two down). The stimulus level is increased after one incorrect response (i.e., one up), as in the classic procedure. Critical for all sorts of up–down procedures is the selection of the initial stimulus level. The first level needs to be above but not too far away from the final threshold. Then, the step-size of the stimulus level to change from one trial to another has to be defined. Moreover, these tracking procedures do not stop after a certain number of trials. Instead, the number of reversals has to be defined of when to stop the track. A

reversal is in principal a turning point where the stimulus level leads to an incorrect response, followed by a stimulus level leading to a correct response or vice-versa (see Fig. 4.2). When the pre-defined number number of reversals is reached, the track is stopped. The final threshold corresponds to the average of the stimulus levels of the reversals. Note that, usually, the initial reversals are skipped for averaging in order to attain a more valid threshold estimate. An example track of the 2-down–1-up staircase procedure in Experiment I is displayed in Figure 4.2. Note that the specifications of the adaptive tracking procedures such as step-size, initial stimulus level, and number of reversals will be specified in each experiment's method section.

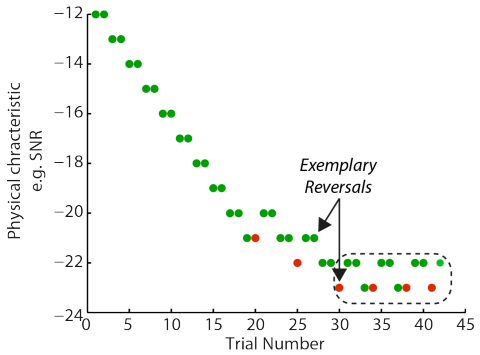


***Figure 4.2.*** **2-down–1-up adaptive tracking.** Example track of one representative participant of Experiment I. Green dots indicate a correct responded trial. Red dots indicate incorrect trials. Step-size was 1 dB throughout the entire track. Tracking was stopped after 12 reversals, see black arrows. The SNRs of the last eight reversals were averaged and indicated the participant's threshold, see dashed line.

For sensory discrimination and the individual differences as described above, signal-detection theory (SDT) plays a crucial role. SDT is able to quantify the ability to discriminate sensory stimuli which essentially serves as a basis of individual threshold estimation. Therefore, SDT as a technique to compute behavioral task performance is described in the next section.

### 4.3.2 Signal-Detection Theory

Signal-Detection Theory (SDT) is a psychophysical approach that assess the performance in experimental tasks, such as stimulus discrimination, similarly to percentage correct. However, in contrast to percentage correct, SDT takes the participant's individual sensitivity (i.e., ability to discriminate between stimulus category) and response bias (i.e., tendency to give one response more often than the other) into account.

**Sensitivity and Response bias** In the experiments conducted in the present thesis, participants had to indicate whether S1 and S2 were same or different. In Experiments I,

IIa, and IIb, participants discriminated the initial consonant of the presented syllables. In Experiment IVa and IVb, they had to discriminate subtle pitch differences between S1 and S2. Despite the difference in stimulus material, both tasks underlie the same conceptual idea that participants have their individual internal distribution of stimulus representations which result in a "same" response and which result in a"different" response (i.e., decision model; Henry and McAuley, 2013). The distance of the internal "same"-distribution and the internal "different"-distribution (a.k.a perceptual distance; Macmillan and Creelman, 2004) corresponds to the participant's sensitivity: the greater the distance, the greater the sensitivity, and consequently, the better the task performance. Sensitivity provides information about the perceptual difference of two response categories. Response bias informs about the individual decision rule, the cut-off where one or the other response is selected (i.e., "same" vs. "different"). It is denoted $d'$ and is calculated by subtracting the z-scored false alarm rate (FAR) from the z-scored hit rate (HR). HR corresponds to the proportion of same-trials responded to with "same" and FAR corresponds to the proportion of different-trials responded to with "same". Note that $d'$ is independent of the response bias (but see below), whereas sensitivity and response bias are intermixed in percentage correct. The response bias is denoted $C$ where $C = 0$ indicates an equal probability of each response. $C > 0$ favors one response, and $C < 0$ is in favor of the other response category. $C$ is calculated by averaging z-scored HR and z-scored FAR.

However, a problem arises, when the variance of the "same" distribution is different from the variance in "different" distribution. Due to the z-transformation of HR and FAR which has then to be computed on either one of the distributions' variance, d' is not independent from c anymore. The registration of confidence ratings on each trial allows to correct for unequal variance in the "same"- and "different"-distributions.

Confidence ratings The binary response paradigm of "same"/"different" tasks can be extended by adding confidence ratings after each binary response. The way it was implemented in the experiments of the current thesis was to indicate on a ternary scale the confidence about the binary response ranging from "very" low to "high". This resulted in six different responses, three "same" and three "different" responses. This in turn could be transformed into 5 C-values spanned across the two internal response-distributions, instead of only one C (Macmillan and Creelman, 2004). Similarly as

described above, HR and FAR were calculated. An empirical receiver-operating characteristic (ROC) was plotted where HR and FAR were plotted against each other along the five criterion positions. Then, linear fits to z-transformed ROCs (zROCs) yielded a slope estimate for each participant. Separately for each condition, zROC slopes were then tested against unity (slope = 1) using a single-sample t-test. Significant deviations from unit slope indicate asymmetric ROC curves and thus non-independence of perceptual sensitivity and response bias in parametric performance measures (e.g., PC, d'). Thus, nonparametric performance measures derived from the ROCs themselves, like $A_z$, are considered more accurate performance measures. $A_z$ is expressed in proportions similarly to percentage correct and represents the area under the ROC curve. It is a measure of sensitivity taking into account the difference in variance of the "same"- and "different"-distribution.

## 4.4 Magnetoencephalography

In order to analyze all consecutive stages of short-term memory in a DMTS it is useful to measure brain responses with a high temporal resolution.

Electroencephaolgraphy (EEG) and magnetoencephalography (MEG) are non-invasive methods that measure brain activity with a temporal resolution; ~1 ms. Both, EEG and MEG are based on the principle that signals in the brain are transmitted via fluctuations of the electric current: A stimulation of a neuron elicits a depolarization of the neuron. This change of current is conducted along the axon of the neuron to the synapses where the signal is transmitted to adjacent neurons (for a detailed description see Kandel, 2000; Hämäläinen et al., 1993). The change of electric current is measured with EEG (Berger, 1929). The neuronal activity which is recoded with EEG is essentially the extracellular, local field potential of the post-synaptic activity. MEG, on the other hand, measures the magnetic field (Cohen, 1972) that is concomitantly generated by the current change in the neuron. The activity recorded with MEG is the local magnetic field or dipole. Both, the local field potential as well as the local magnetic field are generated through synchronized depolarization of bundles of pyramidal neurons (Lopes da Silva, 2013; Elbert et al., 2001; Schnitzler and Gross, 2005) where the electric current measured with EEG travels along the axon, whereas the magnetic

field circulates around the axon. The pyramidal neurons are oriented parallel in the cortex and perpendicular to the cortical surface.

The cortical currents either flow radial or tangential to the skull, depending on the orientation of pyramidal cells and the folding of the cortical surface. Since the MEG sensors detect only dipoles that produce external magnetic fields the MEG is sensitive to fields which are tangential to the surface (Ahlfors et al., 2010; Vrba and Robinson, 2001). These signals are primarily generated by pyramidal cells located in cortical fissures. Thus, signals measured with MEG are locally more focused than the signals measured by EEG which emerge from radial and tangential dipoles simultaneously (Hämäläinen et al., 1993).

In the present thesis, all experiments were conducted in MEG because not only is the temporal resolution very high, but also it is possible to localize the neural sources of the measured brain activity (see below). Source analyses can also be conducted on EEG signals but have some disadvantages compared to MEG. First, the magnetic field is less disturbed through head movements as is the electric potential in EEG. Second, other than for the EEG signal, the tissue outside the brain (i.e., cerebro-spinal fluid (CSF), skull, and skin) hardly disturb the MEG signal (e.g.; Hari et al., 2000). For that reason a single compartment volume conductor is sufficient to model the sources of the MEG signal, whereas for EEG the conductivity of the different tissues has to be taken into account (Lopes da Silva, 2013).

### 4.4.1 MEG recording and pre-processing

All experiments reported in the present thesis were measured with the same MEG system in the same set up. Also, initial pre-processing steps were identical throughout experiments. Participants were seated in an electromagnetically shielded room (Vacuumschmelze, Hanau, Germany), necessary to protect the weak brain signal from interfering stronger magnetic signals. Magnetic fields were recorded using a 306-sensor Neuromag Vectorview MEG (Elekta, Helsinki, Finland) with 204 orthogonal planar gradiometers and 102 magnetometers at 102 locations. Two electrode pairs recorded a bipolar electrooculogram (EOG) for horizontal and vertical eye movements. The participants' head positions were monitored during the measurement by five head position indicator (HPI) coils. Signals were sampled at a rate of 1000 Hz with a bandwidth ranging from direct current (DC) to 330 Hz.

The signal space separation method (Taulu et al., 2004) was applied offline to suppress external interferences in the data and to transform individual data to a default head position that allows statistical analyses across participants in sensor space.

Following data analyses were carried out with Matlab (The MathWorks Inc., Massachusetts, USA) and the FieldTrip toolbox (Oostenveld et al., 2011). Analyses were conducted using only the 204 gradiometer sensors, as they are most sensitive to magnetic fields originating directly underneath the sensor (Hämäläinen et al., 1993). If not stated differently, the continuous data were filtered offline with a 0.5-Hz high pass filter, specifically designed to provide a strong suppression of DC signals in the data (>140 dB at DC, 3493 points, Hamming window; e.g., Ruhnau et al., 2012).

Subsequent pre-processing steps such as the timing of the extracted trial epochs as well as the method of artifact rejection are described in each experimental chapter separately because of the different configurations and approaches in each experiment.

### 4.4.2 The MEG signal – neural oscillations

Traditionally, the MEG signal is averaged across epochs time-locked to a specific stimulus event (cf., event related fields; ERFs) in order to find differences in the amplitude of the ERFs between contrasted conditions. More recently, MEG (and also EEG) methodology was expanded by investigating neural oscillations (e.g., David and Friston, 2003; Tallon-Baudry, 2009; Ward, 2003). Neural oscillations refer to periodic variations in the recordings of neural activity. The emergence of oscillations and the frequencies of these oscillations depend on cellular pacemaker mechanisms and neuronal network properties (Buzsáki and Draguhn, 2004; Buzsáki, 2006; Schnitzler and Gross, 2005).

Neural oscillations are inherent to the brain because the neural activity in the brain fluctuates permanently. However, the oscillatory activity does not only underlie random fluctuations. As already elaborated in Section 1.2.2, neural oscillations (similar to ERFs) reflect cognitive processes and provide the link between brain and behavior. Here it is important to consider specific frequency bands and their respective purported functions.

The basic idea is that signals that are strong enough to be detected by MEG sensors are only generated by synchronous neural activity. Signal amplitude increases with the number of neurons being synchronously active in the same frequency. Neural synchrony implies systematic brain activity in contrast to random neural fluctuations.

An increased amplitude in slower frequencies is an indicator for widespread neural activity, whereas increased amplitude in high frequencies (i.e., gamma > 40 Hz) reflects rather local processes (Lopes da Silva, 2013).

**(Time–)frequency representations** Power spectra and time–frequency representations (TFRs) were computed to attain differences in power and phase alignment between experimental conditions as well as as a function of behavioral performance. The power spectra of neural oscillations were calculated by multiplying the time-domain signal with a Hann taper and then using a fast Fourier transform (FFT) approach (Mitra and Pesaran, 1999; Percival and Walden, 1993). To inspect the time course of the frequency effects, TFRs were calculated also by convolving the time-domain signal with a Hann taper. Here, the output of the analysis was complex Fourier data, allowing for analyses of phase and of power over time. The complex Fourier output consists of a complex part and a real part. Both contain the information about the phase and the amplitude of the signal at a certain point in time in a certain frequency band.

For the FFT and TFR analyses, a frequency range of interest as well as the resolution or size of single frequency bins within this range was pre-defined. Since the focus of the conducted experiments was mainly on alpha power and in general on slower neural oscillations, the frequency range never exceeded 30 Hz. The frequency bins were logarithmically spaced to account for the inverse relationship of power and frequency ($1/f$; Buzsáki and Draguhn, 2004).

For the calculation of the TFRs the time-window of interest within a trial epoch was selected, as well as the temporal resolution, which was 0.02 s in all experiments. Furthermore, the width of the Hann tapers was determined in each experiment separately. In all analyses, the width was adapted to the frequency range: a certain number of cycles per frequency were determined, in most cases four cycles ($\Delta t = 4/f$), which covers enough oscillatory fluctuations to allow for a valid estimate. TFR and FFT analyses were calculated for each gradiometer resulting in a $trial \times sensors \times frequencies (\times time)$ matrix.

Based on the complex Fourier output, up to three neural activity measures were calculated for each time-frequency-sensor data bin: Inter-trial phase coherence (ITPC; Lachaux et al., 1999), total power, and evoked power (David et al., 2006; Ding and Simon, 2013). ITPC corresponds to the magnitude of the amplitude-normalized com-

plex numbers averaged across trials of the TFR estimates for each time-frequency bin, channel, and foreperiod bin (Thorne et al., 2011). Total power was expressed as the average power (squared magnitude of the complex-valued TFR estimates) across single trials (see below), while evoked power was calculated for each channel by first averaging single-trial time domain data, then calculating the power as the squared magnitude of the complex-valued TFR estimation.

The configurations of the analyses are specified in each experimental chapter separately.

### 4.4.3 Source analysis

The generators of the MEG signals measured outside of the head can be localized by means of source reconstruction algorithms. With the forward model or lead field one can predict the magnetic field measured externally using realistic data based on individual MRI scans and the volume conductor model that contains information about about surrounding tissue (i.e.; CSF, scull, and skin Lopes da Silva, 2013; Hämäläinen et al., 1993). However, the source reconstruction also involves an inverse problem, which means that there is an infinite number of solutions for the deduction of the source of a magnetic field outside the volume conductor (Hämäläinen et al., 1993; Hari et al., 2000; Helmholtz, 1853; Lopes da Silva, 2013). The inverse problem can be solved by having specific assumptions about the sources such as number of brain areas involved or the spatial extent of the source (Ramirez et al., 2010).

**Source projections based on individual T1-weighted MRI images** In the present experiments source localizations were computed as described in the following paragraphs. On the basis of individual T1-weighted MRI images (3T Magnetom Trio, Siemens AG, Germany), topographical representations of the cortical surface of each hemisphere were constructed with Freesurfer (`http://surfer.nmr.mgh.harvard.edu/`). The MR coordinate system was co-registered with the MEG coordinate system using the head-position indicators (HPIs) and about 100 additional digitized points on the head surface (Polhemus FASTRAK 3D digitizer). For forward and inverse calculations, boundary element models were computed for each participant using the inner skull surface as volume conductor (using the MNE toolbox; `http://www.nmr.mgh.harvard.edu/martinos/userInfo/data/index.php`). Individual mid-gray matter surfaces were used as source

model by reducing the approximately 150,000 vertices needed to describe single hemispheres to 10,242 vertices.

The FieldTrip-implemented beamformer approach (DICS, dynamic imaging of coherent sources; Gross et al., 2001) was used to project alpha power to source space, employing the cross-spectral density (CSD) across sensors. The CSD was calculated based on results of the sensor-space analysis: Using a multitaper FFT (Fast Fourier Transform) applied to single trials. The multitaper FFT was centered on the frequency of interest (either 10.5 Hz or 11 Hz; smoothing with three Slepian tapers; Percival and Walden, 1993) and a complex filter (either common for all epochs analyzed or separately for each group of epochs) was calculated (Gross et al., 2001; Schoffelen et al., 2008). Data were then projected through the filter, separately for each condition. Then, projections of (relative, only when a baseline was applied) power change per condition averaged over trials were attained. For visualization, the (relative) power source projection of each condition was morphed onto a common surface (Freesurfer average brain; Fischl et al., 1999).

## 4.5 Statistical analyses

In this section, the basic principles of the statistical analyses are described that were applied on the MEG data on the sensor level and the source level.

### 4.5.1 Analyses on the sensor level

Statistical analyses on the sensor level were conducted on the power and phase data per or across epochs. Based on the time- and frequency resolution of the time-frequency estimation, power and phase values were attained for each time-point at each calculated frequency at each MEG sensor. Statistical analyses were calculated on each of these time-, frequency bins and sensors. Therefore, it was necessary to correct for multiple comparisons by means of cluster tests (see below). Statistical contrasts were calculated in a multi-level fashion which is described in the next section.

**Multi-level tests** Multi-level statistics as computed in the present thesis comprised analyses on the single-subject level and a subsequent analyses on the group level across all participants. On the first (single-subject) level, specific contrasts were conducted using

single-trial data to test for differences in the frequency range of interest between conditions. Contrasts of all conditions were performed using the Fieldtrip-implemented independent-samples regression t-test with contrast coefficients according to the contrasts of interest. The regression t-test provided partial-correlation coefficients or beta coefficients for each time–frequency bin at each of the 102 sensor positions indicating the strength of the tested contrast. For the statistical analyses on the second (group) level, beta-values resulting from the single-subject first level statistics were tested against zero with cluster based permutation tests (dependent samples t-tests, 1000 iterations; Maris and Oostenveld, 2007) which will be described in the next section.

Cluster test Because of the multiple comparisons at each time-frequency-sensor it becomes more likely that the tested contrasts become significant. For that reason, cluster tests were calculated that protect against this so-called inflated type-1 error due to the multiple comparisons. To this end, a second-level t-statistic was calculated on the beta coefficients (derived from alpha power first-level analysis, see above) for each time–sensor bin. Then, clusters were formed based on combining adjacent time-sensor bins with t-values exceeding a threshold of $p < 0.05$. Within each cluster, t-values were summed. Using a permutation-based approach, time–sensor values were randomly assigned to two "conditions" without regard for their true condition labels on each of 1000 iterations. On each iteration, clusters were again formed based on combining neighboring bins with statistically significant t-values, and the t-value from the cluster with the largest summed statistic was added to a permutation distribution. Finally, any clusters with t-values exceeding 95 % of those from the permutation distribution were considered statistically significant. All cluster tests were two-tailed and were thus considered significant when $p < 0.025$.

### 4.5.2 Analyses on the source level

To illustrate condition effects observed in sensor-space at the source level, the same contrasts as described for the first-level of the sensor data were computed on the sources data. That is, vertex-wise t-tests or regression analyses were computed. The resulting t-values were z-transformed and displayed on the average brain surface. Given that the goal of source reconstruction was to localize the neural generators of sensor-space

effects previously identified as significant, z-value maps will be displayed with contrast specific uncorrected vertex-wise thresholds.

# 5 Experiment I: Alpha oscillatory dynamics index temporal expectation benefits in working memory[1]

## 5.1 Introduction

Oscillatory alpha power recorded with magneto- or electroencephalography (M/EEG; 8–13 Hz) is studied extensively in the fields of attention and working memory. In the current study, we were particularly interested in the cognitive load associated with the retention of to-be-remembered items in working memory. In the visual, somatosensory, and auditory domains, increases in alpha power have been associated with performance of working memory tasks (Jensen et al., 2002; Leiberg et al., 2006b; Haegens et al., 2010). Moreover, alpha power parametrically increases with the number of to-be-remembered items (Jensen et al., 2002; Leiberg et al., 2006b; Obleser et al., 2012), and thus provides further evidence that alpha indexes cognitive load associated with item retention. In particular, within the framework of the "functional inhibition" hypothesis, it has been argued that higher alpha power during item retention in working memory reflects the inhibition of task-irrelevant information (for review see Klimesch, 2012) and/or brain regions (for review see Jensen and Mazaheri, 2010).

Compatible with the "functional inhibition" framework, a decrease of alpha power can be related to active stimulus processing (e.g., Hanslmayr et al., 2012) and to increased excitability in sensory cortices (e.g., Jensen et al., 2012; Lange, 2013). Moreover, controlled inhibition (as reflected by alpha power increases) and active processing (as reflected by alpha power decreases) are likely to play a role in improving the signal-to-

[1]This chapter has been adapted from the article published in *Cerebral Cortex* by Wilsch, Henry, Herrmann, Maess, and Obleser (2014).

noise ratio (SNR) of the relevant information stored in memory (for review see Weisz et al., 2011; Klimesch, 2012).

Reasoning from the "functional inhibition" hypothesis, we chose to examine working memory performance for speech items embedded in noise, where the noise creates cognitive load that raises the need to increase functional inhibition. Degraded speech is hypothesized to increase memory load mainly due to the additional resources and time needed to encode and subsequently process the speech signal (Pichora-Fuller and Singh, 2006). In line with this claim, a previous study observed increased alpha power during the retention of degraded speech items in working memory (Obleser et al., 2012). In particular, Obleser et al. noted parametric increases in alpha power both with the number of to be remembered items and with the decline in acoustic signal quality, suggesting that cognitive load is increased by task detrimental acoustic factors as well.

The primary goal of the present study was to explore the potential of temporal cueing (Nobre, 2001; Coull and Nobre, 2008; Jaramillo and Zador, 2011) to improve working memory performance and concomitantly reduce alpha power. Temporal expectations have been shown to enhance the precision of stimulus encoding (Rohenkohl et al., 2012) as well as to improve behavioral performance (Coull and Nobre, 1998). Thus, we hypothesized that behaviorally, cueing participants to the time of occurrence of a to-be-remembered speech item would improve working memory performance (for a review see Gazzaley and Nobre, 2012). Critically, we expected that alpha power would be reduced when to-be-remembered items were temporally cued, reflecting the potentially reduced demand for functional inhibition.

We devised an MEG experiment using an auditory delayed-matching-to-sample task on speech in noise: Retaining a syllable in memory for two seconds introduced memory load. A priori, we provided listeners with potentially facilitating visual cues that contained probabilistic information about the duration of the foreperiod preceding the syllable pair (Nobre, 2001; Coull and Nobre, 2008; Kaiser et al., 2009; Jaramillo and Zador, 2011). The experiment addressed three specific questions: First, do temporal expectations reduce cognitive load imposed by retention of a target stimulus presented in noise, as reflected in a relative alpha power decrease? Second, what are the underlying neural sources of alpha power modulations due to temporal cueing? Third, if individuals differ in their ability to behaviorally profit from temporal expectation, is

individual alpha power during memory retention predictive of individuals‘ behavioral performance?

## 5.2 Methods

### 5.2.1 Participants

Twenty healthy right-handed participants took part in this study. Data of two participants were discarded from further analyses because more than 50 % of their trials were rejected due to artifacts. This led to the inclusion of data for eighteen participants (9 females) ranging in age from 21 to 35. All participants had self-reported normal hearing. Participants were fully debriefed about the nature and goals of this study, and received financial compensation of 7€ per hour for their participation. The study was approved of by the local ethics committee (University of Leipzig), and written informed consent was obtained from all participants prior to testing.

### 5.2.2 Experimental task and stimuli

The time course of an example trial is depicted in Figure 5.1A. Each trial began with the simultaneous onset of speech-shaped noise and a fixation cross. The noise lasted throughout the entire trial. A visual cue was presented approximately one second after noise onset (jittered between 750 ms to 1250 ms). Cues were presented for 1500 ms, and indicated the approximate onset time of S1. The onset time of S1 was measured from the offset time of the cue. Participants had to retain S1 in memory during a two-second retention period following S1-offset. Then, a second syllable, S2, was presented, and participants judged whether S2 had the same or different initial consonant as S1. Approximately one second (jittered between 900 ms to 1100 ms) after the presentation of S2, participants were prompted to give a response via button press. Finally, participants indicated their confidence in their “same”/“different” response on a 3-level confidence scale (“not at all confident”: 1, “somewhat confident” : 2, “very confident”: 3). Trials were separated by an inter-trial interval of approximately one second that was free of stimulation or responses. Three types of cues were presented: “early”, “late”, and “neutral”. Early and late cues were specific, meaning that cues provided meaningful information about when S1 would occur following cue offset. S1-onset times for early and late cues were randomly drawn from Gaussian distributions (early: =

850 ms, $\sigma$ = 85 ms; late: = 1300 ms, $\sigma$ = 130 ms). On the other hand, neutral cues were unspecific, and S1-onset times were randomly drawn from a uniform distribution ranging between 700 ms and 1500 ms (see Figure 5.1B).

S1 and S2 stimuli consisted of four different syllables: “da”, “de”, “ga”, and “ge”. For information about the recording and the processing of the sound files see Section 4.2.

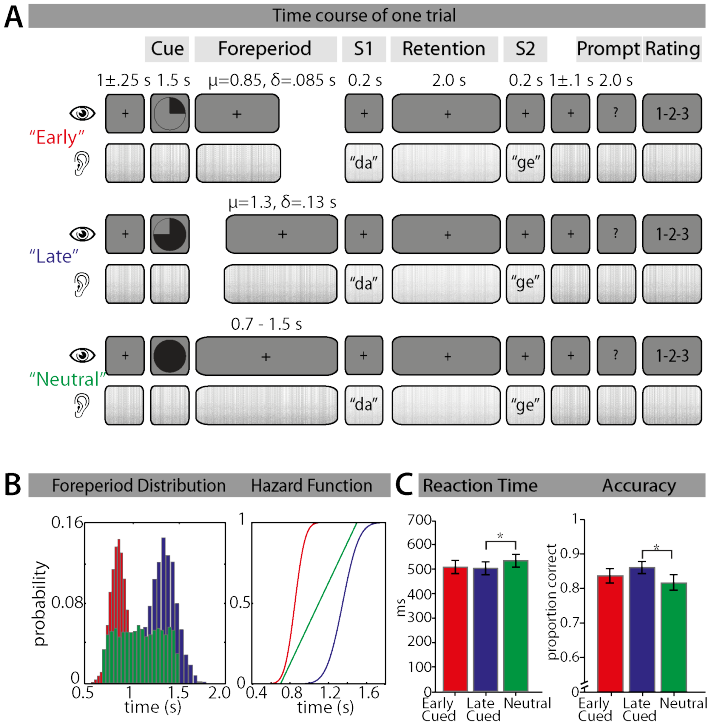


***Figure 5.1.*** **Temporal expectation combined with speech-in-noise memory task and behavioral performance. A.** A schematic timeline of three trials, one for each cueing condition (early-cued, late-cued, neutral). The upper panel of each trial symbolizes visual stimulation, the lower panel the concurrent auditory stimulation. The gray background of the auditory stream symbolizes ongoing speech-shaped noise. Differences in the foreperiod represent the manipulation of temporal expectation. The S1-S2 memory task was the same for all conditions: listeners remembered S1 during a 2-s retention period; then following presentation of S2, they indicated whether the syllables had the same initial consonant and additionally rated their confidence in their response. **B.** Left panel: Histogram of actual foreperiod duration probabilities of all trials: early foreperiod durations are shown in red, late in blue, and neutral in green. Right panel: Probability of S1 occurrence as a function of time (given that it has not already occurred; i.e., hazard function) for each cueing condition. **C.** Mean (±SEM) reaction time and accuracy for each condition (early-cued, late-cued, neutral). Asterisks indicate differences between conditions that are significant at $p < 0.05$.

Speech-shaped noise was generated by filtering white noise to approximate the long-term average spectrum of speech (e.g., Peters et al., 1998). Power per frequency band from a concatenated set of 60 German nouns (female speaker) served as input for the filter, which was subsequently applied to white noise. This resulted in noise with an approximately speech-shaped spectral envelope and an approximately flat amplitude envelope (i.e., a non fluctuating noise masker).

### 5.2.3 Procedure

Prior to the MEG measurement, participants completed three blocks of an adaptive tracking procedure in order to estimate individual signal-to-noise ratios (SNR) yielding 70.7 % correct responses (Levitt, 1971, i.e., two-down-one-up;). Participants performed the same task as they did in the experiment proper, with the exception that no cues to the timing of S1 onset were provided. The intensity of the noise was kept constant at 50-dB sensation level, and the relative intensity of the syllables was adjusted in 1-dB steps. Each block terminated after 12 reversals. Thresholds were taken as the arithmetic average of the final 8 reversals in each block, and additionally averaged across blocks.

Next, brain activity was recorded with MEG during the performance of 360 trials completed in 18 blocks of 20 trials each. Cue type (early-cued, late-cued, neutral) was constant within a block, and participants were informed at the start of each block about the type of temporal cue they would receive on each trial. The order of trials within a block and order of blocks were randomized for each participant. Button assignments were counterbalanced across participants, such that half of the participants indicated that S1 and S2 started with the same consonant using the left button, and half did so with the right button.

The testing took approximately 2.5 hours per subject and was conducted within one session. The overall session including adaptive tracking and preparation of the MEG setup took about 3.5 hours.

### 5.2.4 Data recording and analysis

See section 4.4 for detailed information about MEG recording.

Data analyses were carried out with Matlab (The MathWorks Inc., Massachusetts, USA) and the FieldTrip toolbox (Oostenveld et al., 2011) using only trials to which

correct responses were provided (“correct trials”). Analyses were conducted using only the 204 gradiometer sensors, as they are most sensitive to magnetic fields originating directly underneath the sensor (Hämäläinen et al., 1993). The continuous data were filtered offline with a 0.5-Hz high pass filter, specifically designed to provide a strong suppression of DC signals in the data (>140 dB at DC, 3493 points, Hamming window; e.g., Ruhnau et al., 2012).

Subsequently, trial epochs ranging from –1 to 3 s time-locked to the onset of S1 were extracted. Additionally, 4 s epochs were extracted from –2.25 s to 1.75 s time locked to noise onset providing the baseline window (–1.0 s to –0.25 s) for a remote baseline correction of the time–frequency data. These rather long epochs were extracted to circumvent windowing artifacts in the time–frequency analysis; the intervals analyzed statistically were shorter (see below). Trial and baseline data were low-pass filtered at 150 Hz and subsequently down-sampled to 500 Hz. Epochs were rejected when the signal range within one epoch exceeded 200 pT/m (gradiometer) or 100 V (EOG). Additionally, trials for which variance was deemed high relative to all others (per participant, per condition) based on visual inspection were rejected manually.

### 5.2.5 Time–frequency representation (TFR)

Time–frequency representations (TFRs) were calculated for each trial and 4-s baseline epoch (with 20-ms time resolution) for frequencies ranging between 2 Hz to 30 Hz (logarithmically spaced, in 15 bins). Time-domain data were convolved with a Hann taper, with an adaptive width of four cycles per frequency ($\Delta t = 4/f$). An event-free 750-ms interval ranging between –1 to –0.25 s prior to noise onset (i.e., during the inter-trial interval) was used as baseline period. For each participant, single-trial relative power changes were calculated with respect to mean baseline power (averaged over trials and time; separately for each condition, sensor, and time–frequency bin). Power estimates for each trial were baseline corrected by subtracting and dividing by average baseline power. The average baseline provides a possibility to adjust for block-specific differences. Therefore, we accept that this baseline does not account for between-trial variance. Thus, the condition-specific baseline correction reflects changes in alpha power during stimulation in contrast to no stimulation and might contain between-trial differences.

### 5.2.6 Statistical analysis

Behavioral responses (i.e., proportion correct, PC; and response times, RTs) were analyzed with a one-way repeated-measures ANOVA followed by paired-samples t-tests to resolve differences between individual cueing conditions (early, late, and neutral). Statistical analyses of the time–frequency data comprised a multi-level approach on alpha power data (Obleser et al., 2012; van Dijk et al., 2010a): On the first (single-subject) level, specific contrasts were conducted using single-trial data to test for alpha power differences (8–13 Hz) between cueing conditions. Contrasts of all single conditions (neutral vs. late-cued, neutral vs. early-cued, early-cued vs. late-cued) were performed within the framework of Fieldtrip's independent sample t-tests. The contrast of the cued (early-cued and late-cued combined) and neutral conditions was conducted using the Fieldtrip-implemented independent-samples regression t-test with contrast coefficients *neutral = 2, early-cued = –1, late-cued = –1*. Beta values for all contrasts were obtained for each time–frequency bin at each of the 102 sensor positions. Next, beta-values were averaged across 8–13 Hz to derive an aggregated alpha-frequency estimate for each time point and sensor. Time points from –0.5 s to 2.5 s relative to S1 onset and each sensor were included in the analyses. For the statistical analyses on the second (group) level, beta-values resulting from the single subject first level statistics were tested against zero with cluster based permutation tests (dependent samples t-tests, 1000 iterations; Maris and Oostenveld, 2007, see Section 4.5.1).

We also tested for correlations of alpha power with an in-depth measure of behavioral performance. Confidence ratings served to construct receiver operating characteristic (ROC) curves (Macmillan and Creelman, 2004) for each condition that were used to derive $A_z$, a non-parametric performance measure corresponding to the area under the ROC curve (see Fig. 5.4A). Based on our analyses on alpha power and $A_z$, differences between the late-cued and neutral conditions were the largest (see below). In order to test how the dynamic ranges of $A_z$ and of alpha power are related to each other in individual participants, the difference $A_{zNeutral} - A_{zLate}$ was correlated with the difference $alpha_{Neutral} - alpha_{Late}$. We used the permutation-cluster approach across time points and sensors to identify clusters of significant alpha power–behavior correlation.

### 5.2.7 Source localization

For general information about the source analysis see Section 4.4.3.

The beamformer approach (DICS, dynamic imaging of coherent sources; Gross et al., 2001) was used to project alpha power during the retention of S1 (1.25–2.0 s after S1 onset) to source space. The multitaper FFT was centered at 10.5 Hz (+- 2.5 Hz smoothing with three Slepian tapers; Percival and Walden, 1993) and the complex filter was a common filter based on all conditions and baseline (Gross et al., 2001; Schoffelen et al., 2008). Then each condition was baseline corrected (relative change, comparable to sensor space). The relative power change was morphed onto a common surface (Freesurfer average brain; Fischl et al., 1999).

Analogous to the sensor space, source-projected conditions were contrasted against each other by means of vertex-wise t tests (neutral vs. late-cued, neutral vs. early-cued, early vs. late-cued). Z-value maps on the average brain surface were displayed with an uncorrected vertex-wise threshold of $|z| >= 2.5$ (Sohoglu et al., 2012).

Additionally, for each condition we extracted source-projected alpha power (baseline corrected) from the vertices yielding $|z| >= 2.5$ (resulting from the neutral greater than late-cued contrast) within the right insula cluster, where z-values showed the greatest condition effects (see more on the insula below). Extracted activity was then averaged across vertices for each condition separately and used for visualization. A repeated measures ANOVA was conducted across the averaged activity in order to reveal condition differences in this exact area.

## 5.3 Results

### 5.3.1 Effects of temporal cueing on behavioral performance

The participants‘ task was to retain syllable S1 in memory for two seconds and then to decide, after the offset of S2, whether S1 and S2 had the same syllable-initial consonant.

A one-way repeated-measures ANOVA on proportion correct (Fig. 5.1B) indicated that performance depended on cueing ($F(2, 34) = 4.15, p = 0.024$). Participants responded more accurately in the late-cued condition compared to the neutral condition ($t(17) = 2.53, p = 0.009$). Participants benefited less robustly from early cues, as this condition did not differ significantly from the late-cued ($t(17) = -1.49, p = 0.155$)

or the neutral condition ($t(17) = -1.44, p = 0.169$). A repeated-measures ANOVA on response times (measured relative to a response prompt that occurred one second after S2 offset) revealed a main effect of condition ($F(2, 34) = 7.30, p = 0.035$). Post-hoc paired-samples t-tests revealed that responses to late-cued trials were significantly faster than to neutral trials (neutral vs. late: $t(17) = 2.58, p = 0.019$). Similar to the accuracy results, there were no significant differences between RTs for early-cued and late-cued conditions ($t(17) = 0.50, p = 0.622$) or the early and neutral conditions ($t(17) = 1.95, p = 0.0678$; Fig. 5.1B).

### 5.3.2 Effects of temporal cueing on alpha power changes

As predicted, alpha power increased across the entire trial in all three conditions, relative to baseline (see Figure 5.2A). We compared the post-baseline interval (–0.5 to 2.5 s after S1 onset) and the baseline interval (–1.0 to –0.25 s,prior to noise onset), both averaged across time–sensor bins in the alpha range, with t-tests. Each condition in the post-baseline interval presented a significant increased compared to the baseline interval in the alpha range (all $p < 0.05$).

Statistical contrasts between conditions revealed a strong difference in alpha power between neutral and late-cued trials. Two significant clusters (1. $p = 0.010$, –0.42 to 0.98 s; 2. $p = 0.018$, 1.4 to 2.5 s) during S1 and S2 encoding, as well as during retention of S1 indicated that alpha power was reduced in late-cued trials relative to neutral trials (see Fig. 5.2B, upper panel).

Alpha power in the early-cued condition did not differ significantly from the neutral condition. Moreover, no significant clusters obtained for the contrast between the cued and neutral conditions. However, in an early time window around syllable S1, early-cued trials exhibited larger alpha power than late-cued trials in a right-frontal positive cluster ($p = 0.033$; –0.42 to 0.32 s; Fig. 5.2B, lower panel).

In sum, late-cued trials showed reduced alpha power compared to neutral and early cued trials. The late cue was thus most effective in providing temporal expectations that yielded the hypothesized alpha power decrease.

### 5.3.3 Source localization of alpha power changes

We tested whether the alpha-power source projections (see *Methods*) presented less activity in the late-cued condition than in the neutral condition (Fig. 5.3), to confirm

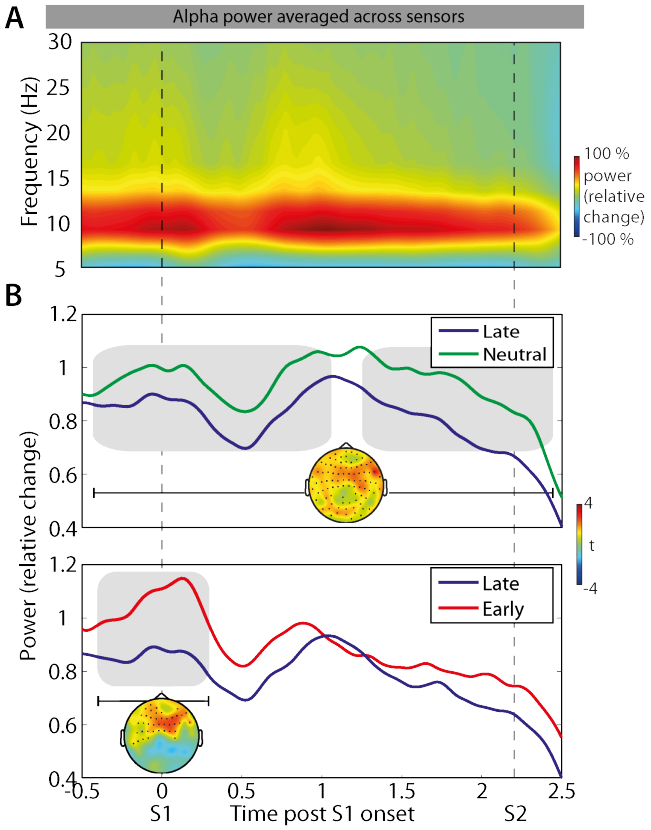


***Figure 5.2.*** **Effects of temporal cues on alpha power throughout syllable encoding and retention.** **A.** Grand average of lower frequency power (percent change relative to baseline) from 5 to 30 Hz; alpha power is averaged over participants, sensors, and conditions. The time window shown here ranges from –5 to 2.5 s, with S1 onset at t = 0 s and S2 onset at t = 2.2 s. **B.** Relative change alpha power of neutral and late-cued conditions (upper panel) and of early-cued and late-cued conditions (lower panel) drawn from the significant clusters indicating condition differences (both –0.5–2.5 s, relative to S1-onset). Gray areas indicate temporal dimension of condition differences. Topographic plots illustrate the location of the statistical effects, printed sensors are part of the significant clusters.

results from sensor space (Medendorp et al., 2007; Haegens et al., 2010; Obleser et al., 2012). Source space results corroborated the findings in sensor space: Late-cued trials led to a reduction of alpha power compared to early-cued and neutral trials. Locations of the alpha power reduction in the late-cued condition were strongly overlapping. In general, the alpha power differences ($z > 2.5$) were found in the right hemisphere emerging from the right anterior insular cortex [peak activity at MNI: 28; 23; –6]. A repeated measures ANOVA ($F(2, 34) = 7.70, p = 0.006$) on the condition-wise averaged

alpha power projection in the insula showed that late-cued trials present significantly less activity than neutral trials ($t(17) = -4.21, p = 0.002$), whereas this reduction in late-cued trials compared to early-cued trials is only significant on trend level ( $t(17) = -2.09, p = 0.078$). Activity in early-cued and neutral trials does not differ at all ($t(17) = -1.57, p = 0.135$; Fig, 4.4.3A). Figure 4.4.3A depicts the source-projected alpha power in the insula for each condition. Condition-specific power values show the same pattern as our sensor-space analysis, thereby confirming the right insula as the main source of our alpha effects.

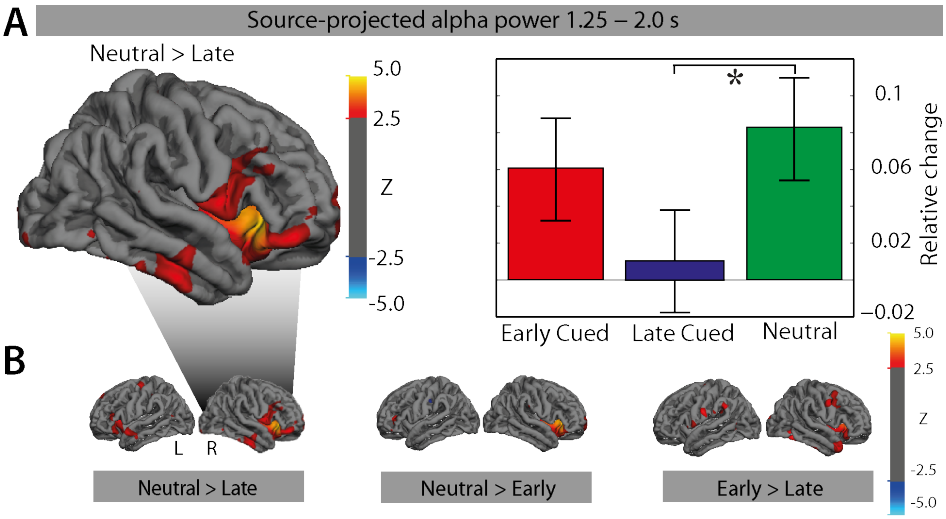


***Figure 5.3.*** **Alpha power effects (8–13 Hz; z-values) in source space during syllable retention (1.25–2.0 s after S1 onset).A.** Positive and negative z-values of the neutral and late-cued condition contrast are plotted on a template. Bar graphs represent condition-wise activity drawn and averaged from the vertices presenting z >= 2.5 around insula (peak activity, MNI: 28; 23; –6). Error bars represent within-subject errors. **B.** Z-values (z <= –2.5 & z >= 2.5) of all condition contrasts at left and right hemispheres. Z-values are greatest at the contrast of late-cued and neutral conditions.

### 5.3.4 Alpha power reduction during memory retention predicts behavioral performance

In a final analysis, we aimed to relate the observed modulation of behavioral performance by temporal cueing to the alpha power differences between cue conditions. Specifically, we contrasted the two conditions for which we observed the largest difference in both behavior and alpha power (i.e., the neutral and late-cued conditions).

We asked whether the degree to which alpha power was decreased by temporal cueing (indexed by $alpha_{Neutral} - alpha_{Late}$) would predict the degree to which participants were able to profit from the temporal cue ($A_{zNeutral} - A_{zLate}$).

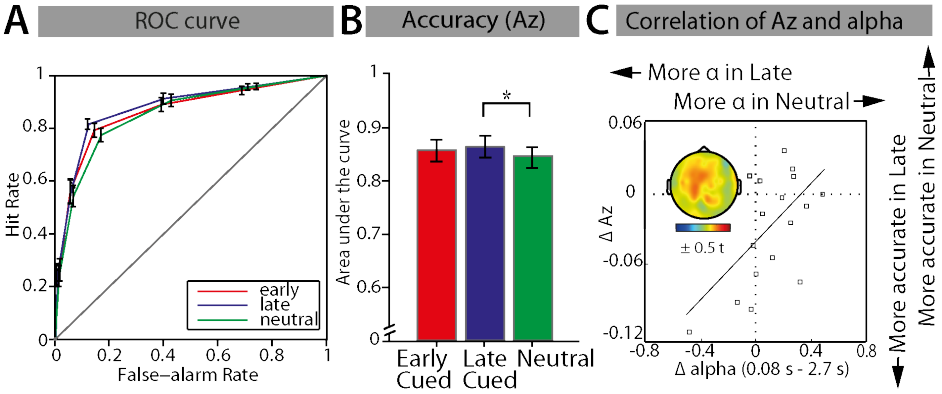


***Figure 5.4.*** **Correlation of behavioral dynamics with brain dynamics. A. Receiver-operating characteristics (ROC) curves.** False-alarm rates versus hit rates for each condition. The greater the area under the curve, the better the perceptual sensitivity. **B. Area under the curve ($A_z$).** Following from the ROC curve, this denotes a corrected measure of accuracy for each condition. The asterisk indicates a significant difference with p $< 0.05$. **C. Correlation of $A_z$ changes with alpha power changes.** $A_{zNeutral} - A_{zLate}$ is plotted against $alpha_{Neutral} - alpha_{Late}$, averaged over 0.08 to 2.7 s after S1 onset and the corresponding topographical effect that belonged to the significant-correlation cluster (t-values marked red in topography). Dotted lines indicate zero, meaning no difference between neutral and late. Note that listeners who profited behaviorally least from specific late cues (y-axis) showed relatively most alpha power (x-axis; upper right corner of the scatter plot).

This analysis focused on the performance measure $A_z$, a nonparametric measure derived from the receiver operating characteristics (ROC) curve (see Methods and Fig. 5.4A) which can be interpreted similarly to proportion correct (Fig. 5.4B). In brief, recall that confidence ratings were collected for "same"/"different" responses on each trial, and these were used to construct ROC curves. Then, ROC curves were tested for asymmetry around the minor diagonal (Henry and McAuley, 2013). Linear fits to z-transformed ROCs (zROCs) yielded a slope estimate for each participant. Separately for each condition, zROC slopes were then tested against unity (slope = 1) using a single-sample t-test. Significant deviations from unit slope (as was the case here; all $.07 > p > .01$) indicate asymmetric ROC curves and non independence of perceptual sensitivity and response bias in parametric performance measures (e.g., PC, d'). Thus,

nonparametric performance measures derived from the ROCs themselves, like $A_z$, are considered more accurate performance measures.

Next, we calculated an "alpha-power modulation index" that reflects the difference for each participant between alpha power in the neutral and late-cued conditions (i.e., $\text{alpha}_{\text{Neutral}}$ – $\text{alpha}_{\text{Late}}$), and correlated these values with a "behavioral-performance modulation index" calculated for the same two conditions ( $\text{A}_{\text{zNeutral}}$ – $\text{A}_{\text{zLate}}$). We then correlated these values for individual time–sensor bins, again using a cluster-based approach. This revealed a broad positive fronto-central cluster (0.08–2.7 s, $p = 0.007$) ranging across the entire retention phase including encoding of S1 and S2.

The correlation of the alpha power differences extracted from this cluster and the behavioral differences ($r = 0.51$) are shown in Figure 5.4C.

## 5.4 Discussion

The present study investigated whether temporal cues improved behavioral performance and decreased alpha power in a delayed-matching-to-sample working-memory task, where to-be-remembered syllables were embedded in masking noise. We observed that knowing when to listen facilitated retention of a syllable in ongoing noise, as indexed by higher accuracy and faster response times in the late cued compared to the neutral condition. This finding is in line with previous research indicating that temporal cues and long foreperiods lead to better stimulus encoding (Correa et al., 2005; Rohenkohl et al., 2012) and behavioral performance (Coull and Nobre, 1998). Moreover, we observed that, along with the overall increase of alpha power in all conditions, temporal cues (in particular when coupled with a relatively long foreperiod) caused a reduction of the magnitude of this alpha power increase, suggesting that knowing when to listen also decreased the necessity to functionally inhibit task-irrelevant information. In particular, largest differences in alpha power between temporal cueing conditions were observed in the right insula. Overall, the reduction of alpha power as well as the increase of behavioral performance imply that temporal expectations (i.e., late-cued condition) are able to reduce the cognitive load elicited by stimuli presented in noise (see Zanto and Gazzaley, 2009).

In the following sections we will put the current findings in context, in particular emphasizing how the facilitatory effects of temporal cues might be realized neurally in

terms of alpha power modulations. The discussion will be structured in three parts: (1) How do temporal expectations affect alpha power and cognitive load?; (2) What are the underlying neural sources of alpha-power modulations?; (3) How do alpha-power modulations predict modulations of behavioral performance?.

### 5.4.1 How does temporal expectation affect alpha power and cognitive load?

Temporal expectations in the current study led to a decrease of alpha power during syllable retention, relative to when the onset of the syllable pair could not be expected even though stimulation (syllables, noise, and SNR) were identical across conditions. In particular, we observed the largest differences in terms of both behavior and alpha-power effects when we contrasted the late-cued with the neutral conditions. That is, although early and late cues both provided information about the onset time of the syllable, the late-cued condition was more effective in reducing alpha power than the early-cued condition (see also the behavioral results in Fig 5.1B). This effect of foreperiod duration corresponds to previous behavioral results showing that longer foreperiod durations lead to increased encoding precision (Correa et al., 2005) and better stimulus detection (Niemi and Näätänen, 1981).

We interpret reduced alpha power for the late-cued relative to the neutral condition to mean that temporal expectations reduced the need for functional inhibition. The reason is that, in all temporal cueing conditions (early, late, neutral), alpha power was generally increased relative to baseline. Thus, we suggest that alpha power played an inhibiting role in the speech-in-noise working-memory task regardless of temporal cueing condition. For the late-cued condition, alpha power increased less relative to baseline than in the neutral condition, suggesting that alpha power still played an inhibiting role, albeit a less strong one. In particular, we suggest that more specific temporal expectations may have allowed for an a priori suppression of irrelevant, potentially interfering information. Concomitantly, less functional inhibition was needed, which was reflected in reduced alpha power.

Along these lines, previous studies have shown that knowing when to listen enhances stimulus encoding (e.g., Posner, 1980; Correa et al., 2005; Rohenkohl et al., 2012; Vangkilde et al., 2012; Cravo et al., 2013). We suggest that improved encoding could have been allowed for by the stronger suppression of irrelevant information (e.g., Hillyard et al., 1998) in the late-cued relative to the neutral condition. Moreover, less degraded

stimuli elicit less cognitive load and less alpha power during maintenance in working memory (Obleser et al., 2012), suggesting that the beneficial effects of temporal expectations cascaded into the retention interval in the current study, thereby triggering the observed alpha effects.

It is worth pointing out that alpha power rather serves as an indirect measure not reflecting active maintenance but functional inhibition of irrelevant information (termed working memory "protection", Roux and Uhlhaas, 2013), whereas stimulus maintenance in memory per se has previously been associated with gamma oscillations ($> 30$ Hz; e.g., Howard et al., 2003; Jensen et al., 2007; Lisman and Jensen, 2013; Roux et al., 2013). Essentially, alpha and gamma are inversely related: brain areas presenting high alpha power are inhibited and present low gamma power because active processing is suppressed, and vice-versa (Jokisch and Jensen, 2007; for a review see Klimesch et al., 2007; Jensen and Mazaheri, 2010).

So far we have only discussed less alpha power as reflecting less functional inhibition. However, an alternative (although not mutually exclusive) explanation is that reduced alpha power associated with temporal expectations has been interpreted to reflect increased cortical excitability (e.g., Jensen et al., 2012; Lange, 2013). The association between reduced alpha and increased excitability comes specifically from studies involving focusing attention either spatially (Weisz et al., 2014; Whitmarsh et al., 2014) or temporally (Rohenkohl et al., 2012), where focused attention also results in improved task performance. With our design, it is not possible to completely disentangle whether reduced alpha power reflects reduced functional inhibition or enhanced cortical excitability. However our overall alpha effects reflect synchronization (i.e., a power increase compared to baseline; Klimesch et al., 2012) rather than desynchronization (i.e., power decrease relative to baseline). Moreover, our primary effect localized not to sensory/domain-specific, but rather to domain-general cortex (i.e., the insula, see below). Thus, we suggest that the functional inhibition framework and a relative decrease in the need for such functional inhibition offer the more parsimonious explanation for our observed alpha effects. More generally, the current results fit within the context of an extensive literature relating alpha oscillations to attention and working memory. Studies manipulating selective attention (for a review see Foxe and Snyder, 2011), along with studies using comparable delayed-matching-to-sample tasks in the somatosensory (e.g. Haegens et al., 2010, Haegens et al., 2011a) and in the auditory domain (Kaiser

et al., 2007a), imply that increased alpha power effectively inhibits interference from other processes and/or brain sites.

### 5.4.2 What are the underlying neural sources of alpha power modulations?

Source analyses of alpha power revealed that effects between conditions were confined mainly to the right insular cortex (see Fig. 5.3 3). We suggest that lateralization to the right-hemisphere generally reflects inhibition of the hemisphere that is arguably task-irrelevant when it comes to retaining verbal material (i.e., syllables) in working memory (e.g., Smith and Jonides, 1998). Previous research supports this proposition. Specifically, right-hemispheric alpha power effects were observed in another working memory study making use of syllable material (Leiberg et al. 2006; see also results by Obleser et al. 2012). Although the authors interpreted their alpha effects as reflecting executive processes operating on verbal material, (van Dijk et al. 2010) re-interpreted the findings of Leiberg and colleagues as meaning that alpha power was inhibiting the right hemisphere, which (similar to the current study) was task-irrelevant during syllable retention. Conversely, van Dijk et al. (2010) made use of a non verbal, pitch memory task, and found increased alpha power in the left hemisphere. The authors argued that enhanced alpha power reflected a functional inhibition of the hemisphere that was again task-irrelevant, this time during retention of pitch information. Finally, during a working memory task in the somatosensory domain, Haegens et al. (2010) showed that alpha power increased at sensors ipsilateral to the side of stimulation (i.e., the task-irrelevant hemisphere). With respect to localization to the insula more specifically (see Fig. 5.3) several previous fMRI studies have shown that the processing of degraded speech (not unlike the present stimulus setup) is accompanied by increased insular activity reflecting the difficulty of comprehension (Vaden et al., 2013; Erb et al., 2013). Converging evdience for increased insula activity in a difficult listening situation comes from an fMRI study of Sadaghiani et al. (2009), who found that increased pre-stimulus BOLD activity in the insula was associated with enhanced detection of near-threshold auditory stimuli in a sustained attention task. According to Sadaghiani et al., activity in the insula is a marker of fluctuations of sustained attention. Dosenbach et al. (2007) and Eckert et al. (2009) more genrally see that the anterior insula not only enhances sustained attention but, is part of a network which is responsible for sustained task-related cognitive control.

We would like to suggest that the insula plays an active role in functional inhibition, in line with the localization of our alpha effects to this region. A recent fMRI study from our group found upregulation of insula activity associated not only with selective attention to task-relevant information, but also with selective ignoring of task-irrelevant Henry et al. (2013). Work using combined EEG/fMRI has typically shown a negative relation between BOLD signal and alpha power in much of cortex (Laufs et al., 2006; Scheeringa et al., 2011). This correlation has been interpreted within the context of alpha as a marker of inhibition (e.g., Jensen and Mazaheri, 2010). However, a combined EEG/fMRI resting state study (Sadaghiani et al., 2010) indicated that the BOLD signal and alpha power, specifically in the right anterior insular cortex, were positively correlated. On these grounds, we propose that the right insula may act as a generator for alpha power and the neural source for functional inhibition.

### 5.4.3 How do alpha-power modulations predict modulations of behavioral performance?

Lastly, a correlation analysis revealed that a listener's behavioral-performance modulation was predictable from her/his own alpha-power modulation between temporal expectation conditions. Performance was in general better for late-cued trials than for neutral trials, but the correlation of the behavioral differences and alpha power differences between neutral and late-cued conditions (Fig. 5.4) conveys one central conjecture: Participants who had relatively large alpha power in neutral trials performed in these trials as well as, or even better than, in late-cue trials. Thus, both (exogenous) temporal cues and (endogenous) alpha power are means that can lead to the same end, that is, a performance benefit: Either listeners form and utilize specific temporal expectations to reduce cognitive load up front (the arguably more adaptive strategy), or, alternatively, listeners do not utilize the cues as much but succeed in good performance in neutral trials nevertheless. This latter strategy then comes at the "cost' ' of increased alpha power to boost working memory performance. We propose to label such alpha power increases a "compensatory" process, as these increases might come at a neural or metabolic cost to the system (see also the previous section on insular activity), but they can be beneficial to performance. This view is supported by a study from Haegens et al. (2010) showing that alpha power increases were strongest during successful working memory performance.

We conclude that alpha power is instrumental for performance in cognitively demanding tasks. It can partly make up for (or trade off with) other task-beneficial factors, such as the temporal expectation cues provided here.

### 5.4.4 Conclusion

Alpha power changes are a sensitive neural marker of cognitive load, particularly so when the task requires memorizing and matching auditory syllables in task-detrimental noise. Cues that allow listeners to form a specific temporal expectation about when target syllables will occur can counteract and reduce alpha power. Furthermore, the facilitatory or task-beneficial effects of cueing are not limited to sensory encoding but extend to later stages of memory retention. Here, the magnitude of alpha oscillations emerging from right insular cortex scales directly with listeners‘ performance benefits. Thus, alpha power appears as a costly but effective neural mechanism to boost performance in difficult listening situations.

# 6 Experiment IIa: Temporal expectations exert differential effects on alpha power in clear speech and in noise

## 6.1 Introduction

In the previous Chapter (*Experiment I*) we have shown that temporal expectations for syllables in noise reduce memory load throughout syllable retention reflected in a decrease in alpha power and an increase in behavioral performance. The degradation of the speech signal by adding a noise masker has been shown to increase memory load (Pichora-Fuller and Singh, 2006, see previous Chapter, Section 5.1) and alpha power has appeared to be a suitable marker to reflect this kind of modulations of memory load. Moreover, with the previous experiment we were able to demonstrate that a gain in stimulus encoding precision due to temporal expectations reduced subsequent memory load during stimulus retention. Alpha power has been argued to inhibit irrelevant information and brain areas (Jensen et al., 2002; Klimesch et al., 2007) to gate information processing in cognitive demanding settings.

However, it remains to be shown in how far alpha power is modulated when memory load is low and whether temporal expectations then still have a similar effect on alpha power. Therefore, the exact same paradigm of the previous study was tested without the noise on ten participants that already took part in *Experiment I*. Here we hypothesized that the effect of temporal cues on alpha power is reduced for clear speech compared to speech-in-noise because the enhancement of encoding precision will not be played out to full extent when stimuli are presented clearly. Specifically, the aim of the

present study was to show that the alpha power decrease with temporal expectations, as shown in the previous study, is weaker or even gone when syllables are presented clearly. For that reason we contrasted the temporal-expectations effect of *Experiment I* with the temporal-expectations effect of this clear-speech experiment.

## 6.2 Methods

For detailed information on participants, experimental design, stimuli, and data pre-processing see Chapter 7 (*Experiment IIb*). Processing steps that deviate from those in the following chapter will be described in the following section. The processing steps described here only refer to the data of the clear speech experiment. Data of the noise experiment that was included in the statistical analysis (see below) was analyzed as described in *Experiment I*. Importantly, the ten participants of the present study also took part in the previous study (*Experiment IIb*) which allowed for a statistical comparison of these two data-sets.

In brief, temporal expectations for a syllable (S1), which had to be retained in memory for two seconds, was manipulated by means of three conditions. The "late" condition provided information about the onset of S1 with a longer foreperiod. The "early" condition also provided information about S1-onset but with a shorter foreperiod. The "neutral" condition was not informative about the onset-time of S1.

### 6.2.1 Data analysis

After pre-processing the data with the Neuromag software (see Section 4.4), data analyses were carried out with Matlab (The MathWorks Inc., Massachusetts, USA) and the FieldTrip toolbox (Oostenveld et al., 2011). First, the continuous data were filtered offline with a 0.5-Hz high pass filter, specifically designed to provide a strong suppression of DC signals in the data (>140 dB at DC, 3493 points, Hamming window; e.g., Ruhnau et al., 2012). Further analyses were conducted using only the 204 gradiometer sensors, as they are most sensitive to magnetic fields originating directly underneath the sensor (Hämäläinen et al., 1993).

Trial epochs ranging from –2.5 to 9.5 s time-locked to the onset of the cue were extracted, and down-sampled to 200 Hz. These rather long epochs were extracted to circumvent windowing artifacts in the time–frequency analysis; the intervals analyzed

statistically were shorter (see below). Epochs were low-pass filtered at 150 Hz. Then, epochs with strong artifacts were rejected when the signal range at any sensor exceeded 800 pT/m (gradiometer) and independent component analysis (ICA) was applied in order to exclude artifacts mainly due to eye blinks and heart beat. Following ICA, remaining epochs containing artifacts exceeding a threshold of 200 pT/m were rejected.

Subsequent time–frequency representations (TFRs) were calculated for the preprocessed 11-s epochs for each trial (with 20-ms time resolution) and for frequencies ranging between 0.5 Hz to 20 Hz (logarithmically spaced, in 20 bins). Time-domain data were convolved with a Hann taper, with an adaptive width of two to four cycles per frequency; i.e., the number of cycles increased logarithmically with frequency in twenty steps. The output of the analysis was complex Fourier data that was transformed into power by computing the squared magnitude of the complex-valued TFR estimates. Then, data were baseline corrected with a 0.750 s interval in the inter-trial interval ranging from –2 to –1.25 s time-locked to cue onset. After baseline-correction, trial timing was scaled to be t = 0 at S1-onset.

### 6.2.2 Statistical analyses

Percentage correct (PC) was analyzed by means of a repeated measures ANOVA with the factors experiment (clear vs. noise) and temporal expectations (early, late, neutral). Response times were not analyzed because responses were prompted and hence provide no valid information about the processing demands.

Multi-level cluster tests (see Section 4.5) were conducted on epochs ranging from –0.5 to 2.5 s time-locked to S1-onset. On the first level statistics were calculated across the whole frequency range. Here, the neutral condition was contrasted with the late condition separately for the ten participants of the clear-speech experiment and for the exact same ten participants of the noise experiment by means of an independent-sample regression t-test.

On the second level, beta-values from the first level were contrasted against zero, again separately for each experiment by means of independent t-tests and the cluster approach to correct for multiple comparisons. We wanted to show first, whether the neutral–late effect from the full-sample experiment in noise (previous chapter) was replicated and second, whether there was an effect of temporal expectations in the clear speech experiment. Next, the beta-values from the clear-speech experiment were

contrasted with the beta-values from the noise experiment in order to test, whether the temporal-expectations effect differed across experiments.

Due to our strong hypothesis derived from the findings of the previous experiment, all second-level t-test were one-sided in favor of the neutral condition presenting more alpha power than late as well as the effect in the noise-experiment being stronger than in the clear-speech experiment. The tests reached significance when $p < 0.05$.

## 6.3 Results

The ANOVA on percentage correct (PC) with the factors experiment (clear vs. noise) and temporal expectations (early, late, neutral) revealed a main effect of experiment ($F(1, 9) = 32.54, p < 0.0001$; clear speech: $mean = 0.998$, $sd = 0.002$, speech in noise: $mean = 0.826$, $sd = 0.013$), whereas there was neither an effect of temporal expectations ($F(2, 18) = 0.91, p = 0.369$, Greenhouse-Geisser corrected), nor an interaction of both factors ($F(2, 18) = 1.38, p = 0.271$, Greenhouse-Geisser corrected).

The results on alpha power are depicted in Figure 6.1. The upper panel illustrates the time course of alpha power for the ten participants in the noise experiment (left panel) and the clear-speech experiment (right panel) for all three manipulations of temporal expectations. Both line-graphs show that, on average, alpha power was increased compared to baseline, throughout the retention phase. For speech-in-noise, the neutral condition showed increased alpha power compared to late and early, whereas there is no such difference in clear speech.

Statistical analyses on the contrast of speech-in-noise revealed a right-frontal cluster (–0.5 to 0.5 s, $p = 0.048$) and a central cluster (2.0 to 2.5 s, $p = 0.048$; see Fig. 6.1, lower panel, first row) indicating that alpha power was significantly decreased in the late condition compared to the neutral condition. As expected, the clear-speech experiment did not present this effect ($p = 0.58$; see Fig. 6.1, lower panel, second row). Consequently, contrasting the noise effect with the clear-speech effect revealed a significant right-frontal cluster (0.0 –1.5 s, $p = 0.041$) and another centrally distributed cluster on trend-level (2.0 to 2.5 s, $p = 0.091$; see Fig. 6.1, lower panel, third row) showing that the impact of temporal expectations was significantly greater when syllables were presented in noise. The bar-graphs in Figure 6.1 show the beta-values of

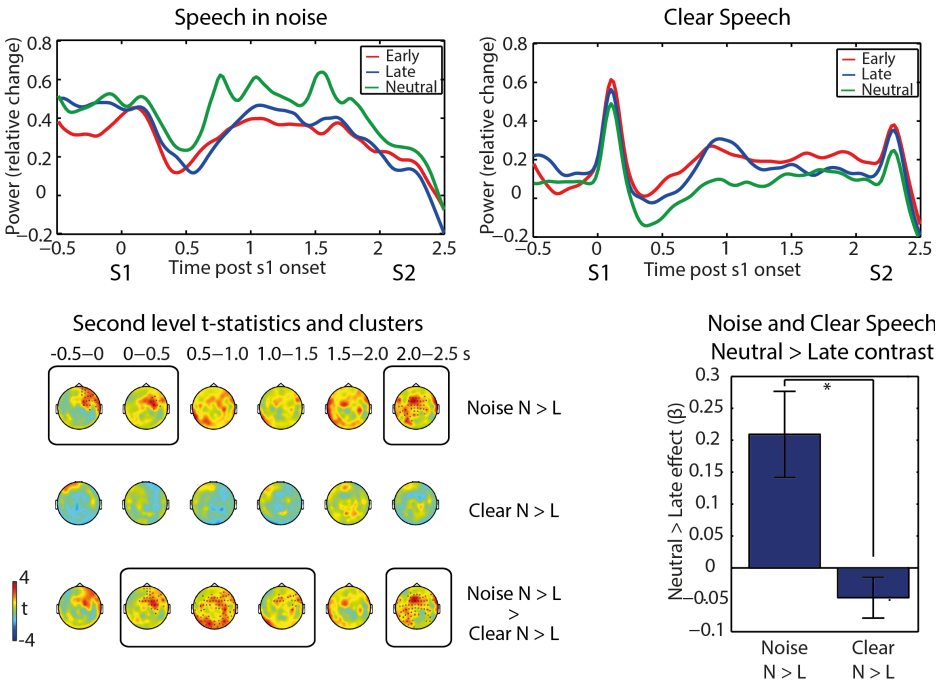


***Figure 6.1.*** **Interaction effect of temporal expectations on alpha power in noise and in clear.** Upper panels present alpha power (8–13 Hz) relative change for each cueing condition for speech-in-noise and clear speech, time-locked to S1-onset. Lower panels present statistical contrast in alpha power between the neutral and the late cueing condition. Left panel first row depicts the topography of alpha power differences for speech-in-noise. Second row illustrates the same effect for clear speech. The third row illustrates the differences in neutral–late effects between speech-in-noise and clear speech. Depicted channels indicate clusters presenting the effects. The bar graph presents the neutral–late effect in noise and clear speech averaged across the respective clusters. Error-bars indicate standard error of the mean.

the noise effect and the clear-speech effect averaged across the clusters of the contrast of the two experiments.

## 6.4 Discussion

First of all, we were able to show that only with ten participants alpha power was decreased when syllables presented in noise were temporally expected. This effect emerged predominantly from right-frontal sensors, analogous to the full sample effect in *Experiment I*. This topography has previously been identified to origin from the right

insula, part of the cingulo-opercular attention network. Thus, a decrease in alpha power emerging from this attention network has been discussed before as reflecting a decreased need for cognitive control-like mechanisms such as enhanced stimulus maintenance (see Chapter 5 and Chapter: 8).

Even though, alpha power was slightly increased in the clear-speech experiment, no effect between neutral and late conditions were found. Hence, temporal expectations did not affect alpha power during stimulus retention. Moreover, we could show that the effect of temporal expectations on alpha power was significantly stronger in noise than in clear speech. The topography of this contrast is similar to and presumably driven by the temporal-expectations effect in the noise experiment.

The null-effect in the clear speech experiment was expected in so far that temporal expectations affect stimulus processing more effectively or stronger when stimuli are presented near-threshold (e.g., Lange and Schnuerch, 2014). Since temporal expectations have been shown to enhance encoding precision and we assumed that to be the mediating effect which led to a reduction in memory load in the previous experiment, it appears to be trivial that the encoding of a clearly presented syllable will not be necessarily enhanced by temporal expectations. Moreover, the behavioral performance was at ceiling indicating that in all conditions memory load was very low (see Zanto and Gazzaley, 2009). Hence, if temporal expectations have had an enhancing effect on stimulus encoding reflected by a different measure than alpha power, it is just likely that enhanced stimulus encoding did not not lead to a subsequent reduction of memory load.

We can only speculate whether participants' have actually payed attention to the temporal cues or if the rather unnecessary cue-information was just too costly to process. Therefore, we assume that the data indicate that the cognitive system adapts to the demands of listening situations reflecting an optimized use of available resources. See the following chapter for a more in-depth analysis of these data on the effects of temporal expectations on supra-threshold (clear speech) stimuli.

# 7 Experiment IIb: Slow-delta phase concentration marks improved temporal expectations based on the passage of time[1]

## 7.1 Introduction

Temporal orienting guides the focus of attention to a point in time when a target stimulus is expected to occur (i.e., "temporal expectations"; Coull and Nobre, 1998). The ability to direct attention in time is testimony to the temporal flexibility of attentional functions in the human brain (Nobre, 2001) and is gaining scientific interest from both a psychological and a neuroscientific viewpoint.

A distinction can be made between different sources of temporal expectations. First, the presentation of a symbolic temporal cue may allow the prediction of the onset-time of an expected event (referred to by Nobre and colleagues as "controlled" temporal expectation; Coull and Nobre, 1998). Second, temporal expectations can arise from rhythmic structure such that the onset times of each stimulus in a rhythmic sequence become highly predictable (Large and Jones, 1999; Barnes and Jones, 2000; Jones et al., 2002). Third, for a situation in which an event is certain to occur, but the exact time of occurrence is not known, temporal expectation follows a "hazard rate function", meaning that expectation for the event's onset increases with passage of time (referred to as "automatic" temporal expectations by Nobre et al., 2007; Janssen and Shadlen, 2005).

[1]This chapter has been adapted from the article submitted to *Psychophysiology* by Wilsch, Henry, Herrmann, Maess, and Obleser (in revision).

All three types of temporal expectations have been shown to enhance perceptual processing of the expected stimulus (Correa and Nobre, 2008), which is reflected by decreasing response times (Correa et al., 2006; Doherty et al., 2005; Nobre, 2001; Rohenkohl et al., 2012; Stefanics et al., 2010; Sanabria and Correa, 2013) and increasing encoding precision (Rohenkohl et al., 2012; Cravo et al., 2013).

Slow neural oscillations constitute a parsimonious neural mechanism for facilitatory effects of temporal expectations (Henry and Herrmann, 2014). By this account, the brain capitalizes on temporal regularities to be in its optimal (i.e., high-excitability) state when the relevant stimulus occurs (Schroeder and Lakatos, 2009). Accordingly, expectations generated by symbolic cues about time-of-occurrence have been shown to reorganize slow neural oscillatory phase (Stefanics et al., 2010). For the most part, however, the relationship between the phase of slow neural oscillations and temporal expectations has been studied using rhythmically presented stimuli. In this case, neural oscillations are entrained by temporal regularities leading to increased neural phase concentration across trials in the frequency range corresponding to the stimulation rate (2.5 Hz: Cravo et al., 2013; 1.5 Hz: Lakatos et al., 2008, 2013; 3.95 Hz: Herrmann et al., 2013; 3 Hz: Henry and Obleser, 2012; 0.67 Hz: Lakatos et al., 2013). However, to date it is unknown whether instantaneous temporal expectations resulting from passage of time (i.e., as a function of foreperiod duration) are related to the organization of delta phase in a similar manner. If so, we expect delta phase coherence to increase with increasing temporal expectations coupled to the passage of time.

So far, temporal expectations have most successfully been studied with near-threshold stimuli (Rohenkohl et al., 2012; Cravo et al., 2013; Lawrance et al., 2014) where expectation effects are behaviorally and neurally strongest (e.g., Lange and Schnuerch, 2014). In the present study, we were interested in how temporal expectations play out in a more ecologically valid setting with supra-threshold spoken syllables. Extending a previous experiment on near-threshold stimuli (Wilsch et al., 2014), we manipulated the temporal structure of trials and the expectations coupled to the trial structure: Explicit temporal cues allowed for the formation of temporal expectations, but we hypothesized that these would be less relevant for supra-threshold stimuli. More importantly, however, stimulus-onset times were variable within a 0.6-s ($\sim$ 1.7 Hz) to 1.8-s ($\sim$ 0.6-Hz) range and longer foreperiod durations were expected to prompt stronger temporal expectations. Our results demonstrate that slow-delta phase coherence is a sensitive

marker of the degree of temporal expectations for the occurrence of supra-threshold stimuli.

## 7.2 Methods

### 7.2.1 Participants

Ten healthy right-handed participants (ranging in age from 24 to 36; five females) took part in this study. All participants had self-reported normal hearing. Participants were fully debriefed about the nature and goals of this study, and received financial compensation of 7€ per hour for their participation. The study was approved of by the local ethics committee (University of Leipzig), and written informed consent was obtained from all participants prior to testing.

### 7.2.2 Experimental task and stimuli

Two spoken syllables were presented per trial, and participants had to indicate whether the syllables shared the same initial consonant by responding “same” or “different”. The time course of an example trial is depicted in Figure 1A. Each trial began with the onset of a fixation cross, followed by a visual cue (fixation–cue interval jittered between 750 ms to 1250 ms). Cues were presented for 1500 ms, and indicated the approximate onset time of the first syllable, S1. Note that the cue presentation time was comparably long but fixed. Thus, the foreperiod leading up to the first target S1 was measured from the offset time of the cue. Participants had to retain S1 in memory during a two-second retention period before the presentation of the second syllable, S2.

Critically, the foreperiod duration varied from trial to trial between 0.6 to 1.8 s. The variable foreperiod duration induced temporal expectations by increasing the probability of S1-onset occurrence with the passage of time (see 7.1B). Furthermore, foreperiod durations were split into three groups according to the preceding cue: “early”, “late”, and “neutral”. That is, S1-onset times for early and late cues were randomly drawn from Gaussian distributions (early: $= 850$ ms, $\sigma = 85$ ms; late: $= 1300$ ms, $\sigma = 130$ ms). S1-onset times after neutral cues were randomly drawn from a uniform distribution ranging between 700 ms and 1500 ms. S1 and S2 stimuli consisted of four different syllables: “da”, “de”, “ga”, and “ge” spoken by a female voice. For more details on the experimental task and stimuli see Section 4.2.

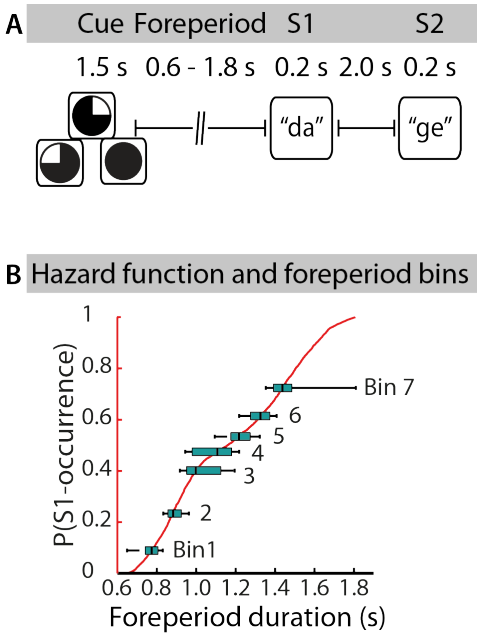


***Figure 7.1.*** **Experimental manipulation and characteristics of the foreperiod. A. Outline of a trial.** Each trial started with the presentation of one of three visual cues. The foreperiod between cue-offset and S1-onset varied between 0.6 and 1.8 s. Both syllables lasted 0.2 s. The first syllable had to be retained in memory for 2 s, then the second syllable was presented. 1 s after S2 presentation, a response prompt appeared, and subjects indicated whether S2 started with the same or with a different consonant as S1. **B. Temporal hazard function and the foreperiod bins.** The hazard function was calculated as the cumulative probability of S1 occurrence according to the foreperiod duration, across the experiment. Seven foreperiod bins are depicted by means of box plots, where the black central line illustrates the median foreperiod of each bin, linearly spaced across all trials. Error bars indicate the percentiles of trials of each bin.

### 7.2.3 Procedure

While brain activity was recorded with MEG (see below), participants performed 360 trials, organized in 18 blocks of 20 trials each. Cue type (early, late, neutral) was constant within a block, and participants were informed at the start of each block about the type of temporal cue they would receive on each trial. The order of trials within a block and order of blocks were randomized for each participant. Button assignments were counterbalanced across participants, such that half of the participants indicated that S1–S2 shared the same initial consonant using the left button, and half did so with the right button. The testing took approximately 1.5 hours per participant and was conducted within one session.

### 7.2.4 Data recording and analysis

See Section 4.4 for detailed information about MEG recording.

Subsequent data analyses were carried out with Matlab (The MathWorks Inc., Massachusetts, USA) and the FieldTrip toolbox (Oostenveld et al., 2011) using only trials to which correct responses were provided ("correct trials", percentage correct >98 %).

Analyses were conducted using only the 204 gradiometer sensors, as they are most sensitive to magnetic fields originating directly underneath the sensor (H m l inen et al., 1993). The continuous data were filtered off-line with a 70-Hz low pass filter. No high pass filter was applied in order to analyze neural oscillations in the slow-delta (< 1 Hz) frequency band.

Subsequently, trial epochs ranging from –4 to 7 s time-locked to the onset of S1 were extracted, and down-sampled to 200 Hz. First, epochs with strong artifacts were rejected when the signal range at any sensor exceeded 800 pT/m (gradiometer). Then, the mean of each epoch was subtracted and independent component analysis (ICA) was applied to the epochs in order to exclude artifacts mainly due to eye blinks and heart beat. Following ICA, remaining epochs containing artifacts exceeding a threshold of 200 pT/m were rejected.

### 7.2.5 Time–frequency representations (TFRs)

Time–frequency representations (TFRs) were calculated for the preprocessed 11-s epochs for each trial (with 20-ms time resolution) and for frequencies ranging between 0.5 Hz to 20 Hz (logarithmically spaced, in 20 bins). Time-domain data were convolved with a Hann taper, with an adaptive width of two to four cycles per frequency; i.e., the number of cycles increased logarithmically with frequency in twenty steps. The output of the analysis was complex Fourier data, allowing for analyses of phase and of power.

### 7.2.6 Correlation of time–frequency representations with S1-onset time

Instantaneous temporal expectations increase with longer foreperiod durations (Nobre et al, 2007). Hence, in order to test whether slow-delta phase coherence, or other measures of slow-delta oscillatory activity, reflects the strength of temporal expectations, measures of slow neural oscillatory activity were correlated with foreperiod duration. To this end, trials were grouped into seven bins according to their individual foreperiod duration according to the following procedure: First, all trials of each participant were sorted in order of increasing foreperiod duration. Then, seven trials were selected that were equally (linearly) spaced in terms of foreperiod duration (in seconds) and that also spanned the entire set of durations. These trials served as bin centers. A bin contained 37 adjacent trials with shorter foreperiod durations and 37 adjacent trials with longer foreperiod durations. That way, the bin centers were equal to the median

of each bin, which served as a regressor in the subsequent correlation analyses. This procedure ensures equal trial numbers per bin, whereas bins have variable widths in terms of foreperiod duration. See 7.1B for an example.

Next, three neural activity measures were calculated for each time-frequency-sensor data bin and for each foreperiod bin: Inter-trial phase coherence (ITPC; Lachaux et al., 1999), total power, and evoked power (David et al., 2006; Ding and Simon, 2013). ITPC corresponds to the magnitude of the amplitude-normalized complex numbers averaged across trials of the TFR estimates for each time-frequency bin, channel and foreperiod bin (Thorne et al., 2011). Total power was expressed as the average power (squared magnitude of the complex-valued TFR estimates) across single trials (see below), while evoked power was calculated for each channel and foreperiod bin by first averaging single-trial time domain data, then calculating the power as the squared magnitude of the complex-valued TFR estimation.

Lastly, we normalized total power and evoked power by means of z-transformation taking full 11s-epochs as reference. Note that our experimental design did not allow the definition of a long enough time interval to serve as a conventional reference baseline for subtraction. For the z transform, we computed the trial-mean and the trial-standard-deviation (SD) of power in each trial, channel, and frequency-bin. z-transformed total power as a function of time (i.e., for each individual time bin) was then computed by first subtracting the trial-mean and subsequently dividing by the trial-SD. Finally, normalized power was averaged across trials within each foreperiod bin at each time-frequency bin, and channel. Evoked power normalization was performed on overall power representations per foreperiod bin at each time-frequency-channel bin, again by subtracting the mean over time bins and dividing by the standard deviation across time bins.

Prior to the statistical analyses (see next section) gradiometer pairs were combined by means of averaging across two gradiometers of a pair for ITPC, total power, and evoked power, respectively. For each dependent measure, this procedure resulted in one value for each time point, frequency bin, sensor position, and foreperiod duration.

### 7.2.7 Statistical analysis

Behavioral dependent measures (i.e., proportion correct, PC; and response times, RTs) were correlated with foreperiod duration in order to test for increases in performance

with increasing temporal expectations due to longer foreperiods. Additionally, behavioral measures were analyzed with separated one-way repeated-measures ANOVAs (early, late, and neutral) to test for effects of temporal cues.

Statistical analyses of the correlation of foreperiod duration with ITPC, total power, and evoked power followed a multi-level approach (Wilsch et al., 2014; Obleser et al., 2012, van Dijk et al., 2010): On the first (single-subject) level, the median duration of the seven foreperiod bins was correlated with a particular dependent measure in each time-frequency-channel bin. Statistical tests were performed within the framework of Fieldtrip's independent-samples regression t-test with contrast coefficients corresponding to the medians of the foreperiod duration bins. Linear coefficients for all contrasts (ITPC, total power, evoked power) were obtained for each time-frequency bin at each of the 102 sensor positions.

The focus of the correlation analysis was on effects in the frequency range that corresponded to the range of rates that were most likely to correspond to temporal expectations due to foreperiod duration. Here, foreperiod durations varied from 0.6 s to 1.8 s, and we hypothesized that temporal orienting within this range of durations would be reflected in phase organization in the corresponding about 0.6 to about 1.7 Hz frequency range. Therefore, the statistical analyses on the second (group) level were conducted on exactly that frequency range (i.e., 0.6–1.7 Hz). Our time-window of interest was –0.5 to 0.5 s time-locked to S1-onset in order to cover pre- and peri-stimulus effects after cue presentation.

In a previous study, we observed variations in alpha power during the S1-retention period due to cued temporal expectations (Wilsch et al., 2014). Thus, in the current study we additionally examined the correlation between alpha power (8–13 Hz) and foreperiod duration using the same multi-level correlation analysis described above. In order to capture activity during retention, the time window of interest ranged from –0.5 to 2.5 s time-locked to S1.

For all correlation analyses, linear coefficients resulting from the single-subject first-level statistics were tested on the group level against zero with cluster-based permutation tests (dependent samples t-tests, 1000 iterations; Maris and Oostenveld, 2007). The cluster approach protects against inflated type-1 error due to multiple comparisons. All cluster tests were one-tailed in favor of a positive correlation for the delta frequency

band and one-tailed in favor of a negative correlation for the alpha frequency band and were thus considered significant when $p < 0.05$.

Post-hoc correlations were conducted on the clusters resulting from the correlations between delta ITPC and alpha power with foreperiod duration (see below). Here, delta ITPC and alpha power were averaged across the channel-time-frequency bins belonging to their respective significant cluster. Averages were calculated separately for each foreperiod bin and for each subject. Then two correlations were calculated, one across foreperiod bins and one across participants. For the correlation across foreperiod bins, the delta ITPC values and the alpha power values were averaged across participants, resulting in in a single delta ITPC and a single alpha power value per foreperiod bin which were then correlated. Similarly, for the correlation across participants, dependent measures were averaged over foreperiod durations, yielding a single delta ITPC and a single alpha power value per participant, which were then correlated.

Effect sizes for all measures reported were calculated by estimating the effect size measure $r_{equivalent}$ (denoted r) which is bound between 0 and 1 (Rosenthal, 1994). In the case of cluster tests where t-statistics were obtained for all time–frequency–channel bins, r values were averaged across all bins belonging to a significant cluster (denoted R).

## 7.3 Results

Behavioral performance did not vary with foreperiod duration ($t = -0.017$, $p = 0.507$, $r = 0.006$) or cueing condition ($F(2, 18) = 0.35, p = 0.71, r = 0.18$), most likely because performance was at ceiling for all conditions (PC $>$ 98 %). In order to test whether explicit temporal cues did elicit variations in neural measures reflecting temporal expectations, inter-trial phase coherence (ITPC), total power, and evoked power were compared across the three cueing conditions (early, late, neutral) using multi-level cluster t-tests. These statistical contrasts on ITPC, total power, and evoked power did not reveal any effects beyond cue-evoked responses (data not shown here). Therefore we will focus on the effects of temporal expectations induced by the passage of time as indexed by correlations between brain measures (ITPC, total power, evoked power) and foreperiod duration.

With respect to delta ITPC, statistical analyses revealed one positive cluster (–0.5 to 0.46 s, $p = 0.045, R = 0.63$) at right fronto-temporal sensors (see Fig. 7.2A, left panel and Fig. 7.2B) ranging from 0.6 to 0.9 Hz. This effect peaked between 0.7 and 0.9 Hz and at 120 ms, that is, around S1 onset. Fig. 7.2B illustrates the enhancement in slow-delta ITPC and phase distributions for the first and last foreperiod bins. ITPC is consistent with auditory generators (Fig. 2B: left and right topographical plots). As illustrated for two single participants, the phase concentration was higher in the last bin compared to the first (Fig. 7.2D).

Unsurprisingly, analyses on evoked power revealed qualitatively similar effects as for ITPC (e.g. Henry & Obleser, 2012). Here, however, the slow-delta cluster did not attain significance on a conventional 5 % level (positive cluster: –0.5 to 0.5 s, $p = 0.12, R = 0.64$). Similarly, total power did not present any clusters in the slow-delta range (see Fig. 7.2, center and right panel).

The analysis on alpha power revealed a centrally distributed negative cluster (1.12 to 1.92 s, $p = 0.013, R = 0.71$) indicating less alpha power during S1 retention after longer foreperiods (see Fig. 7.3A). This alpha power decrease and the delta ITPC increase both reflect the brain's sensitivity to variable foreperiods raising the question whether delta ITPC and alpha power are mutually dependent. Therefore, we correlated delta ITPC and alpha power (data were averaged across participants) across foreperiod durations, which revealed a negative dependency ($r = -0.77, p = 0.044, df = 5$; see Fig 7.3, left panel). For each participant individually, this ITPC–alpha power correlation was calculated and subsequently transformed to Fisher's z. Mean Fisher's z coefficients were significantly smaller than zero ($t = -3.10, p = 0.013, r = 0.72$). Although the partial correlation between delta ITPC and alpha power (regressing out the bins‘ foreperiod duration) was non-significant ($r = 0.62, p = 0.191, df = 5$), this finding illustrates the modulatory effect that foreperiod duration exerts on delta phase concentration and later alpha-power modulation. However, another correlation between slow-delta ITPC and alpha power across participants (data were averaged across foreperiod bins) also addressed the question of a mutual dependency of delta ITPC and alpha power and revealed another significant negative correlation ($r = -0.71, p = 0.02, df = 8$; see Fig. 7.3B, right panel). Thus, participants presenting high slow-delta ITPC at S1 showed a decease in alpha power during S1-retention, independent of foreperiod duration.

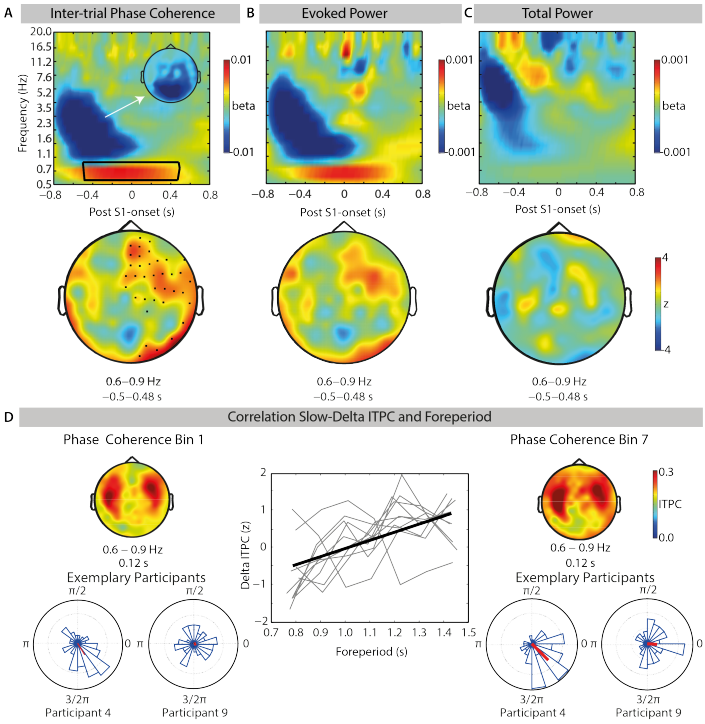


***Figure 7.2.*** **A-C. Correlation of foreperiod duration with ITPC, total power, and evoked power.**A (inter-trial phase coherence, ITPC), B (evoked power), and C (total power) time–frequency plots display first-level correlation coefficients (beta-values averaged over participants) of the correlation between foreperiod duration (1 to 7 bins) and the respective neural measure from 0.5 to 20 Hz and –0.8 to 0.8 s time-locked to S1 onset. Topographies illustrate the distribution of z-values averaged across the slow-delta range (0.6-0.9) during the duration of the delta effect (–0.5–0.48 s). Marked channels in the left plot show the location of the significant cluster. Small topography in ITPC single plot illustrates beta-values in higher frequencies averaged across all channels. **D. Correlation of slow-delta ITPC and foreperiod duration.** The central plot illustrates variations of slow-delta ITPC with foreperiod duration for each subject averaged across the significant positive cluster. The thick black line represents the average of all single-subject linear fits. Topographic plots on the left and right show slow-delta (0.6–0.9 Hz) at 0.12 s after S1-onset (peak of effect). The left plot represents ITPC and in the first foreperiod bin and the right plot in last (7th) foreperiod bin. Rose plots underneath illustrate slow-delta phase distribution at 0.12 s in bin 1 (left) and bin7 (right) of two representative participants. The red line corresponds to the resultant vector.

Less relevant for the present research question, negative effects of foreperiod duration on ITPC, total power, and evoked power were also observable (Fig. 7.2A–C). These effects are a more trivial reflection of the cue offset response shifting and being closer to S1 (i.e., in the –.8–0-s range relative to S1) for shorter foreperiods. The occipito-

parietal distribution of these effects (see blue colors in Fig. 7.2A) strongly implies that they were primarily caused by the change in visual stimulation at cue offset. These effects will thus not be further discussed here.

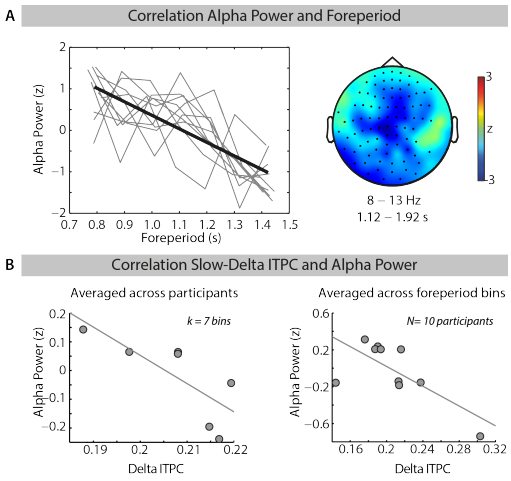


***Figure 7.3.*** **A. Correlation of foreperiod duration with alpha power.** Left panel illustrates variations in alpha power with foreperiod duration for each individual subject averaged across the significant negative cluster. The thick line represents the linear fit averaged across subjects. The topography presents the significant negative cluster (8–13 Hz, 1.12–1.92 s). Illustrated sensors mark cluster membership. **B. Correlation of delta ITPC and alpha power.** The left panel shows the correlation of slow-delta ITPC and alpha power on foreperiod bins averaged across subjects. The right panel shows the correlation of slow-delta ITPC and alpha power on participants averaged across foreperiod bins.

## 7.4 Discussion

In the current study, we have shown that temporal expectations for stimulus occurrence based on the passage of time are reflected in a gradual increase of phase coherence of slow-frequency oscillatory activity. Furthermore, these temporal expectations exert also a "remote" impact and reduce the magnitude of the typical alpha power increase observed during later retention of sensory information in memory. In notable contrast to the same task using near-threshold stimuli (speech in noise; Wilsch et al., 2014), explicit temporal cues here had no discernible impact, as cues failed to elicit neural or behavioral markers of temporal expectation.

Unsurprisingly for supra-threshold stimulation with highly familiar syllables, no behavioral effect of temporal expectancy occurred (> 98 % accuracy). On a neural level, however, temporal expectancy did affect the processing of these syllables: Very slow

neural oscillations (< 1 Hz; corresponding to the frequency range of the so called "slow 1" band, 0.5–2 Hz; Penttonen, 2003) turned out to be a sensitive marker for variations in the strength of temporal expectation induced by varying foreperiod durations. Foreperiod duration correlated significantly with slow-delta phase coherence around the onset of the target syllable at right fronto-temporal sensors. We tested for phase coherence effects specifically in the low delta range (0.6–1.7 Hz) because we hypothesized a correspondence between the variable onset times of stimulus events across the experiment (foreperiod durations between 0.6 and 1.8 s) and the frequency of the recruited neural oscillator. In previous studies, increased neural phase locking has been found at the stimulation frequency of rhythmically presented stimuli (de Graaf et al., 2013; Henry and Obleser, 2012; Herrmann et al., 2013; Cravo et al., 2013; Lakatos et al., 2013; Mathewson et al., 2012). In the present study the stimulation frequency varied considerably across trials, but the instantaneous probability of stimulus occurrence always increased with the passage of time within a limited range (see Figure 7.1B). The present data suggest that in particular low frequency neural oscillations matched best to the longest foreperiods occurring across an experiment (here 1.8 s, relating to $\sim$ 0.6 Hz) can reflect the formation of temporal expectations.

These data fit previous observations that delta band phase locking increases with increasing probability of stimulus occurrence (Stefanics et al., 2010), but extend these to a more implicit and variable scenario of expectations formed only from the passage of time. In general, low frequency neural oscillations have been related to neural excitability fluctuations (Lakatos et al., 2005; Steriade et al., 1993). Our data suggest that temporal expectations as a function of foreperiod duration tuned slow-delta oscillations to be in a high-excitable phase just before and during occurrence of the first target syllable (–0.5 to 0.48 s; covering approximately a half cycle of these very slow oscillations).

Interestingly, despite the absence of a behavioral modulation by foreperiod duration, a benefit from increased temporal expectations emerged in the neural dynamics during subsequent syllable retention in memory: the better the expectation, the lower centroparietal alpha power during retention of the first syllable. High alpha power can be seen as a marker for cognitive load (e.g. Jensen et al., 2002; Klimesch, 2012; Leiberg et al. 2006; Haegens et al. 2010) and has been shown to be relatively decreased under the beneficial influence of temporal cues in a near-threshold study (Wilsch et al., 2014) or

with improved quality of the sensory input (Obleser et al., 2012). Hence, the lowered alpha power during syllable retention after longer foreperiods is the best indicator in the present data that temporal expectations as a function of foreperiod duration not only optimize sensory processes but also reduce markers of cognitive load.

But can we establish direct links between temporal expectation, slow neural phase concentration, and later alpha power effects? Average Slow-delta phase locking across participants and the respective alpha power correlated negatively when treating foreperiods bins as the units of observation (Fig. 7.3A). However, a partial correlation controlling for foreperiod duration showed that increased temporal expectations (from bin 1 to bin 7) were the common driver of the increase in slow-delta phase locking and the decrease in alpha power, respectively. More interestingly, individuals‘ average degree of slow-delta phase locking directly predicted their later average degree of alpha power (Fig. 7.3B, right panel). Thus, individuals with a higher slow-delta phase coherence during stimulus encoding exhibit lower alpha power during later memory retention. This is at least initial evidence that temporal expectations benefit retention in memory (Wilsch et al., 2014) by way of optimized neural phase organization around the time point of stimulus encoding.

The observed slow-delta band phase locking difference emerged most prominently at right fronto-temporal sensors. This topography suggests at least two possible generators. First, the topographies in Fig. 2D indicate that slow-delta ITPC has its peak at temporal sites and thus most likely emerged from sources in the superior temporal gyrus or the auditory cortex. This possibility is in line with previous studies that have reported that increased delta-phase coherence predominantly in the primary sensory areas corresponding to the modality of the anticipated stimulus (Lakatos et al., 2005, Lakatos et al., 2008). The statistical effect, however, appears to be more frontally located. Thus, the same topographical distribution of statistical effects also allows for the possibility that phase locking effects emerged at least partly from the cingulo-opercular network. This network plays a critical role in attentional control over diverse cognitive processes such as perception and decision-making (Dosenbach et al., 2007; Eckert et al., 2009; Sadaghiani et al., 2009). Hence, enhancement in these brain regions has been shown to be favorable for stimulus processing. A previous, near-threshold instantiation of the present design also yielded neural oscillatory (alpha power) modulations with

a comparable topography and right-anterior insula source localization (Wilsch et al., 2014).

The former interpretation supports the idea that changes in slow-delta phase coherence reflect perceptual modulation directly at sensory regions (i.e., auditory cortex), whereas the latter suggests that slow-delta phase coherence is an attentional signal originating from domain-general cortex. While obviously requiring future disambiguation, both interpretations are in line with improved stimulus processing through temporal expectations, by way of neural phase realignment.

Acknowledging the summated and indirect nature of the MEG signal, the current data cannot separate changes in evoked magnetic field activity from true altered phase concentration of ongoing neural oscillations. According to Ding and Simon (2013), inter-trial phase coherence is much more sensitive to stimulus-synchronized neural activity than are measures of power. In our study, neither total nor evoked power was sensitive enough to capture significant variations whereas phase coherence was. However, the similarity of patterns between phase-locking and evoked power leaves open whether the underlying neural process is a change in oscillatory phase patterns or in amplitude, or in both.

Note that in the present study the explicit temporal cue that indicated the onset of the foreperiod was a visual stimulus whereas the target was auditory. Hence, increased neural phase coherence in the delta band might be caused by a cross-modal phase reset where the attended stimuli in one sensory modality can affect processing of inputs in another modality (Busse et al., 2005). Specifically, a visual stimulus signaling an upcoming auditory stimulus has been shown to reset auditory cortical oscillations to a state of high excitability (Lakatos et al., 2009; Thorne et al., 2011; Thorne and Debener, 2013). Despite the fact that the mentioned studies applied a much shorter stimulus onset asynchrony between a visual and an auditory target (30 to 75 ms Thorne et al., 2011) our design with much longer stimulus onset asynchronies (i.e. foreperiod durations between 0.6 and 1.8 seconds) might be reflecting an extended, but closely related form of cross-modal phase reset.

### 7.4.1 Conclusions

In sum, we here have shown that temporal expectations are formed and utilized based on highly variable, probabilistic event occurrences. Furthermore, unlike more explicit,

controlled expectations (like those elicited by the cues in the current study), these temporal expectations also impact the sensory processing of supra-threshold stimuli. Phase precision of slow neural oscillations in a slow-delta frequency range that matched the temporal scale of the experimental manipulation increases as temporal expectations become more precise. These data thus underline the utility of slow neural oscillations in understanding processes of perceptual organization and attentional control.

# 8 Experiment III: Cortical patterns of alpha power in sensory memory decay[1]

## 8.1 Introduction

Working memory as one on of the main executive functions allows us to focus our attention on representations of perceptions that are not physically present anymore (Baddeley, 2012). This particular ability comes at the cost of limited processing capacity: only a limited amount of memory load which is represented by either the number or the complexity/precision of information which can be stored and manipulated in working memory (e.g., Luck and Vogel, 1997; van den Berg et al., 2012). Information exceeding these limits is not stored correctly, as is reflected by a decrease in working memory task performance (e.g., Norman and Bobrow, 1975).

As already discussed in previous sections of this thesis (see Chapter 5), alpha power has been observed to be a sensitive marker of working memory load: according to the "functional inhibition" hypothesis, an increase of alpha power gates the processing of information by inhibiting task-irrelevant information and/or brain regions (for a review see Klimesch et al., 2007).

Specifically, alpha power was increased during the delay phase when memory load was increased due to the number of items-to-be stored (Jensen et al., 2002; Leiberg et al., 2006b; Obleser et al., 2012) or due to degraded speech signals (Obleser et al., 2012; Wilsch et al., 2014). This alpha power increase has been argued to functionally inhibit irrelevant brain regions.

However, working memory was not just characterized by its limitations in terms of number of items and stimulus precision, but also with respect to duration of item

[1]This chapter has been adapted from a manuscript in preparation for submission by Wilsch, Henry, Herrmann, and Obleser.

maintenance (see Chapter 1): the encoded memory representation fades away after a brief period of time (i.e., memory decay; Brown, 1958; Posner and Keele, 1967).

The current study investigates memory decay. To that end, it focuses on auditory sensory memory (Cowan, 1984; Cowan et al., 1997) with pre-lexical stimuli (sensu Obleser and Eisner, 2009) to avoid rehearsal effects (Oberauer and Lewandowsky, 2013). Auditory sensory memory enables integration of auditory information and preservation of information over brief periods of time (for a review see Schröger, 2007).

The modulation of alpha power as a function of memory decay has not yet been investigated. We think that this would add to the role of alpha power for working memory. We are able to derive two different hypothesis on the modulation of alpha power by memory decay from previous findings. First, the *alpha-decrease hypothesis* takes into account that previous neural findings on memory decay indicate a decline of neural response during the delay phase: This decline has been observed in single-cell recordings of monkeys' neural activation during the delay phase (Fuster, 1999). Similarly, Jha and McCarthy (2000) found a decline in the BOLD response of posterior regions during the visual memory delay phase. Thus, with respect to modulations in the alpha range, we assume to observe a decrease with longer delay phase duration. In addition, alpha power has also been shown to be directly linked to memory performance. That is, increased alpha power is associated with improved memory performance (Wilsch et al., 2014; Haegens et al., 2010). Since sensory memory performance decreases with longer delay phases (for a review see McKeown and Mercer, 2012; Mercer and McKeown, 2014) this decline in performance might also be accompanied by a decline in alpha power.

Second, the *alpha-increase hypothesis* is based on the additional effort needed to maintain a memory representation over time. One possibility is that alpha power increases with longer delay phase duration because more cognitive resources are needed to keep the memory representation from fading away. These allocated cognitive resources could be reflected by alpha power which has been argued to protect the storage of items in memory (Roux and Uhlhaas, 2013).

In a previous study (*Experiment I*) we have shown that temporal expectations reduce memory load of speech-in-noise. This reduction was reflected in decreased alpha power during stimulus retention and improved working memory performance (see Chapter 5; Wilsch et al., 2014). This facilitating effect of temporal expectations was most likely

mediated by the enhanced encoding precision of the expected stimulus (see Rohenkohl et al., 2012). It has not been decided, however, whether temporal expectations not only reduce memory load but also have a protective effect on memory decay. Specifically, the question arises whether temporal expectations are able to counteract the decay over the passage of time in auditory sensory memory.

In the present magnetoencephalography (MEG) experiment we investigated to what extent sensory memory decay was reflected by modulations in alpha power during stimulus retention. To that end, we conducted a *delayed two-stimulus pitch comparison procedure* (e.g., Bachem, 1954; Bull and Cuddy, 1972; Harris, 1952; Keller et al., 1995) with two brief pure-tone sequences separated by variable delay phases. Pure-tone sequences were embedded in the noise in order to increase memory load (Pichora-Fuller and Singh, 2006). We also varied the delay phase duration parametrically which allowed for a correlation with alpha power and, thus, would indicate a positive or negative relationship of memory decay and alpha power.

Moreover, we wanted to determine whether temporal expectations for stimuli, which are masked with noise, counteract memory decay. There also was a manipulation of temporal expectations orthogonally to the delay phase manipulation. Temporal expectations were manipulated by presenting temporal cues that indicated either a fixed onset time of the first pure-tone sequence or a jittered, hence unknown, onset time. The aim was to find out whether temporal expectations counteracted memory decay that is reflected by modulations of performance and alpha power. In addition to analyses on the sensor level, we conducted a source localization of alpha power modulations. We expected to find different sources for the different experimental manipulations. That is, effects of temporal expectations most probably arose from frontal regions, specifically the cingulo-opercular attention network (see Chapter: 5 Wilsch et al., 2014; Triviño et al. (2010)). We assumed that effects related to the manipulation of memory decay emerge from posterior brain areas instead. Alpha power in posterior regions was often reported to reflect disengagement of these regions during memory maintenance (Haegens et al., 2010; Jensen et al., 2007; Tuladhar et al., 2007). However, we did not know which brain regions would show a possible interaction of temporal expectations and memory decay. Source localizations of the different effects allowed for a disambiguation and hence a differential perspective on possible alpha power modulations throughout stimulus maintenance.

## 8.2 Methods

### 8.2.1 Participants

Twenty healthy right-handed participants took part in this study (10 females) ranging in age from 23 to 33 years. All participants had self-reported normal hearing. Participants were fully debriefed about the nature and goals of this study, and received financial compensation of 7 € per hour for their participation. The study was approved of by the local ethics committee (University of Leipzig), and written informed consent was obtained from all participants prior to testing.

### 8.2.2 Experimental task and stimuli

The time course of an example trial is depicted in Figure 8.1A. Each trial began with the presentation of a fixation cross. Approximately one second later (jittered between 750 ms to 1250 ms) white noise and a visual cue were presented simultaneously. The onset of the cue indicated the onset time of the first sound (S1). The onset time of this sound was measured from the onset of the cue. Participants had to retain the sound in memory during a one-,two-, or four-second delay phase following the sound's offset. Then, a second sound (S2) was presented, and participants judged whether the second was same or different from the first sound. Approximately one second (jittered between 900 ms to 1100 ms) after the presentation of S2, participants were prompted to respond by a button press. Finally, participants indicated their confidence in their "same"/"different" response on a 3-level confidence scale ("not at all confident", "somewhat confident", "very confident"). Trials were separated by an inter-trial interval of approximately one second that was free of stimulation or responses. The entire trial was embedded in white noise to decrease the sounds' precision and to concomitantly increase their memory load.

Memory decay was manipulated by having variable delay phases (i.e., 1-, 2-, 4-seconds) throughout which S1 had to be retained in memory. Temporal expectations were manipulated by the duration of the interval between cue-onset and S1-onset (i.e., foreperiod). The foreperiod was either "fixed" (i.e., fixed foreperiod, 1300 ms) or "jittered", in which case the onset times of the first sound were randomly drawn from a

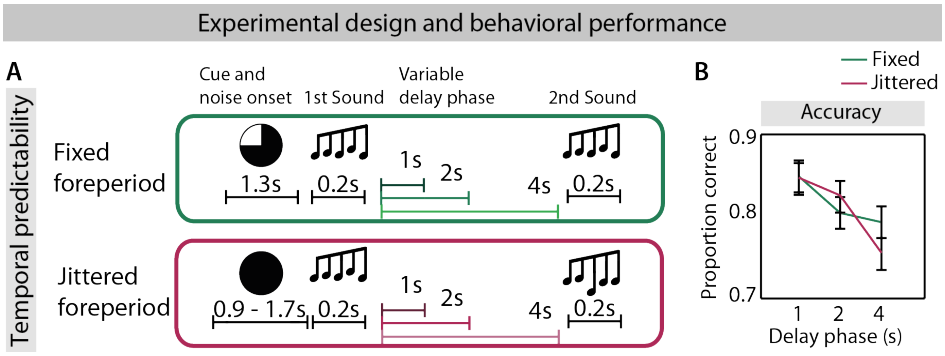


***Figure 8.1.*** **Experimental design and behavioral performance.** **A.** Experimental design. Upper panel illustrates a "same" trial with fixed foreperiod. Lower panel illustrates a "different" trial with jittered foreperiod. **B.** Accuracy for each condition. The green line displays fixed and the red line displays accuracy after jittered foreperiods

uniform distribution ranging between 900 ms and 1700 ms (i.e., jittered foreperiod). The mean onset times were 1300 ms corresponding to the fixed cue.

Characteristics of the sound stimuli Sound pairs were created for the "same"/ "different" task, a standard sound and a deviant sound. The deviant was higher in pitch than the standard. See Section 4.2 for a precise description of the sound characteristics.

The noise masker was white noise. Sound sequences and noise were presented with a constant signal-to-noise ratio (SNR) of -17, which, after piloting, turned out to increase the difficulty but still allowed all participants with their individual sensitivity towards the SNR to perform the task.

### 8.2.3 Procedure

Prior to the MEG measurement, participants were introduced to stimuli and task and performed a few practice trials. Then, the individual threshold (pitch-differences between standard and deviant in third and fourth pure tone) was titrated aiming for a performance between 65 % and 85 % correct across all experimental conditions (2 foreperiod conditions, 3 delay-phase conditions). For that reason, participants performed a practice block of 18 trials containing all conditions. The initial threshold applied here was kept constant throughout the block. This starting value was derived from an adaptive tracking procedure in order to estimate individual signal-to-noise ratios (SNR) yielding 70.7 % correct responses (i.e., two-down-one-up; Levitt, 1971).

Eight different participants had performed the adaptive tracking with the same task as described before. The individual thresholds were averaged and used a starting value for each participant in the current experiment.

Depending on the participant's performance in this practice block the initial threshold was adapted and applied to the stimuli for a second practice block. Here again, in case that participants' have not performed yet at a level of 65 % to 85 % the threshold was adapted again. After the second practice block the actual experiment and the MEG measurement started.

Brain activity was recorded with MEG during the performance of 396 trials completed in 12 blocks of 33 trials each. Foreperiod duration (fixed, jittered) was constant within a block, and participants were informed at the start of each block about the type of temporal/foreperiod cue they would receive on each trial. Delay-phase durations (1-, 2-, 4-seconds) were equally distributed across blocks. The order of trials within a block and order of blocks were randomized for each participant. Button assignments were counterbalanced across participants, such that half of the participants indicated that the first and the second sound were the same using the left button, and half did so with the right button.

The testing took approximately 2.5 hours per subject and was conducted within one session. The overall session including practice blocks and preparation of the MEG setup took about 4 hours.

### 8.2.4 Data recording and analysis

See Section 4.4 for detailed information about MEG recording.

Subsequent data analyses were carried out with Matlab (The MathWorks Inc., Massachusetts, USA) and the FieldTrip toolbox (Oostenveld et al. 2011) using only trials to which correct responses were provided ("correct trials"). Analyses were conducted using only the 204 gradiometer sensors, as they are most sensitive to magnetic fields originating directly underneath the sensor (Hämäläinen et al., 1993). The continuous data were filtered offline with a 0.5-Hz high pass filter, specifically designed to provide a strong suppression of DC signals in the data (>140 dB at DC, 3493 points, Hamming window; e.g., Ruhnau et al., 2012).

Subsequently, trial epochs ranging from –1.5 to 11.5 s time-locked to the onset of the first sound were extracted. These rather long epochs were extracted to circumvent

windowing artifacts in the time–frequency analysis; the intervals analyzed statistically were shorter (see below). Epochs were low-pass filtered at 80 Hz and subsequently down-sampled to 200 Hz.

First, epochs with strong artifacts were rejected when the signal range at any sensor exceeded 800 pT/m (gradiometer). Then, independent component analysis (ICA) was applied to the epochs in order to exclude artifacts mainly due to eye blinks and heart beat. Following ICA, remaining epochs containing artifacts exceeding a threshold of 200 pT/m were rejected. Epochs were rejected when the signal range within one epoch exceeded 200 pT/m (gradiometer) or 100  V (EOG). Additionally, trials were rejected manually for which variance was deemed high relative to all others (per participant, per condition) based on visual inspection. Prior to the time–frequency analyses, trial time was changed so that the onset of the second sound was t = 0 s. That resulted in two sets of epochs, one being time-locked to the first, the other one being time-locked to the second sound. Due to the variable trial length (different delay phase duration) these two trial sets allowed for analyses during the delay phase right after presentation of the first sound (post-S1) and right before the presentation of the second sound (pre-S2).

### 8.2.5 Spectral analysis

Power spectra were calculated at each gradiometer independently for the trial sets time-locked to S1 and time-locked to S2. From each trial set, a 0.7 s segment was extracted (0.4 to 1.1 s time-locked to S1, –0.8 to –0.1 s time-locked to S2 excluding evoked responses due to sound presentation). Segments were multiplied with a Hann taper and power of 8–13 Hz was computed using a fast Fourier transform (FFT) approach.

To inspect the time course of the frequency effects, we also computed time–frequency representations (TFRs). TFRs were calculated only on the trial sets time-locked to S1. Time–frequency analysis was conducted on a trial epoch ranging from -2.0 to 7.6 s for each trial (with 20-ms time resolution) for frequencies ranging between 0.5 Hz to 20 Hz (logarithmically spaced, in 20 bins). Time-domain data were convolved with a Hann taper, with an adaptive width of two to four cycles per frequency; i.e., the number of cycles increased logarithmically in twenty steps corresponding to the frequency bins. The output of the analysis was complex Fourier data.

Power was calculated as the average of power (squared magnitude of the complex-valued TFR estimates) across single trials. Inter-trial phase coherence (ITPC) was

calculated by averaging across all trials after normalizing the complex values with the absolute TFR estimates at every single time-frequency bin and channel for each foreperiod bin (Thorne et al. 2012).

Prior to the statistical analyses (see next section) gradiometer pairs were combined by means of averaging across two gradiometers of a pair for FFT power spectra, and power and ITPC attained from the TFRs, respectively. For each dependent measure, this procedure resulted in one value for each time point, frequency bin, sensor position, and foreperiod duration.

### 8.2.6 Statistical analysis

Behavioral responses (i.e., proportion correct, PC; $A_z$) were analyzed with a repeated-measures ANOVA (foreperiod x delay phase). Greenhouse-Geisser correction was applied if Mauchley's test of sphericity turned out to be significant. ANOVAs were followed by paired-samples t-tests to resolve differences between individual foreperiod conditions (jittered, fixed) and delay phase (1-,2-,4-seconds). T-tests were FDR-corrected. $A_z$ is an in-depth measure of behavioral performance. Confidence ratings served to construct receiver operating characteristic (ROC) curves (Macmillan and Creelman, 2004) for each condition that were used to derive $A_z$, a non-parametric performance measure corresponding to the area under the ROC curve (see Fig. 4A). Response times are not reported because responses were prompted and thus do not provide valid information about costs and benefits of the experimental manipulations.

Statistical analyses were only conducted on the FFT power spectra not on the TFRs. Analyses comprised a multi-level approach (see Section 4.5.1). On the first (single-subject) level, specific contrasts were conducted using single-trial data to test for a main effect of temporal expectations (fixed vs. jittered foreperiod) in alpha power (8–13 Hz), a parametric modulation of alpha power by memory decay (1, 2, 4 s delay phase), and an interaction of temporal expectations and memory decay. For the temporal expectation effect, fixed-foreperiod trials were assigned a contrast coefficient of 1 and jittered-foreperiod trials of –1. To test the parametric modulation of memory decay, contrast coefficients corresponded to the actual delay phase in seconds (i.e., 1, 2, 4). In order to test the interaction of both factors the contrast values testing for parametric modulations of memory decay (1, 2, 4) were applied to each foreperiod condition (fixed, jittered) separately.

For the statistical analyses on the second (group) level, beta-values resulting from the single-subject first level statistics testing the main effect of foreperiod condition, as well es the test of parametric modulations of the delay phase were tested against zero. To test, whether the delay phase modulation in the fixed condition differs significantly from the modulation in the jittered condition, beta values attained for each of the foreperiod conditions separately were tested against each other. All tests were conducted with FieldTrips dependent sample t-test in terms of a cluster based permutation tests (see Section 4.5.1).

We also tested for correlations of alpha power with $A_z$ (see above) independent of experimental condition by means of a multi-level cluster test (see above). On the first level, an independent sample regression t-test was performed on the post-S1 and pre-S2 alpha power FFTs. Six $A_z$ values, one per condition served as regression weights for each condition's alpha power modulation, respectively. On the second level, first-level betas were tested against zero with a dependent samples t-test.

### 8.2.7 Source localization

For general information about the source analysis see Section 4.4.3.

The beamformer approach (DICS, dynamic imaging of coherent sources; Gross et al., 2001) was used to project alpha power during the delay phase directly following the first sound (0.4 to 1.1 s after S1-onset and –0.8 to –0.1 s prior to S2-onset) to source space.

The multitaper FFT was centered at 11 Hz (±2 Hz smoothing with three Slepian tapers; Percival and Walden, 1993) and a complex filter, specific for each condition, was calculated (Gross et al., 2001; Schoffelen et al., 2008). FFT data were then projected through the filter, separately for each foreperiod condition and delay phase condition.

We pursued different approaches to morph data to the common surface analogous to the analysis on the sensor level yielding different statistical contrasts: First, in order to illustrate the main effect of temporal expectations, the source projected power values of the data time-locked to S1 were morphed. Then, fixed and jittered foreperiods were contrasted by means of vertex-wise t-tests. Second, in order to test for a correlation of memory decay and alpha power in source space, source projected alpha power and the delay phase regressor (1,2,4) were z-transformed and a function of delay phase was fitted to the source power. The resulting standardized betas were then morphed onto

a common surface. For the interaction of temporal expectations and memory decay, the same correlation approach was applied to the same data (i.e., pre-S2) again but separately for each foreperiod condition. The beta-values of each foreperiod condition were also morphed onto the common surface. Third, correlation of source projected alpha power and $A_z$ was calculated by fitting $A_z$ of each condition onto alpha power of each condition at each vertex point. For each contrast the beta-values were tested against zero with vertex-wise t-tests.

The resulting t-values were z-transformed and displayed on the average brain surface with contrast dependent uncorrected vertex-wise threshold of $|z| \geq 2.0$ (jittered vs. fixed), $|z| \geq 3.0$ (delay phase correlation), $|z| \geq 1.5$ (delay phase correlation of fixed foreperiods vs. delay phase correlation of jittered foreperiods), $|z| \geq 2.0$ ($A_z$ correlation in post-S1), and $|z| \geq 1.7$ ($A_z$ correlation in pre-S2; Sohoglu et al., 2012).

Post-S1–Pre-S2 index of correlation with Az Correlations of alpha power and $A_z$ were found early in the delay phase (i.e., post-S1) as well as during the end of the delay phase (i.e., pre-S2; see below). In order to visualize the temporal specificity (post-S1 vs. pre-S2) of brain areas that present a correlation of alpha power and $A_z$ we calculated an index based on the attained z-values of the correlation with post-S1 FFT alpha and pre-S1 FFT alpha. Due to a combination of positive and negative z-values, post-S1 FFT and pre-S2 z-values had to be scaled into a common space between zero and one before calculating the index: The common mean of both (S1 and S2) z-values of all vertex points was subtracted from each S1 and S2 z-value vector. Then the resulting vectors were both divided by the new common maximum of S1- and S2-values.

The index was then calculated on the transformed z-values of the post-S1 and pre-S2 time windows. Therefore, the difference of S1- and S2-values was divided by the sum of S1- and S2-values. This resulted in a descriptive index for each vertex which was displayed on the average brain surface highlighting brain areas that showed a stronger correlation effect early in the delay phase or at the end of the delay phase.

## 8.3 Results

The present study explored how sensory memory decay of sounds presented in noise is reflected by changes in alpha power. Furthermore, the aim was to find out whether temporal expectations towards the to-be-remembered sound counteracts memory decay

and a potential modulation of alpha power. The participants' task was to retain a sound in memory for one, two, or four seconds and then to decide whether the first and the second sound were the same.

### 8.3.1 Effects of memory decay and temporal expectations on behavioral performance

Figure 8.1B illustrates a decline in behavioral performance (percentage correct) with longer delay phases. The repeated measures ANOVA on percentage correct reveals a main effect of memory decay ($F(2, 19) = 17.21, p < 0.0001$), no main effect of temporal expectations ($F(1, 19) = 0.89, p = 0.36$), and a significant interaction of memory decay and temporal expectations ($F(2, 19) = 4.90, p < 0.014$). We resolved the interaction by the factor memory decay to find out whether the decay in performance with longer delay phase is modulated by the foreperiod. A contrast of foreperiod conditions within each delay phase conditions shows that PC after a fixed foreperiod is slightly increased after a 4-second delay phase compared to the jittered condition ($t(19) = 2.49, p = 0.066$, see figure 8.1B), whereas there is no difference between foreperiods in the other two delay phase conditions (1 s: $t(19) = 0.28, p = 0.779$; 2 s: $t(19) = -1.49, p = 0.228$).

In addition to PC, we analyzed the performance measure $A_z$, a nonparametric measure derived from the receiver operating characteristics (ROC) curve (see Section 8.2 and Figure8.4A) which can be interpreted similarly to proportion correct. but, by taking the confidence ratings into account, $A_z$ is adjusted for response bias. The ANOVA on $A_z$ revealed a main effect of temporal expectations ($F(1, 19) = 101.31, p < 0.0001$), a main effect of memory decay ($F(2, 38) = 44.75, p < 0.0001$), and an interaction of both factors ($F(2, 38) = 17.52, p < 0.0001$). As for PC, the interaction was resolved by the factor memory decay in order to test whether there are effects in performance depending on the foreperiod. T-tests revealed that there was no differences between fixed and jittered foreperiods with a delay phase of one second ($t(19) = 0.24, p = 0.813$). $A_z$ after 2-second and 4-second delay phases differed significantly between foreperiod conditions (2 s: $t(19) = 6.69, p < 0.0001$, 4 s: $t(19) = 8.6, p < 0.0001$; see Fig 8.4A).

### 8.3.2 Effects of memory decay and temporal expectations on alpha power changes

We were interested in how stimulus encoding and stimulus retention was affected by temporal expectations and memory decay reflected by alpha power. Figure 8.2 illustrates overall power (A) and inter-trial phase coherence (ITPC, B) across all frequency

bands (5–20 Hz) time-locked to the S1. Figure 8.2C presents the time-course of alpha power averaged across trials for each condition separately. Interestingly, alpha power increases until the potential onset of the earliest second sound (shortest delay phase of one second) and then decreases slowly.

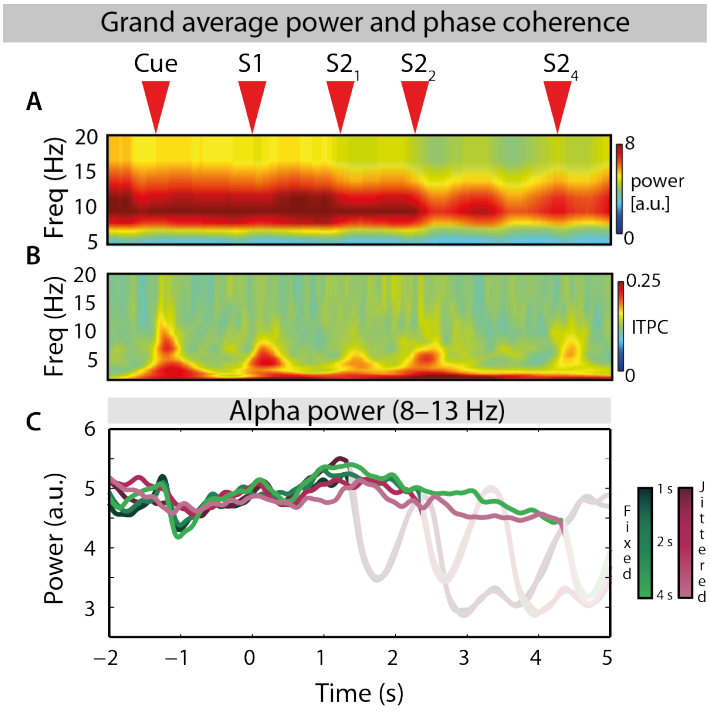


***Figure 8.2.*** **Time–Frequency grand averages power and phase coherence. A.** Power grand average 5–20 Hz. Red arrows on top indicate onset of each stimulus. **B.** Inter-trial phase coherence grand average 0.5–20 Hz. **C.** Alpha power (8–13 Hz) grand-average and power-spectrum across channels per condition.

Statistical analyses on alpha power aimed to find effects during the delay phase after presentation of S1 (0.4 to 1.1 s) and before presentation of S2 (–0.8 to –0.1 s, compare Fig. 8.1). First, we tested for an effect of memory decay on alpha power by correlating the delay phase with alpha power. We also tested for an effect of temporal expectations contrasting fixed and jittered foreperiods and additionally we tested whether the effect of memory decay on alpha power is modulated by temporal expectations.

The correlation of delay phase and alpha power revealed a broad posterior, negative cluster before the onset of the second sound ($p < 0.0001$; see Figure 8.3A, left panel), showing that alpha power decreases with longer delay phase (see also Figure 8.2C).

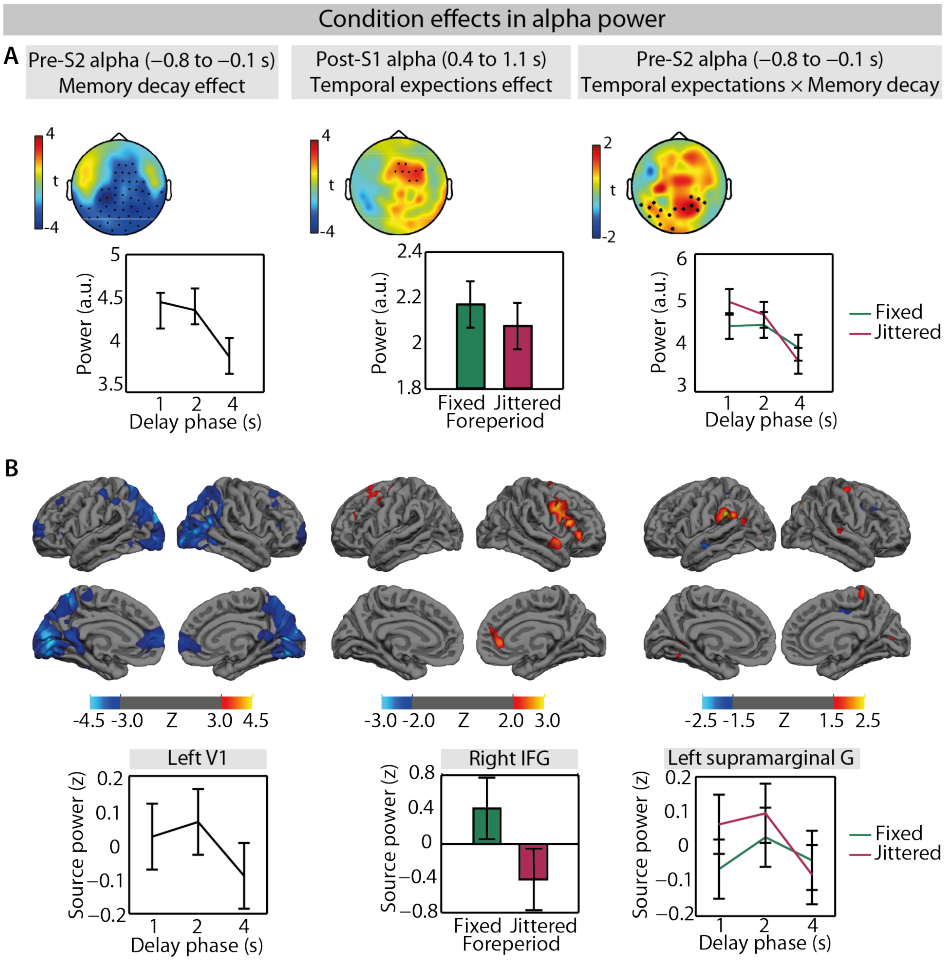


***Figure 8.3.*** **Condition effects in alpha power**. Left column: Effect of memory decay (1,2,4 s delay phase). Middle column: Effect of temporal predictability (fixed vs. jittered foreperiod).Right column: Interaction of temporal predictability and memory decay. **A.** Topographies of the t-values of the respective analyses on alpha power on the sensor level. Displayed channels present significant effects. Bar- and line graphs represent alpha power extracted from the displayed channels. **B.** Source projected alpha power effects, i.e. z-transformed t-values of the respective contrasts. Bar- and line graphs represent z-scored source power extracted from the (plotted) peak activity. All error bars display within-subject standard error.

Unsurprisingly, there was no effect of memory decay right after presentation of the first sound, at a time where the duration of the delay phase was still unknown.

The comparison of fixed and jittered foreperiods revealed a frontally distributed positive cluster after the onset of S1 indicating more alpha power in the fixed foreperiod

condition ($p = 0.047$; see Figure 8.3A, middle panel). No clusters were found before the onset of S2. Thus, a main effect of temporal expectations became only evident in the beginning of the delay phase.

Interestingly, the interaction of temporal expectations and memory decay revealed that the decrease of alpha power with delay phase was less strong after fixed foreperiods than after jittered foreperiod. The effect was shown by a significant positive cluster ($p = 0.025$) contrasting first-level betas in the fixed foreperiod condition with beta coefficients in the jittered foreperiod condition (see Figure 8.3A, right panel). No such interaction effect was found right after presentation of the first sound.

### 8.3.3 Source localization of alpha power changes

A source localization was conducted to identify the origins in the brain of the reported alpha power effects on the sensor level. The effect of memory decay on alpha power was localized at posterior sites. The peak of the effect emerged from the left primary visual cortex (V1, [MNI: –7, –81, 2]). Comparably strong effects were found in the right V1 ([MNI: 16, –77, 8]), the right inferior parietal lobe (IPL, [MNI: –49, –58, 19]) and precuneus [MNI: –9, –53, 56]. Z-transformed effects in source space and Z-values greater than 3.0 for each foreperiod condition averaged across vertices around the peak effect in V1 are illustrated in the line graph of figure 8.3B, left panel.

The main effect of temporal expectations during the early part of the delay phase (after the first sound) was localized in the right hemisphere. The peak of the effect was found in the right inferior frontal gyrus (IFG, [MNI: 46, 22, 19]) areas presenting this effect as well were right superior temporal gyrus (STG, [MNI: 58, 1, –1]) and right anterior cingulate cortex (ACC, [MNI: 8, 66, 3]). Z-transformed condition contrasts in source space and Z-values greater than 2.0 for jittered and fixed foreperiods averaged across vertices around the peak effect in IFG are illustrated in the bar graph of figure 8.3B, middle panel.

The differential effect of fixed and jittered foreperiods on the delay phase modulation on alpha power originated in the left supramarginal Gyrus ([MNI: –55, –48, 26]). Z-values greater than 1.5 are illustrated in figure 8.3B, right panel.

### 8.3.4 Alpha power predicts behavioral performance

In a final analysis, we aimed to relate the observed modulation of behavioral memory performance (i.e. $A_z$) to the alpha power modulations. We correlated condition-specific $A_z$ and alpha power by means of a cluster test which revealed a positive cluster post-S1 ($p = 0.023$) and another positive cluster pre-S2 ($p = 0.013$). Figure 8.4B illustrates these effects projected to source space: In the post-S1 time window (left panel), the alpha power correlation with $A_z$ emerges from bilateral anterior cingulate cortices (ACC, [left, MNI: ; right: MNI:]), as well as from right midfrontal gyrus (MFG, [MNI: 39, 7, 48]), right IFG [MNI:, 52, 9, 4], and right STG [MNI:, 6, –10. –2]. Note the overlap with the brain regions presenting the foreperiod effect (i.e., IFG; ACC, STG). In the pre-S2 time window (right panel), the correlation of alpha power and $A_z$ is also mostly emerging from bilateral ACC [MNI: –14, 47, 2; MNI: 13,43 – 5] and right IFG ([MNI: 53, 15, 2]), as well as left V1 [MNI: –14, –90, 3] and left SMG [MNI: –49, –25, 47]. Note here as well that these brain regions overlap with the regions observed for the main effect of delay phase (i.e., V1) and the interaction of delay phase and temporal expectations (i.e., SMG).

In a purely descriptive manner, the post-S1–pre-S2 index of correlation visualizes that the correlation of alpha power and $a_z$ emerges from different brain regions early in the delay phase compared to later in the delay phase. That is, in the early post-S1 time window correlation effects are stronger in the right hemisphere including STG, precuneous, cuneal, and motor cortices. The correlation effect in the later pre-S2 time window is stronger in the left hemisphere including MTG and ITG but also presents effects in the rigth hamisphere at SMG, angular gyrus, and insula.

## 8.4 Discussion

With the current experiment we wanted to explore memory decay in auditory sensory memory. Specifically, we raised the question in how far memory decay is reflected by modulations of alpha power. Moreover, we manipulated temporal expectations in order to find out whether the focus of attention towards the time-of-occurrence of the to-be-remembered sound stimulus counteracts the stimulus‘ decay over time.

Behavioral responses indicate that, as expected, memory decays over time. Both, proportion correct (PC) and $A_z$ present a decline in performance with longer delay

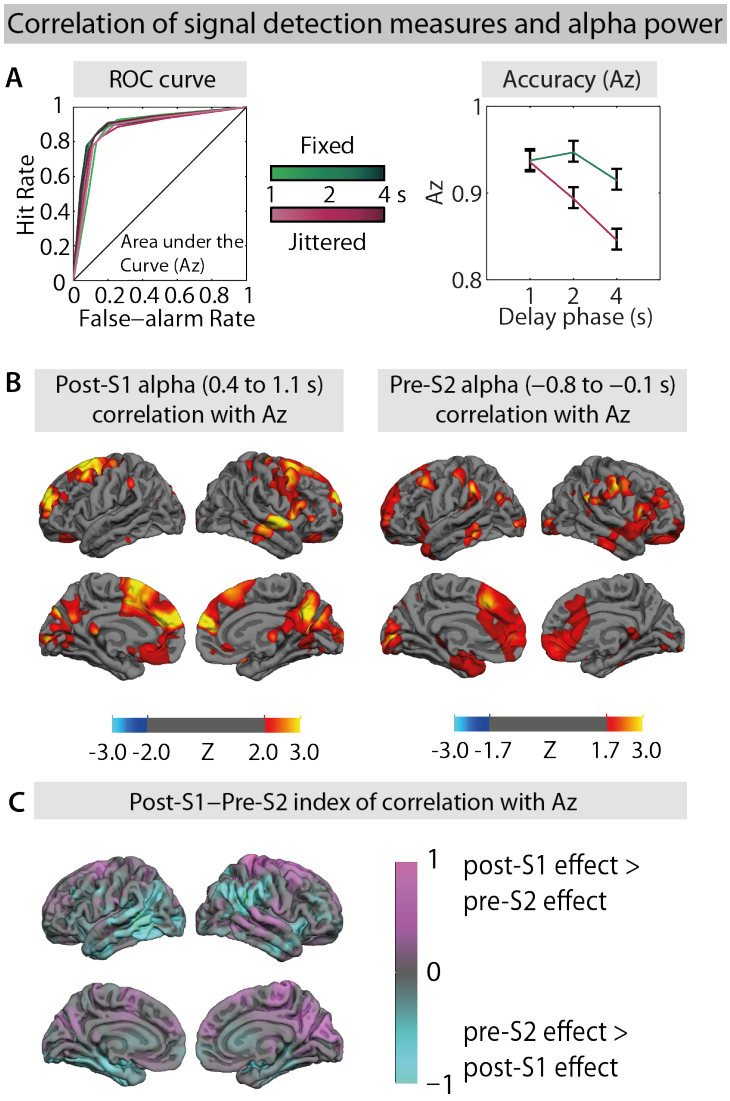


***Figure 8.4.*** **Correlation of signal detection measures and alpha power A.** Receiver-Operator Characteristics curves for each condition and Az. Errorbars represent within subject standard error. **B. Correlation of Az and source projected alpha power.** Left panel highlights brain areas correlating with Az in the post-S1 time window. Right panel highlights brain areas correlating with Az in pre-S2 time window.**C. Post-S1–Pre-S2 index of correlation with Az.** Purple-colored areas depict a stronger correlation with Az in the post-S1 time window. Cyan-colored areas depict stronger correlation with Az in pre-S2 time window.

phase. The interaction of temporal expectations and memory decay in PC as well as

in $A_z$ show that the decline in performance was reduced when foreperiods were fixed. Thus, on the behavioral level we could show that temporal expectations counteracted the decay in auditory sensory memory. However, this effect was more evident in the more sensitive measure $A_z$ than in PC.

### 8.4.1 Memory decay reflected by alpha power modulations

A correlation of alpha power and delay phase duration revealed that alpha power decreased with the passage of time, prior to the onset of the second sound. This finding is in line with previous studies reporting a decline of neural responses with memory decay (Fuster, 1999; Jha and McCarthy, 2000). From the "functional inhibition" perspective our findings lead to the assumption that a reduction in alpha power reflected reduced gating of information by means of inhibiting irrelevant information (e.g. Klimesch et al., 2007). Source projections of this effect indicated that the strongest modulation emerged from V1. But also other parietal areas, such as right IPL and precuneus were origins of the alpha power decrease. These source projections match very well to the broad range of working memory literature reporting an increase of parieto-occipital alpha power during the delay phase reflecting memory load, specifically reflecting the inhibition of visual areas (Bonnefond and Jensen, 2012; Haegens et al., 2010; Jensen et al., 2002; Jokisch and Jensen, 2007; Krause, 1996; Leiberg et al., 2006b; Sauseng et al., 2009; Tuladhar et al., 2007).

Increased right IPL BOLD response with increasing memory load has been found during the delay phase of an auditory working memory task (Leung and Alain, 2011). More generally, precuneus and IPL are part of the fronto-parietal network (Dosenbach et al., 2008). Sadaghiani et al. (2012) reported a positive correlation of alpha power and right and left inferior parietal lobe during resting state which points to a rather active process reflected by alpha power in IPL, contrary to the presumably inhibiting effect in V1. The involvement of these different areas seemed to be reflecting different processes. Effects emerging from V1 presumably reflected the inhibitory activity of alpha power, whereas IPL and precuneus rather reflected active attentional control during memory delay.

However, alpha power in these areas decreased with longer delay phase. As shown by behavioral performance, maintaining information in memory became more demanding as time passed. Why did we not observe an increase of alpha power with longer delay

phase indicating increased inhibition in V1, as well as increased attentional processing in IPL and precuneus? One explanation could be provided by the ongoing debate about memory decay: Does memory performance decrease because the memory trace fades away over the passage of time (Barrouillet et al., 2011; Mercer and McKeown, 2014)? Or does performance decrease because interferences become stronger over time (Lewandowsky et al., 2010; Oberauer et al., 2012; Oberauer and Lewandowsky, 2014)? A stronger interference implies a stronger need for inhibition of irrelevant/interfering information as well as stronger attentional control to protect the information stored in memory. As discussed above, greater protection of the stimulus in memory by means of inhibition of irrelevant information was shown to be reflected by an increase in alpha power. On the other hand, when the stored information fades away one could also expect before-mentioned mechanisms to be activated. But if the representations in memory (i.e., memory trace) vanishes, it might be possible that the stimulus that activates inhibitory and attentional processes is just not strong enough. Interestingly, the argumentation of interference holds best for verbal working memory (Oberauer and Lewandowsky, 2013). Therefore, we take the present findings as a support for the trace decay theory at least in auditory short term memory rather than as reflecting memory performance decline due to interference.

### 8.4.2 The effect of temporal expectations reflected by alpha power modulations

**Jittered and fixed foreperiods elicit differential effects on alpha power** We contrasted fixed and jittered foreperiods in order to find out whether temporal expectations modulate alpha power during the delay phase. A cluster test revealed that alpha power after fixed foreperiods was increased compared to jittered foreperiods just after the presentation of the first sound. This effect was independent of memory decay because at this point in time during the delay phase the duration of the delay phase was unknown. The origins of these effects were found in the right hemisphere, specifically, in inferior frontal gyrus (IFG), anterior cingulate cortex (ACC) and superior temporal gyrus (STG).

IFG, and STG are part of the ventral attention network with a strong right-hemisphere dominance. The network's main function is to direct attention to behavioral relevant stimuli and is responsive to sensory events or bottom-up driven (for reviews see Corbetta and Shulman, 2002; Shulman et al., 2009; Petersen and Posner, 2012). This

network is relevant for orienting and re-orienting attention based on cues (Driver et al., 2004).

The ACC as a part of the cingulo-opercular network has been argued to be involved in cognitive control and goal directed behavior (Dosenbach et al., 2007). Cognitive control in the framework of the current design would refer to the storage of the sound in memory. As discussed in a previous study (Wilsch et al., 2014), increased alpha power from the right cingulo-opercular attention network (i.e., insula) presumably reflects a controlling or 'gating' mechanism of stimulus maintenance (by inhibition).

The present data does not provide information about whether activity in rSTG is reflecting top-down processes related to attention, because rSTG as a primarily auditory brain area also has been shown to play a key role in retaining auditory information in sensory memory (Zatorre and Samson, 1991). Thus, increased alpha power might represent active stimulus maintenance processes, as alpha power has also been interpreted as a marker of internally directed attention (Ray and Cole, 1985). In contrast to the present alpha power increase at rSTG after presentation of the first sound, for instance Weisz et al. (2014) found pre-stimulus decrease in rSTG when attention was focused towards an external/physically present auditory stimulus.

How to interpret the increase of alpha power for fixed foreperiods then? With a fixed foreperiod duration attention is directed to a specific point in time. A jittered foreperiod, on the contrary, only allows for less precise focusing of attention. Because IFG and STG have been argued to respond rather stimulus driven, their alpha power increase might reflect the effect of temporal expectations towards the sound onset. Alpha power increase in ACC, on the other hand, could already reflect memory related control mechanisms, such as top-down modulated attention enhancing stimulus maintenance.

More specifically, these regions might present a network activated by temporal expectation that conveys stimulus maintenance in STG. Frontal brain regions have been found to be connected to and performing top-down control of STG. For example, the frontal eye fields have been found to be involved in top-down modulations of auditory cortical activity, which are part of the dorsal attention network and hence relevant for spatial attention (Müller and Weisz, 2012). Analogous in the visual domain, inferior frontal junction (IFJ) has been shown to drive top-down modulations in selective attention working memory tasks (Baldauf and Desimone, 2014; Zanto et al., 2013).

In order to clarify whether the identified brain regions (rACC and rIFG) are connected with rSTG in a similar manner as reported by M ller and Weisz, connectivity analyses would be needed. Here, complex valued spectral data in the alpha range is projected to source space and then phase-locking values of the regions of interests are calculated (see Müller and Weisz, 2012). In the present case, the goal would be to identify covariations of alpha phase locking in STG with phase locking in ACC and IFG.

Jittered and fixed foreperiods elicit different effects on decay related decline in alpha power Since the main effect of temporal expectations indicated that different foreperiod timings had an effect on alpha power per se, the aim was to find out whether a manipulation of temporal expectation might also have an effect on memory decay. In fact, an interaction of temporal expectations and delay phase revealed that the decline in alpha power after jittered foreperiods was stronger than after fixed foreperiods at the end of the delay phase. A similar pattern became also evident for the behavioral performance (i.e., PC and $A_z$). If temporal expectations counteracted memory decay behaviorally, these differential effects in alpha power decline might have indicated the corresponding effect for alpha power. As discussed above, increased alpha power presumably reflects the gating of the representation in memory and a decline in alpha power over time could be interpreted as an indicator for a vanishing memory trace or representation. Thus, a lesser decline in alpha power could imply a stronger and still actively maintained memory trace after fixed foreperiods. Mechanistically speaking, a fixed foreperiod elicited greater temporal expectations which are known to enhance the encoding precision (Rohenkohl et al., 2012). Enhanced precision of a sound masked by noise might have resulted in a clearer representation of the sound which first could lead to a more stable memory trace and further enabled facilitated pitch discrimination when the second sound was presented.

The interaction effect was localized to the left supramarginal gyrus (SMG) which has been shown before to be crucial for pitch memory (Gaab et al., 2003; van Dijk et al., 2010b). Van Dijk and colleagues localized alpha power to emerge from left SMG during the delay phase in a pitch discrimination task. They interpreted this alpha-power effect as inhibition of task irrelevant brain regions, since pitch is predominantly processed in the right hemisphere (Zatorre et al., 1992). Gaab et al. (2003) conducted an fMRI study

to also investigate pitch memory. They showed increased BOLD responses in bilateral SMG, whereas the response was stronger in the left hemisphere. They interpreted the left SMG to be a short-term pitch information storage site which is contradictory to the interpretation of van Dijk et al. (2010b). Furthermore, the BOLD signal emerging from the left SMG correlated positively with performance at the pitch-memory task. Critically, Gaab et al. applied a sparse sampling procedure which allowed for six different scanning time points ranging from zero seconds into the delay phase to six seconds into the delay phase. These six scanning points showed that the decay of left SMG BOLD response is less strong than in right SMG again underlining the importance of left SMG for pitch memory.

Thus, lSMG is crucial for pitch memory and the increased alpha power activity as presented in the present fixed foreperiod condition was beneficial for auditory sensory memory. However, we are not able to completely distinguish whether increased alpha power in lSMG reflects the inhibition of this region or rather active storage of the sensory information in memory.

### 8.4.3 Correlation of $A_z$ and alpha power

The present results indicated that temporal expectations and memory decay had similar effects on alpha power as on behavioral performance. In order to test whether there was a direct link between alpha power and performance (i.e., $A_z$) we correlated both variables independent of the experimental manipulations. The significant positive clusters we found on the sensor level in the beginning of the delay phase (post-S1) as well as in the end of the delay phase (pre-S2) replicated previous findings that also showed that an increase in alpha power is beneficial for working memory or short-term memory performance (Haegens et al., 2010; Roux et al., 2012; Wilsch et al., 2014).

Figure, 8.4C shows an index that depicts, on a descriptive level, that alpha power correlations with $A_z$ partially emerged from different sites in early delay phase stages than in the end of the delay phase. Therefore, we will discuss brain regions presenting this effect early on (post-S1) and at the end of the delay phase (pre-S2) separately. Source projections of the effects in both time windows (post-S1 and pre-S2) provided insightful information about the origins of this correlation. In the early time window, correlations of $A_z$ and alpha power emerged from the ventral attention network (STG and IFG), as well as from cingulo-opercular regions (ACC) and the fronto-parietal

network (precuneus). Similar to the effects of comparing jittered and fixed foreperiods (see above) alpha power was increased in regions which have been shown to orient attention in a bottom-up manner oriented towards the stimulus (ventral network) and top-down control (cingulo-opercular and fronto-parietal networks). Here again, the assumption is that alpha power did not inhibit these brain regions that are essential for task monitoring and task performance (Dosenbach et al., 2007; Dosenbach et al., 2008; Petersen and Posner, 2012). Instead, we would rather postulate that the alpha power increase in these areas reflected task beneficial activation of relevant attention networks. Again, connectivity analyses would give rise to connections with other brain areas maybe also providing evidence for inhibition of irrelevant, (maybe sensory) brain regions caused by activity emerging from the attention networks.

In the pre-S2 time window at the end of the delay phase, the correlation of alpha power and $A_z$ emerged primarily from bilateral ACC, left SMG, right IFG, and bilateral V1. As discussed before, increased alpha power most probably reflected the inhibition of visual information flow in order to gate auditory information in memory. Increased alpha power in ACC (cingulo-opercular network) was already found early in the delay phase and was interpreted as reflecting top-down modulation of maintaining the memory representation. Similarly, alpha power arising from rIFG correlated with $A_z$ already in the earlier time window. The involvement of ACC and rIFG during early and later stages of the delay phase implies an important role of alpha power emerging from these areas for auditory sensory memory from early stages of stimulus maintenance until the end of the stimulus maintenance.

Left SMG BOLD response has been reported to correlate positively with pitch memory performance (Gaab et al., 2003) and so does increased alpha power emerging from lSMG. Even though we discussed in a previous section that we are unable to tell whether the present SMG alpha activity reflects inhibition or active processing, the parallel between the effect reported by Gaab et al. (2003) and the present alpha power– $A_z$ correlation rather leads to the conclusion that increased alpha power reflects active processing in lSMG.

### 8.4.4 Conclusion

Altogether, we showed that alpha power and behavioral performance both declined with longer delay phase and that temporal expectations counteracted this decline on

the behavioral level as well as in alpha power. Source localizations of alpha power effects revealed numerous brain regions that, because of the positive correlation with $A_z$, appeared beneficial for auditory sensory memory. We found a strong involvement of the attention networks as well as visual and auditory sensory regions. However, the present data show that the mechanisms of alpha power are complex and one should be careful just assigning alpha power a single mechanism, such as functional inhibition. In order to attain a better understanding in how far the localized brain areas and the role of the respective increase of alpha power interacted and consequently enhanced memory performance, it will be necessary to perform connectivity analyses.

The present findings altogether encourage a more specific perspective on alpha power and its inhibitory role across brain areas and (trial) time.

# 9 Experiment IV: Temporal expectations modulate the forgetting curve

## 9.1 Introduction

In the previous chapter we demonstrated that temporal expectations counteract memory decay on the behavioral level as well as reflected by alpha power modulations. We also showed that behaviorally, the impact of temporal expectations was more evident for the performance measure $A_z$ (see Chapter: 4) than for proportion correct. However, since memory decay was manipulated with three different delay phase durations we were only able to fit a linear function onto $A_z$ in order to describe memory decay per se, as well as differences in decay according to manipulations of temporal expectations.

Peterson and Peterson (1959) were one of the first to show that short-term memory declines exponentially with the passage of time by fitting an exponential function to behavioral memory performance data. For that reason, in the context of memory, the exponential decay function is also known as the forgetting curve. Exponential decay functions have often been applied to describe the forgetting curve in short-term memory of animals (Zhang et al., 2005; Ziegler and Wehner, 1997) and humans (for a review see Rubin and Wenzel, 1996; Hesse and Franz, 2010; Wickelgren, 1969). Wickelgren (1969), for example, conducted a variety of auditory pitch-memory experiments showing that the exponential decay function explains memory decay for pitch.

Hence, the aim of the present experiment was to fit a forgetting curve or exponential decay function onto $A_z$, separately for fixed and jittered foreperiods in order to describe more precisely the effect of temporal expectations on memory decay. For that reason, memory decay was operationalized by means of six different delay phase durations (see below). We expected to find, similarly to the experiment in the previous chapter,

temporal expectations to counteract memory decay as reflected by less decline of $A_z$ after fixed compared to jittered foreperiods.

## 9.2 Methods

Nineteen healthy right-handed participants took part in this study (10 females) ranging in age from 23 to 33 years. All participants had self-reported normal hearing. Participants performed a delayed matching-to sample task with auditory stimuli presented in noise. The first sound sequence (S1) was presented followed by a variable delay phase. Then a second sound sequence (S2) was presented and participants had to judge whether S2 was same or different from S1 and also to indicate on a ternary scale the confidence on their response. Analogous to the experiment in the previous chapter, temporal expectations were manipulated via the manipulation of S1-onset times. A cue was presented prior to S1-onset indicating either e fixed (1.3 s) interval from cue-onset to S1-onset (i.e., foreperiod) or a jittered (0.7 – 1.5 s) interval. A fixed onset induced temporal expectations for S1-onset, whereas a jittered onset did not.

Since we wanted to assess auditory sensory memory decay by means of fitting an exponential decay function to the behavioral performance data, we needed enough data points to fit this function. For that reason, the delay phase varied in six steps logarithmically spaced between 0.6 and 7 s (i.e., 0.6, 1, 1.6, 2.6, 4.3, 7 s). Moreover, we aimed to observe a stronger decay effect with the longest delay phase of seven seconds compared to four seconds in the previous experiment.

The presented sound sequences were generated the same way as in the previous chapter (see also Section 4.2, for a detailed description). The SNR of sounds and noise was -17, equal to the previous experiment. Threshold estimation of pitch differences between S1 and S2 was estimated via two practice blocks also analogous to the previous experiment. Participants completed 360 trials in 10 blocks of 36 trials each. A block contained either trials with fixed or with jittered foreperiods and participants were informed about the type of foreperiod prior to each block. Delay-phase durations were equally distributed across blocks. The order of trials within a block and the order of blocks was randomized.

### 9.2.1 Data analyses

We investigated the performance measure $A_z$, a more sensitive measure than percentage correct, which takes the confidence ratings of each trial into account. The derivation of $A_z$ is described in Section 4.3.2. $A_z$ was computed for each of the twelve conditions (temporal expectations (2) $\times$ memory decay (6)) allowing for an estimation of memory decay along all delay phase durations separately for fixed and jittered foreperiods. One participant had to be excluded from further analyses because he or she did not make use of the entire confidence rating scale in at least two experimental conditions. For these data points $A_z$ could not be computed. Another participant presented the same behavior but only in one condition. Here, the missing $A_z$ value was interpolated by calculating the mean of the two adjacent conditions. Note that it was necessary for fitting an exponential decay function that participants presented $A_z$ values in each experimental condition.

We fitted function 9.1 (Glass and Mackey, 1988) onto $A_z$ to assess the decay in memory as a function of delay phase duration. This specific function contained a term describing decay and an additional term describing growth. This function has the advantage compared to simple decay functions that it takes the nature of physiological systems into account. That is, it assumes that in physiological systems activation declines and simultaneously new activation arises.

$$x(t) = (x_0 + e^{-\gamma t}) + (\frac{\lambda}{\gamma})(1 - e^{-\gamma t}), \tag{9.1}$$

where $t$ is equal to time (i.e., decay phase duration) $x_0$ corresponds to the intercept, $\gamma$ is the rate of decay, and $\lambda$ is the rate of production. $\frac{\lambda}{\gamma}$ refers to the asymptote when $\lim_{t\to\infty}$.

The initial parameters inserted into the functions were $x_0 = 0$, $\gamma = 0$, and $\lambda = 0.15$ where $x_0$ was bound between zero and one, and $\gamma$ and $\lambda$ were bound between zero and infinity. The model fit was computed with the lsqcurvefit function with Matlab (version 8.2, Optimization Toolbox) that allowed for 1000 iterations in order to find the best model.

In addition, we also fitted the decay term (i.e., first term) of this function and calculated the Bayesian information criterion (BIC; Schwarz, 1978) for each function and

for fixed and jittered foreperiods separately in order to compare the goodness of fit of both functions and to show that the more complex one is more suitable. The BIC corrects for an unequal number of parameters. Then, we averaged the BIC-scores across fixed and jittered foreperiods separately for each function. A t-test comparing the BIC-scores revealed that the scores for the complete function including both terms has lower scores, meaning a better model fit ($t(17) = 4.75, p < 0.0001$, Schwarz, 1978; Priestley, 1981). Therefore, all further analyses were conducted on the parameters resulting from the fit of the complete equation 9.1.

After the fitting of the function, a repeated measures multivariate ANOVA was computed on the resulting parameters $x_0$, $\gamma$, and $\lambda$ separated by jittered and fixed foreperiods in order to find out whether there is a global difference between jittered and fixed foreperiods. Subsequently, the parameters $\gamma$ and $\lambda$ were tested for differences between fixed and jittered foreperiods with t-tests, in order to find out whether temporal expectations counteract memory decay. The parameter $x_0$ was not tested, since first, it became evident from visual inspection of the data (see Fig. 9.2A) that there is no difference in the intercept between fixed and jittered and second, $x_0$ does not provide any information about decay. Four of the participants were excluded from the t-tests, because $R^2$, an indicator for goodness of the model fit, of their fitted models was smaller than 0.3 (see Fig. 9.1 for overall $R^2$ and Fig. 9.2B for individual model fits). The average $R^2$ indicating the goodness of fit was on average 0.66 including all participants and 0.80 without excluded participants for fixed and 0.72 with and 0.81 without excluded participants for jittered (see Fig 9.1).

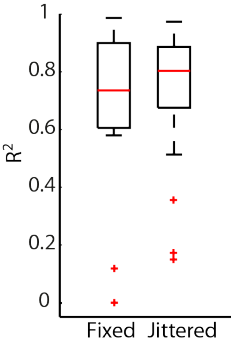


***Figure 9.1.*** **Goodness of fit in $R^2$.** Boxplots display distribution of $R^2$ across participants separately for fixed and jittered foreperiods. The red line indicated the median of the distribution, red crosses represent outliers extending ± 2.7 $\sigma$. Outliers are in total four participants that were excluded from further analyses.

## 9.3 Results and discussion

Figure 9.2A, left panel illustrates the decrease of $A_z$ with longer delay phase durations and shows that performance decayed differently for jittered and fixed foreperiods. The right panel of figure 9.2A illustrates the corresponding decay function averaged across the remaining fourteen participants. The two functions (jittered and fixed) show that until a delay phase duration of one second, memory performance was the same after fixed and jittered foreperiods, whereas after longer delay phases, performance declined less strongly after fixed than after jittered foreperiods.

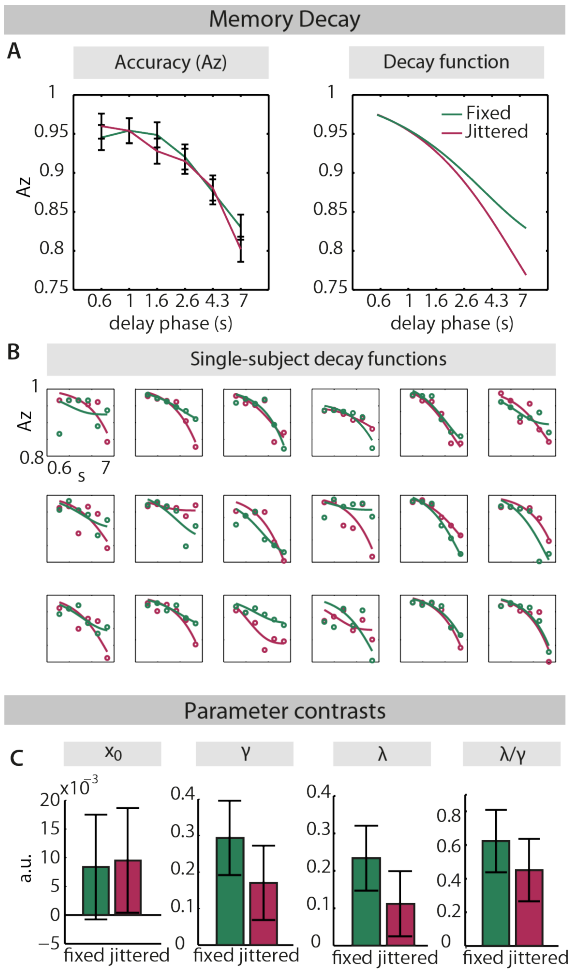


***Figure 9.2.*** **Memory decay A.** Left panel: $A_z$ values for each delay phase duration separated by fixed and jittered foreperiods. Error-bars indicate within-subject standard error. Right panel: Exponential decay function fitted on $A_z$ averaged across participants separated by fixed and jittered foreperiods. **Single-subject decay functions B.** Single-subject fits of exponential decay function (lines) on $A_z$ (dots) separated by fixed and jittered foreperiods. Participants excluded from further analyses because $R^2 < 0.3$ were number 1, 8, 10, and 16. **Parameter contrasts C.** Average parameter estimates for each parameter $x_0$, $\gamma$, $\lambda = 0$, and $\frac{\lambda}{\gamma}$ for fixed and jittered foreperiod trials separately. Errorbars bars depict within-subject standard error.

The least-square model fit led to equation 9.2 for fixed foreperiods and equation 9.3 for jittered foreperiods (see also Fig. 9.2).

$$\text{fixed foreperiods: } x(t) = (0.01 + e^{-0.29t}) + (\frac{0.23}{0.29})(1 - e^{-0.29t}) \tag{9.2}$$

$$\text{jittered foreperiods: } x(t) = (0.01 + e^{-0.17t}) + (\frac{0.11}{0.17})(1 - e^{-0.17t}) \tag{9.3}$$

The repeated measures multivariate ANOVA showed that jittered and fixed foreperiods differed across estimated parameters on trend-level ($F(1, 13) = 4.18, p = 0.062$). Although this effect has not reached our designated level of significance ($p < 0.05$), we considered this trend effect as an indicator that fixed and jittered foreperiods differed with regards to the estimated parameters. A more trivial finding is that parameters differed from each other ($F(2, 26) = 6.137, p = 0.027$). Moreover, there was a significant interaction of foreperiods and parameters ($F(2, 26) = 6.125, p = 0.025$), indicating that parameters did not vary between fixed and jittered foreperiods to the same extent.

Subsequent t-tests on $\gamma$, and $\lambda$ revealed that there was an effect on trend level of $\gamma$ ($t(13) = 1.91, p = 0.077$; see Fig. 9.2C). The t-test on $\lambda$ showed that $\lambda$ was significantly greater for fixed than for jittered foreperiods ($t(13) = 2.23, p = 0.044$; see Fig. 9.2C). The asymptote after fixed foreperiods was significantly larger than 0.5 with a 95 % confidence interval from 0.52 to 0.82 ($t(13) = 2.38, p = 0.029$), whereas the asymptote after jittered foreperiods did not differ from 0.5 with a 95 % confidence interval from 0.26 to 0.64 ($t(13) = -0.54, p = 0.59$).

Despite the fact that $\gamma$ increased by trend in fixed foreperiod trials indicating that memory decays faster, temporal expectations due to the fixed-foreperiod appeared to have counteracted a decline in memory performance. The reason for that is that the production rate $\lambda$ is significantly increased when the to-be-remembered sound was temporally expected. Therefore, $\gamma$ can not be interpreted by itself but $\lambda$ has also be taken into account as a factor counteracting the decay. Critically, the ratio of $\lambda$ and $\gamma$ hence the ratio of decay and production (i.e., asymptote) describes to what level performance can decline, the actual decrease in memory performance. The effect in $\lambda$

being more stronger than the effect in $\gamma$ shows the tendency of the data presenting also a greater effect in $\frac{\lambda}{\gamma}$.

When relating the estimated parameters to actual memory processes, $\gamma$ indicates the speed of the decay or the speed of a memory representation to fade away. $\lambda$ as the production rate is more difficult to interpret. Literally, this rate reflects the production of memory representations. Memory processes that could be interpreted as an internal production of a memory representation is for example rehearsal. Although the presented pure-tones are difficult to rehears, $\lambda$ being greater than zero is an indicator that maintenance processes such as refreshing of the memory representation might have taken place either during the delay phase or during retrieval of the stored stimulus, when S2 is presented (Barrouillet et al., 2004). The asymptote ($\frac{\lambda}{\gamma}$) represents the memory performance after an infinite amount of time. The asymptote for fixed foreperiods was significantly greater than 0.5, the behavioral chance level. That shows that temporal expectations prevented memory performance to decline as strongly as without temporal expectations.

Altogether, the parameter estimations of the exponential decay functions reveals that temporal expectations not exactly counteract the decay process in auditory sensory memory. Instead, temporal expectations rather enhance refreshing of the memory representation throughout the delay phase which ensures a task performance above chance level.

# 10 General discussion

The aim of the present thesis was to assess the potentially facilitating impact of temporal expectations on working memory limitations. Working memory limitations were conceptualized as memory load and memory decay. Memory load was manipulated by means of auditory stimuli (verbal and non-verbal) presented in noise, because degraded speech has been specifically shown to increase memory load and to modulate respective markers of load such as alpha power and behavioral performance. Memory decay was explored by picking up on the concept of auditory sensory memory. For that reason, non-verbal sounds were presented instead of speech signals.

Three magnetoencephalography (MEG) and one behavioral experiment were conducted in order to investigate oscillatory brain responses and behavioral responses to memory load and memory decay as well as their modulation through temporal expectations. In this chapter, the results will be first summarized and then further discussed.

## 10.1 Summary of experimental results

*Experiment I* addressed the question whether temporal expectations for a syllable embedded in noise counteracted memory load. We could demonstrate that due to temporal expectations, indicators of memory load, such as alpha power during the delay phase, were decreased and behavioral performance (percentage correct, $A_z$, response times) was improved. The effect of alpha power was localized in the right insula, part of the cingulo-opercular network (Dosenbach et al., 2008). Moreover, we could show that the effect of temporal expectations in alpha power correlated positively with the effect of temporal expectations in memory performance.

In order to explore whether the effect of temporal expectations on memory load and alpha power, was specific to processing speech-in-noise, the same experiment was conducted without noise (*Experiment IIa*) on a subset of participants of *Experiment I*. This comparably easy working memory task did not elicit as much memory load as the

noise experiment (significantly better task performance compared to noise). Temporal expectations did not modulate alpha power during the delay phase. Also on a statistical level we were able to show that the effect of temporal expectations on alpha power was significantly larger in noise compared to clear speech.

Since the modulation of temporal expectations was induced by variable foreperiod durations, this design allowed for an assessment of temporal expectations based on the passage of time across temporal cues (i.e., hazard rate function, see Section 2.1; *Experiment IIb*). Here, we were able to demonstrate that longer foreperiods resulted in a decrease in alpha power during the delay phase, but also increased the phase coherence of neural oscillations in the slow-delta range during S1 presentation. Interestingly, longer foreperiods additionally increased the phase coherence of neural oscillations in the slow-delta range (corresponding to stimulus presentation frequency) during S1 presentation. Increased phase coherence indicated a state of increased excitability. Independent of foreperiod duration, we could show that increased delta phase coherence at S1 predicted decreased alpha power during the delay phase linking the effect of enhanced excitability (phase-coherence) and reduced memory load (alpha power).

In order to attain a more complete picture of alpha power modulations by working memory limitations, we investigated memory decay in auditory sensory memory in *Experiment III*. Memory decay has been already profoundly investigated before. However, the impact of temporal expectations on memory decay as well as the modulation of alpha power with respect to memory decay seem to not have been explored before. Behaviorally, we showed that, besides the expected decline in performance over time, memory decay was less strong when the to-be-remembered stimulus was temporally expected. Furthermore, it turned out that alpha power declines with memory decay, similarly to the decline in task performance. This effect emerged primarily from visual cortices (V1) and other posterior regions such as right inferior parietal lobe (IPL) and precuneus.

Moreover, temporal expectations exerted an effect on alpha power during early stages of the delay phase independent of memory decay. That is, alpha power was increased in the right hemisphere, when to-be-remembered stimuli were temporally expected. This effect was localized in inferior frontal gyrus (IFG), anterior cingulate cortex (ACC) and superior temporal gyrus (STG). Similarly to the behavioral performance, temporal

expectations counteracted the decline in alpha power with longer delay phases. This effect was localized in the left supramarginal gyrus (SMG).

Lastly, a correlation of alpha power with $A_z$ presented a direct link between alpha modulations and behavioral performance. This effect partially emerged from different sites in early delay-phase stages than in the end of the delay phase. At early stages, correlations of $A_z$ and alpha power emerged from the ventral attention network (STG and IFG), as well as from cingulo-opercular regions (ACC) and the fronto-parietal network (precuneus). At the end of the delay phase, the correlation of alpha power and $A_z$ emerged primarily from bilateral ACC, left SMG, right IFG, and bilateral V1.

The last experiment (*Experiment IV*) picked up on the interaction of temporal expectations and memory decay. In principle, the same design as in the previous experiment was tested behaviorally. This time, memory decay was manipulated by means of six instead of three different delay phase durations. That allowed us to fit an exponential decay function (i.e., forgetting curve) onto the performance data. The aim was to describe memory decay depending on temporal expectations. Two parameters of the function were critical for decay. The first described the actual decay ($\gamma$) and the second described the degree to which memory processes, such as refreshing of the memory representation, were able to counteract the decay ($\lambda$). No significant differences between temporally expected and non-expected trails were found for the decay parameter. However, the second parameter was greater in trials with temporal expectations indicating stronger refreshing of the memory representation resulting in an overall less steeper forgetting curve.

The next section will discuss the initial aim of the present thesis which was to assess in how far temporal expectations modulate memory limitations. First, the behavioral results will be discussed which will serve as a basis for a discussion of the effects of alpha power across all experiments.

## 10.2 How temporal expectations improve auditory memory performance

On the behavioral level, temporal expectations clearly had a beneficial impact on memory performance in high-load settings. Memory performance increased when syllables in noise were temporally expected, reflecting a decrease of memory load (see Zanto and Gazzaley, 2009). It seems as if temporal expectations enhanced the encoding precision

(Rohenkohl et al., 2012; Cravo et al., 2013) which in turn generated a more precise memory representation (see van den Berg et al., 2012) resulting in improved memory performance. For auditory sensory memory, temporal expectations counteracted memory load and memory decay in a similar way.

The beneficial effect of temporal expectations on memory load and memory decay is in line with the Time-Based Resource-Sharing model (TBRS; Barrouillet et al., 2004; Barrouillet et al., 2007) which claims that memory decay depends on memory load. One of the assumptions of the TBRS is that the processing and the maintenance of information rely on the same source of attentional resources. An increase in memory load is reflected in an increased need of attentional resources to process high-load information. That consequently reduces the amount of available resources necessary to activate the maintained representation in order to prevent decay. Due to the high demand of resources when memory load is high, stored information decays faster. Hence, when load is reduced due to temporal expectations, more resources are available to keep the memory representation active and to counteract decay.

Moreover, temporal expectations modulated the forgetting curve that was fitted onto the performance data of an auditory sensory memory task (*Experiment IV*). The fitted curve-parameters indicated that not the fading out of the memory trace per se is slowed down ($\gamma$-parameter) but rather resources refreshing the representation were enhanced by temporal expectations ($\lambda$-parameter). To this end, the speed of decay did not differ between expected and unexpected trials. However, temporally expected trials presented increased refreshing of the memory representation which has been shown to enhance stimulus maintenance (Barrouillet et al., 2007). In principle, the $\lambda$-parameter described an increased amount of attentional resources preventing memory decay as suggested by the TBRS model. Hence, for both, memory load and memory decay, the present thesis provides evidence for a beneficial effect of temporal expectations on memory performance.

### 10.2.1 Implications for resource models of auditory working memory

The presented data showed that the maintenance of auditory stimuli in memory is challenged when stimuli are embedded in noise. The data also revealed that temporal expectations for the to-be-remembered auditory stimulus facilitates the maintenance by reducing memory load, especially when stimuli are degraded by a noise masker.

Pichora-Fuller and Singh (2006) explained that speech-in-noise increases memory load because additional attentional resources are needed to process degraded speech. The reason why these additional demands result in poorer working memory performance is in line with resource models of working memory (Ma et al., 2014) as well as with the Time-Based Resource-Sharing model (TBRS; Barrouillet et al., 2004, for both kind of models see also Chapter 1): The common ground of these models is the main assumption that attentional resources necessary to encode and maintain information in memory are limited. Consequently, higher memory load requires more resources, which in turn leads to decreased precision of the memory representation and to poorer memory acuity.

To reiterate, the precision of a memory representation is essential for memory performance (van den Berg et al., 2012). Memory precision can vary during encoding, maintenance, and retrieval. Variation in memory precision are based to some extend on random neural fluctuations. If degraded information enters working memory or sensory memory, precision will be already decreased at the encoding level. Thus, the neural representation of the stimulus is more noisy which results in less memory acuity (e.g., Bays, 2014). The results of the present thesis reveal, however, that temporal expectations enhanced the encoding precision (Rohenkohl et al., 2012) of degraded auditory signals thereby yielding increased working memory acuity. A better precision of the to-be-stored information at the encoding level benefits a more precise memory representation during the stage of maintenance. Hence, due to temporal expectations, the maintained memory representation is more precise which in turn results in improved memory acuity and memory performance.

In addition, the TBRS claims that resources that are needed to encode information are drawn from the same pool of resources as the ones necessary to maintain the representation. The concept of shared resources among encoding and maintenance explains the lack of memory acuity for degraded signals. It also explains improved memory because of temporal expectations: the more a signal is degraded, the more resources are needed for signal encoding and less resources are available for signal maintenance.

In principle, I suggest that both, the concept of precision and the concept of shared resources provide explanations for the beneficial effect of temporal expectations on auditory working memory: A lack of precision as well as a lack of resources draw

on memory acuity in a similar way because less precision affords more of these limited attentional resources (Bays et al., 2009). Thus, degraded auditory information increases memory load and is consequently not as well maintained as information that requires less processing.

## 10.3 How alpha power fluctuates with memory limitations

In this section, the observed alpha power fluctuations will be discussed, first for memory load, next for memory decay, and then with regards to behavioral performance.

### 10.3.1 Alpha power as a marker of memory load

Alpha power was modulated by the impact of temporal expectations on memory load. In line with the findings of Obleser et al. (2012), we were able to demonstrate that memory load induced by degraded speech led to increased alpha power. A reduction of load by means of temporal expectations concomitantly reduced alpha power (*Experiment I*). This effect was interpreted as a reduced need for functional inhibition (e.g., Jensen et al., 2002).

On the other hand, when the speech signal was clear (no noise-masker), memory load was low as indicated by the high task performance (*Experiment IIa*). In this low-load situation, temporal expectations induced via symbolic cues did not have any impact on alpha power or memory load. Temporal expectations did naturally not enhance the encoding precision of clear speech as much as of speech-in-noise because precision was about to be maximal for clear speech. Instead, alpha power and thus memory load were reduced as a function of foreperiod duration (*Experiment IIb*) a more implicit source of temporal expectations (i.e., hazard rate function, see Section 2.1). Although, memory performance reached a ceiling effect, alpha power still varied with foreperiod duration. These results raise the assumption that temporal cues were ignored, presumably because their processing in such a low-load environment was too costly. Temporal expectations based on the passage of time seemed to be significant enough to modulate neural markers of memory load without affording processing costs that were disproportional high in relation to this overall low-cost task.

Contrary to *Experiment I* and *Experiment II*, in *Experiment III*, alpha power was increased during early stages of the delay phase, when the to-be-remembered stimulus

was temporally expected. Although the topography as well as the source localization in both cases revealed that alpha power effects emerged from the right cingulo-opercular network, the alpha-power effect in *Experiment III* was the opposite from the effects described in *Experiment* I and *Experiment IIb*.

What is causing this reversal of effects? Two differences between *Experiment I* and *Experiment III* could explain the reversal of the alpha power effect: First, differences in the implementation of temporal expectations in the experimental designs and second, differences between the stimuli

In *Experiment I*, temporal expectations were modulated with three different jittered foreperiod durations. In *Experiment III*, temporal expectations were modulated via a fixed foreperiod and a jittered foreperiod. At this point, it is impossible to tell, whether these foreperiod manipulations lead to one or another effect in alpha power during the delay-phase. However, in *Experiment IIb*, temporal expectations were tested based on the foreperiod duration which resulted in a similar effect as in *Experiment I*: less alpha power following temporally more expected stimuli. Thus, it seems as if the way temporal expectations were implemented does not explain different alpha-power effects.

Different stimuli in *Experiment I* and *Experiment III* are another possible reason for a reversal of the alpha power effect. It has been argued before that the maintenance of verbal and non-verbal stimuli relies on different processes: Verbal information is mainly maintained by means of articulatory rehearsal plus additional attentional resources that are focused onto the memory representation (Mora and Camos, 2013). Maintenance of non-verbal information, on the other hand, solely relies on attentional resources that refresh and keep the memory representation active throughout the delay phase (Barrouillet et al., 2004; Camos et al., 2011; Vergauwe et al., 2014).

But why would the difference in maintenance processes result in *reduced* alpha power for temporal expectations on verbal working memory and *increased* alpha power for temporal expectations in auditory sensory memory? Both systems have in common that attentional resources are allocated to store information. It is very likely that alpha power in *Experiment I-III* reflected these attentional resources (see below for a more in depth discussion about alpha power and attentional resources). Under this condition, in *Experiment I* and *II*, allocation of these resources was decreased when stimuli were expected. Therefore, it could be possible that articulatory rehearsal sufficed to main-

tain the stimulus. In contrast, when the stimulus was unexpected and the precision of the memory representation was lower, articulatory rehearsal alone might not have been able to store the stimulus. Additional attentional resources had to be allocated to enable stimulus maintenance. This assumption is supported by the positive correlation of alpha power and performance modulation in *Experiment I* that shows that a lack of temporal expectations can be compensated by increased alpha power and consequently increased attentional resources.

However, the question remains how this logic applies to the opposite alpha power effect in auditory sensory memory where increased alpha power seemed to be necessary to perform the task at all. Again, in non-verbal memory stores such as auditory sensory memory, solely the allocation of attentional resources enables the maintenance of information (Vergauwe et al., 2014). Therefore, it seems as if temporal expectations facilitated the allocation of these attentional resources which were necessary to maintain the representation in memory. These resources were reflected in increased alpha power during the delay phase. Thus, the differences in maintenance between verbal and non-verbal stimuli is more likely to explain the reversal of the alpha power effect from one experiment to another than differences in the implementation of temporal expectations.

Altogether, these findings add up nicely to previous findings on the beneficial effects of top-down modulations of working memory by means of selective attention (for a review see Gazzaley and Nobre, 2012). In the following section changes of alpha power reflecting memory decay per se as well as alpha power reflecting the interaction of temporal expectations and memory decay will be discussed.

### 10.3.2 Alpha power as a marker of memory decay

The studies conducted in the present thesis did not only reveal a beneficial effect of temporal expectations on memory load but also on memory decay (*Experiment III, Experiment IV*). This was shown by improved task performance and also by modulations of alpha power. First of all, we could show that alpha power decreased the longer information was stored in memory. This finding is in line with previous findings indicating a decrease of neural responses the longer information was stored in memory (Fuster, 1999; Jha and McCarthy, 2000). However, when the to-be-remembered stimulus was temporally expected, the decline in behavioral performance as well as in alpha power

was less strong. As already suggested, the TBRS model provides an explanation why temporal expectations counteract decay because they reduce memory load.

But in how far does the concept of the TBRS apply to the modulations of alpha power during the delay phase found for memory decay? Alpha power was increased when stimuli were temporally expected. It is very likely that alpha power reflects the attentional resources that activated and refreshed the memory representation and counteracted memory decay. Thus, it seems as if the reduction of memory load enabled the allocation of more resources that were applied onto the memory representation in order to enhance maintenance.

The decay function that was fitted onto memory performance data (*Experiment IV*) revealed differences in the parameter reflecting refreshing of the memory representation of the decay function ($\lambda$). This finding supports the interpretation of alpha power being a marker of attentional resources enhancing memory maintenance. As suggested before, the $\lambda$-parameter of the curve fit described an increased amount of attentional resources that were allocated to prevent memory decay as suggested by the TBRS model. These additional resources are likely to be reflected by increased alpha power during the delay phase.

These findings altogether show that temporal expectations reduced memory load as well as memory decay, although the direct manipulations of temporal expectations differed across experiments. In order to evaluate the significance of alpha power fluctuations, it is important to elaborate on the relationship between alpha power and behavioral outcome. This will be done in the next section.

### 10.3.3 Alpha power modulates behavioral performance

The results of the present thesis presented positive correlations of alpha power and memory task performance (see also Haegens et al., 2010; Roux and Uhlhaas, 2013). In *Experiment I*, it was shown that the modulation of alpha power by temporal expectations correlated positively with the modulation of task performance by temporal expectations. That indicates that the impact of temporal expectations on alpha power predicted a comparably similar impact on behavioral performance. Furthermore, this correlation also showed that stronger alpha power in the absence of temporal expectations led to increased task performance in a compensatory way. Similarly, in *Experiment III*, alpha power also correlated positively with task performance. Interestingly,

even though this correlation was across experimental conditions, source localization revealed a great overlap with alpha power effects due to experimental manipulations. In Experiment II(a+b) no correlations were found because of the ceiling effect in behavioral performance. The results allow for the conclusion that the modulations of alpha power by the experimental manipulations (i.e., temporal expectations, memory load, and memory decay) were directly linked to the memory outcome.

In the next section, the underlying mechanisms that enabled the reduction of memory load and counteracted memory decay will be discussed.

## 10.4 Neural excitability enables temporal expectation benefits

The facilitatory effect of temporal expectations on stimulus maintenance is a rather remote effect. The actual impact of temporal expectations have already taken place during encoding of the expected target stimulus by increasing the neural excitability at the time of stimulus presentation. Across trials, neural excitability is reflected in increased phase coherence (for a review see Schroeder and Lakatos, 2009).

An increase of phase coherence was shown before when temporal expectations were induced by symbolic cues (Stefanics et al., 2010). More prominent, however, are the findings of increased phase coherence due to neural entrainment to a rhythmically presented stimulus sequence (Cravo et al., 2013; Henry and Obleser, 2012; Herrmann et al., 2013; Lakatos et al., 2013). The presentation of clear speech in *Experiment IIb* allowed for precise analyses of neural phase at stimulus presentation. Note that, when speech was embedded in noise (*Experiment I*), the ongoing noise masker most likely has caused a more noisy neural response preventing the analysis of subtle systematic changes. In fact, delta phase coherence during syllable presentation increased as a function of foreperiod duration at right fronto-temporal sensors. Hence, not only temporal cues and rhythmic stimulus presentation elicit increased excitability, but also temporal expectations based on the passage of time. In addition, it was demonstrated that phase coherence correlated negatively with alpha power during stimulus maintenance. That indicates that temporal expectations increased neural excitability which led to enhanced encoding precision enabling a decrease of memory load reflected by reduced alpha power. Neural excitability is most likely the central link between temporal expectations and memory load.

So far, evidence has been accumulated that temporal expectations alleviate working memory limitations by means of enhancing neural excitability at the to-be-remembered stimulus. Moreover, the beneficial effect of temporal expectations was in most cases reflected by alpha power modulations. In order to understand the functional role of alpha power, underlying neural sources within the framework of functional inhibition will be discussed.

## 10.5 Alpha power and functional inhibition

The source localizations conducted in the present thesis allow for interpretations of the functional role of alpha power throughout stimulus maintenance in working memory and auditory sensory memory. Alpha power effects were found to emerge primarily from regions that are part of attention networks; further effects were found to also emerged from sensory regions. For example, the alpha power effect of temporal expectations in *Experiment I* as well as in *Experiment III* emerged from the cingulo-opercular network. Whereas the effect in *Experiment III* was more spread-out and also showed involvement of the ventral attention network as well as superior temporal gyrus (STG), an auditory region. The decline in alpha power with memory decay (*Experiment III*) was localized in the fronto-parietal network as well as in primary visual cortex (VI). The interaction of temporal expectations and memory decay emerged from left supramarginal gyrus (SMG). Note that the individual functional roles of these localizations are discussed in the discussion sections of the respective chapters. This section here will attempt to generate a more nuanced perspective on the functional role of alpha power across all findings.

Initially, an increase in alpha power was explained within the framework of functional inhibition (see Secition: 1.2.2; Jensen et al., 2002; Klimesch et al., 2007), a mechanism that gates the transmission of information through inhibition and activation of brain regions. Inhibition has been argued to be reflected in increased alpha power whereas decreased alpha power enhances neuronal excitability and thus reflects active processing of information. However, the question that is raised here, is, in how far the present findings are compatible with the concept of functional inhibition. The strong involvement of attention networks implies that alpha power might not just reflect immediate inhibition of the region from where it emerges. As already discussed in Chapter 5

and Chapter 8, the cingulo-opercular network and the fronto-parietal network comprise the executive control system performing top-down focus of attention most likely enhancing stimulus maintenance. The ventral attention system operates in a rather bottom-up stimulus driven fashion (Petersen and Posner, 2012). These networks have been shown before to be active and relevant during working memory maintenance (Leung and Alain, 2011, for reviews see Jonides et al., 2008 and Postle, 2006). Moreover, Sadaghiani et al. (2012) found a positive correlation of alpha power and the BOLD response of the cingulo-opercular network. Therefore, it is not very likely that alpha power emerging from these areas reflected directly an inhibiting mechanism.

Based on the findings of Ray and Cole (1985), alpha power has also been interpreted as a marker of internally directed attention and, more specifically, of transmitting information in working memory (for a review see Palva and Palva, 2007). At least in visual working memory Palva et al. (2010) showed that alpha power played a major role in the communication between frontal regions underlying maintenance of working memory as well as frontal- and visual regions during stimulus maintenance. Hence, their findings are in line with the present interpretation that alpha power from executive control system reflected the system's top-down enhancing of stimulus maintenance.

Now, returning to the framework of functional inhibition, most of these findings supporting direct inhibition are based on alpha power emerging from sensory regions (e.g. Haegens et al., 2010; van Dijk et al., 2010b; Jensen et al., 2002; Whitmarsh et al., 2014). In the present thesis, alpha power declining with memory decay emerged from V1 and is indeed most likely to reflect inhibition of this task-irrelevant sensory area. However, the present localizations of alpha power are also partially in line with claims from Palva and colleagues. Nonetheless, the findings are also commensurate with the concept of alpha power to functional inhibit task-irrelevant (sensory) brain areas to support the gating or transmission of the relevant information. Thus, it seems as if the observed alpha power fluctuations during stimulus maintenance represent a complex network of internally directed attention that enhances working memory processes via active top-down modulations of sensory areas by means of increased alpha power in attention networks. In the sensory areas, either the representation of the stimulus in memory is enhanced or irrelevant areas such as V1 in an auditory memory task are functionally inhibited. Additional connectivity analyses would provide necessary

information that could actually support or reject this interpretation (Hipp et al., 2011; Hipp et al., 2012; Müller and Weisz, 2012).

## 10.6 Conclusions

The presented results indicate that top-down modulations via temporal expectations are beneficial for auditory working memory. Specifically, due to temporal expectations the encoding precision of auditory stimuli presented in noise was enhanced. That in turn resulted in decreased memory load and concomitantly counteracted memory decay. The Time-Based Resource-Sharing model (TBRS; Barrouillet et al., 2004) accounts for these results in so far that it claims that stimulus processing or encoding and stimulus maintenance draw on the same cognitive resources and therefore, memory decay is modulated by memory load. Thus, improved stimulus encoding allowed for the recruitment of more attentional resources which in turn enhanced stimulus maintenance. That means specifically for auditory memory that memory load and memory decay varies with the encoding precision of the to-be-remembered information.

The findings on alpha power during stimulus maintenance are also in line with the TBRS. The maintenance of verbal (Experiment I) and the maintenance of non-verbal stimuli (Experiment III) elicited different alpha power effects, which can be explained by different maintenance strategies (rehearsal vs. attentional resources e.g., Vergauwe et al., 2014). Still, enhanced maintenance activity in terms of increased attentional resources was reflected by increased alpha power. That again explains that alpha power declined faster over time when stimuli were temporally unexpected because more resources were needed for stimulus encoding and less resources were available for stimulus maintenance.

Lastly, alpha power source localizations revealed that attention networks such as the cingulo-opercular, fronto-parietal, and the ventral network were involved in the maintenance of auditory information. The crucial role of these networks for working memory (Postle, 2006) contradicts a direct inhibition of these areas in terms of functional inhibition. Therefore, I suggest that alpha power emerging from these regions rather modulates stimulus maintenance in a top-down fashion by inhibiting task-irrelevant brain regions such as primary visual cortex.

Altogether, the results of the present thesis provide evidence for a beneficial effect of a-priori temporal expectations for an auditory signal on working memory. Moreover, alpha dynamics were shown to be a distinct marker for the neural efficiency of managing working memory limitations.

# 11 Future research implications

The findings of the present thesis accumulated evidence on the role of alpha power during auditory working memory in young adults. However, these findings brought up further questions that, so far, have not been answered, yet. The first question concerns special populations, specifically, healthy aging people. Do they benefit from temporal expectations in auditory working memory? The second field of questions addresses additional methodological approaches such as connectivity analyses and electrocorticography (ECoG). A different methodological scope could provide more information about the functional role of alpha power in auditory working memory.

## 11.1 Temporal expectations and alpha power in a healthy aging population

The results of the present thesis showed that in young adults, temporal expectations reduced memory load imposed by auditory stimuli presented in noise during working memory maintenance. Presumably, encoding of the degraded stimuli was enhanced which resulted in a more precise memory representation. For healthy aging participants with normal hearing, for example, it has been shown to be very effortful to listen to and comprehend speech in noisy environments (Pichora-Fuller, 2003). This raises the question whether temporal expectations for speech signals would be similarly or even more beneficial for older people as for younger people. First, it would be of interest to test whether temporal expectations for clear speech, yet perceived noisy by older participants, improve stimulus encoding and concomitantly reduce memory load. Second, in how far would temporal expectations be beneficial if an additional noise masker would degrade the speech signal?

It is important to note that not only the decline in hearing acuity but also the decline in cognitive processing, both, perturb the comprehension of spoken speech signals

(Pichora-Fuller, 2003). Accordingly, it was shown that the ability to focus attention is reduced in older adults (Gazzaley et al., 2005). This cognitive limitation might also prevent the generation of temporal expectations. In fact, the findings of Zanto et al. (2011) revealed that older participants did not use temporal cues in a visual response task. However, it needs to be shown whether older participants still are able to make use of temporal expectations in so far as expected target stimuli alleviate subsequent memory load.

In the present thesis, alpha power was the crucial marker for memory load. For older participants, alpha power could serve again as an index for whether temporal expectations are beneficial for auditory working memory processes. It has been shown before that alpha power shows less modulation by selective attention in older adults (Vaden et al., 2012; Zanto et al., 2010). The question remains whether reduced alpha power modulation also applies to modulations by temporal expectations and memory load.

Healthy older adults present less hearing acuity, a decreased ability to generate temporal expectations, and reduced alpha power modulations. For these reasons it would be very interesting to find out whether there is a certain way to induce temporal expectations to which older adults are most susceptible. For example, temporal cues might be too costly to process. Instead, temporal expectations based on the passage of time (see Experiment IIb Nobre et al., 2007) might induce expectations in a more automatic fashion. Alpha power could still serve as a marker for memory load fluctuations but would be most probably less modulated as observed in young participants.

## 11.2 Expanding the methodological scope

The results of the present thesis give rise to open questions employing different methods than the ones described here. One question addresses the connectivity of brain regions and the other one considers electrocorticography (ECoG) as a method that provides a great spatial resolution as well as clear signals representing active processing states.

### 11.2.1 Connectivity analyses

Source localizations of alpha power in the present thesis gave rise to a number of different brain regions exhibiting effects of alpha power. Alpha power effects were emerging

from primary auditory and visual brain regions as well as from parts of different attentional networks. These different regions led to implications on the functional role of alpha power in auditory working memory. The question arose whether alpha power in attentional networks modulate activity in sensory regions in order to enhance working memory maintenance (see Section 10.5). In order to accumulate evidence in favor of or against this hypothesis, connectivity analyses could be conducted in a next step.

Most evidence on connectivity of brain areas has been accumulated with fMRI and the correlation of the blood oxygen level-dependent (BOLD) signal of different brain regions (e.g., Dosenbach et al., 2007). In contrast to the BOLD-signal which just indirectly reflects brain activity (Logothetis, 2008), electro- or magnetophysiological data provide a direct measure of brain activity with a high temporal resolution. For example, Hipp et al. (2012) suggested an approach where orthogonalized source estimates of power in various frequency bands of spontaneous activity were recorded with MEG and correlated. They found strong correlations of alpha and beta power.

In a somewhat different approach, Weisz and colleagues conducted connectivity analyses of MEG data measured during auditory tasks, beyond spontaneous activity (Müller and Weisz, 2012; Weisz et al., 2014; Weisz and Obleser, 2014). They projected complex-valued spectral data in the alpha range to source space. Then, phase-locking values, instead of power values, of the regions of interests were calculated, revealing connections between attention networks and primary auditory regions (see also Weisz et al., 2014 for "all-to-all connectivity" and Sporns, 2013 for "small-world" networks).

Both approaches would add up nicely to the analyses already conducted in the present thesis. For example, in Experiment III, the manipulation of both factors, temporal expectations and memory decay, gave rise to a large pattern of alpha power activity involving primary auditory and visual brain regions as well as parts of different attentional networks. In order to provide more information about the alpha power and its functional role during auditory memory it is necessary, in a next step, to assess the connections of the localized brain regions. Specifically, in Experiments I, IIb, and II, alpha power effects of temporal expectations emerged from right frontal sensors and were localized in the cingulo-opercular network (Experiment I and III). In Experiment III, IFG and STG presented the effect as well. Here, connectivity analyses could reveal whether the IFG as part of the bottom-up oriented ventral attention system, is connected to the top-down controlling cingulo-opercular network and in turn whether

both networks modulate auditory processing in STG. To this end, a possible connection could add evidence to the mode of action of temporal expectations on auditory working memory.

### 11.2.2 Electrocorticography

The spatial resolution of MEG is limited in so far as that source localization techniques can only approximate the actual sources of the signal measured on the scalp. These limitations prevent the analysis of brain responses at their immediate origin. The precise location of activity, however, provides further insights on the underlying neural mechanisms. Electrocorticography (ECoG), for example, has a higher temporal and spatial resolution (~4 $mm^2$) than other, non-invasive neuroimaging techniques (Miller et al., 2009). For ECoG recordings, electrodes are surgically implanted into the brain. Because ECoG-patients are not cognitively impaired, it has become very interesting to assess human cognition with ECoG (for a review see Jacobs and Kahana, 2010). Therefore, ECoG would be very suitable to investigate the effect of temporal expectations on auditory working memory in more detail.

For example, ECoG studies assessing visual working memory provided insight of the role of neural oscillations in the gamma frequency band during stages of stimulus encoding and maintenance (Howard et al., 2003; Rizzuto et al., 2003). During the encoding of visual stimuli, gamma power was modulated by attention (Fisch et al., 2009). In a passive visual task, gamma power only increased in primary sensory areas. When attention was focused onto the stimuli, an increase in gamma power was also observed in ventral temporal cortex. In an auditory selective attention task, it was shown that attended sounds elicited an increase of high gamma activity in posterolateral superior temporal gyrus (Nourski et al., 2015). Similarly, the effect of temporal expectations could be assessed. When stimuli are expected,the pattern of gamma activity in primary auditory cortices would most likely change, reflecting enhanced processing. In addition, it is probable that the increased focus of attention could as well be reflected in an increase of gamma power in attentional networks.

Besides alpha power, gamma power was also shown to be a sensitive marker for memory load during working memory maintenance (Jensen et al., 2002; Tallon-Baudry et al., 1998). These findings were also confirmed by ECoG data: A correlation of gamma power and memory load was found in neocortex and hippocampus in visual

working memory (Howard et al., 2003; van Vugt et al., 2010). Here as well, ECoG measures could give rise to a more nuanced perspective on memory load in auditory working memory. For example, the locations of auditory memory representations could be indentified as well as top-down modulations of these representations through attentional networks. Presumably, such findings could unmask the underlying neural mechanisms of memory decay by illustrating a possible "neural" fading out of the memory representation.

Altogether, the expansion of the methodological scope towards connectivity analyses and ECoG could most likely provide in-depth evidence about the complex interactions of brain networks of auditory working memory. This would provide also further insights on the neural efficiency of managing working memory limitations.

# References


Ahlfors, S. P., Han, J., Belliveau, J. W., and Hämäläinen, M. S. (2010). Sensitivity of MEG and EEG to source orientation. *Brain Topography*, 23(3):227–32.

Alvarez, G. A. and Cavanagh, P. (2004). The capacity of visual short-term memory is set both by visual information load and by number of objects. *Psychological Science*, 15(2):106–11.

Anderson, T., McCarthy, P., and Tukey, J. (1946). Staircase methods of sensitivity testing. *NAVORD Report*.

Awh, E., Barton, B., and Vogel, E. K. (2007). Visual working memory represents a fixed number of items regardless of complexity. *Psychological Science*, 18(7):622–8.

Awh, E., Vogel, E. K., and Oh, S.-H. (2006). Interactions between attention and working memory. *Neuroscience*, 139(1):201–8.

Bachem, A. (1954). Time factors in relative and absolute pitch determination. *The Journal of the Acoustical Society of America*, 26(5):751–753.

Baddeley, A. (2003). Working memory: looking back and looking forward. *Nature Reviews Neuroscience*, 4(10):829–39.

Baddeley, A. (2012). Working memory: theories, models, and controversies. *Annual Review of Psychology*, 63:1–29.

Baldauf, D. and Desimone, R. (2014). Neural mechanisms of object-based attention. *Science*, 344(6182):424–7.

Barak, O., Tsodyks, M., and Romo, R. (2010). Neuronal population coding of parametric working memory. *Journal of Neuroscience*, 30(28):9424–30.

Barnes, R. and Jones, M. R. (2000). Expectancy, attention, and time. *Cognitive Psychology*, 41(3):254–311.

Barrouillet, P., Bernardin, S., and Camos, V. (2004). Time constraints and resource sharing in adults' working memory spans. *Journal of Experimental Psychology: General*, 133(1):83–100.

Barrouillet, P., Bernardin, S., Portrat, S., Vergauwe, E., and Camos, V. (2007). Time and cognitive load in working memory. *Journal of Experimental Psychology: Learning, Memory, and Cognition*, 33(3):570–85.

Barrouillet, P., Portrat, S., Vergauwe, E., Diependaele, K., and Camos, V. (2011). Further evidence for temporal decay in working memory: reply to Lewandowsky and Oberauer (2009). *Journal of Experimental Psychology: Learning, Memory, and Cognition*, 37(5):1302–17.

Bays, P. M. (2014). Noise in Neural Populations Accounts for Errors in Working Memory. *Journal of Neuroscience*, 34(10):3632–3645.

Bays, P. M., Catalao, R., and Husain, M. (2009). The precision of visual working memory is set by allocation of a shared resource. *Journal of Vision*, 9(10):1–11.

Bays, P. M., Gorgoraptis, N., and Wee, N. (2011). Temporal dynamics of encoding, storage, and reallocation of visual working memory. *Journal of Vision*, 11(10):1–15.

Bays, P. M. and Husain, M. (2008). Dynamic shifts of limited working memory resources in human vision. *Science*, 321(5890):851–4.

Békésy, G. (1947). A new audiometer. *Acta Oto-Laryngologica*, 35:411–422.

Berger, H. (1929). Über das Elektrenkephalogramm des Menschen. *European Archives of Psychiatry and Clinical Neuroscience*, 87(1):527–570.

Beudel, M., Renken, R., Leenders, K. L., and de Jong, B. M. (2009). Cerebral representations of space and time. *NeuroImage*, 44(3):1032–40.

Blough, D. (1959). Delayed matching in the pigeon. *Journal of the Experimental Analysis of Behavior*, pages 151–160.

Bollinger, J., Rubens, M. T., Zanto, T. P., and Gazzaley, A. (2010). Expectation-driven changes in cortical functional connectivity influence working memory and long-term memory performance. *Journal of Neuroscience*, 30(43):14399–410.

Bonnefond, M. and Jensen, O. (2012). Alpha oscillations serve to protect working memory maintenance against anticipated distracters. *Current Biology*, 22(20):1969–74.

Brown, J. (1958). Some tests of the decay theory of immediate memory. *Quarterly Journal of Experimental Psychology*, 10(1):12–21.

Bull, A. R. and Cuddy, L. L. (1972). Recognition memory for pitch of fixed and roving stimulus tones. *Perception & Psychophysics*, 11(1B):105–109.

Busse, L., Roberts, K. C., Crist, R. E., Weissman, D. H., and Woldorff, M. G. (2005). The spread of attention across modalities and space in a multisensory object. *Proceedings of the National Academy of Sciences of the United States of America*, 102(51):18751–6.

Buzsáki, G. (2006). *Rhythms of the Brain*. Oxford University Press, New York.

Buzsáki, G. and Draguhn, A. (2004). Neuronal oscillations in cortical networks. *Science*, 304(5679):1926–9.

Camos, V., Mora, G., and Oberauer, K. (2011). Adaptive choice between articulatory rehearsal and attentional refreshing in verbal working memory. *Memory & Cognition*, 39(2):231–44.

Chen, A. J.-W., Britton, M., Turner, G. R., Vytlacil, J., Thompson, T. W., and D'Esposito, M. (2012). Goal-directed attention alters the tuning of object-based representations in extrastriate cortex. *Frontiers in Human Neuroscience*, 6:187.

Cohen, D. (1972). Magnetoencephalography: detection of the brain's electrical activity with a superconducting magnetometer. *Science*, 175:664–666.

Cohen, J. R., Sreenivasan, K. K., and D'Esposito, M. (2014). Correspondence between stimulus encoding- and maintenance-related neural processes underlies successful working memory. *Cerebral Cortex*, 24(3):593–9.

Corbetta, M. and Shulman, G. L. (2002). Control of goal-directed and stimulus-driven attention in the brain. *Nature Reviews Neuroscience*, 3(3):201–15.

Correa, A., Lupiáñez, J., Madrid, E., and Tudela, P. (2006). Temporal attention enhances early visual processing: a review and new evidence from event-related potentials. *Brain Research*, 1076(1):116–28.

Correa, A., Lupiáñez, J., Milliken, B., and Tudela, P. (2004). Endogenous temporal orienting of attention in detection and discrimination tasks. *Perception & Psychophysics*, 66(2):264–78.

Correa, A., Lupiáñez, J., and Tudela, P. (2005). Attentional preparation based on temporal expectancy modulates processing at the perceptual level. *Psychonomic Bulletin & Review*, 12(2):328–34.

Correa, A. and Nobre, A. C. (2008). Spatial and temporal acuity of visual perception can be enhanced selectively by attentional set. *Experimental Brain Research*, 189(3):339–44.

Coull, J. T., Cheng, R.-K., and Meck, W. H. (2011). Neuroanatomical and neurochemical substrates of timing. *Neuropsychopharmacology*, 36(1):3–25.

Coull, J. T., Frith, C. D., Büchel, C., and Nobre, A. C. (2000). Orienting attention in time: behavioural and neuroanatomical distinction between exogenous and endogenous shifts. *Neuropsychologia*, 38(6):808–19.

Coull, J. T. and Nobre, A. C. (1998). Where and when to pay attention: The neural Systems for Directing Attention to Spatial Locations and to Time Intervals as Revealed by Both PET and fMRI. *Journal of Neuroscience*, 18(18):7426–35.

Coull, J. T. and Nobre, A. C. (2008). Dissociating explicit timing from temporal expectation with fMRI. *Current Opinion in Neurobiology*, 18(2):137–44.

Cowan, N. (1984). On short and long auditory stores. *Psychological Bulletin*, 96(2):341–70.

Cowan, N. (2000). Processing limits of selective attention and working memory: Potential implications for interpreting. *Interpreting*, 5(2):117–146.

Cowan, N. (2001). The magical number 4 in short-term memory: a reconsideration of mental storage capacity. *The Behavioral and Brain Sciences*, 24(1):87–114.

Cowan, N. and AuBuchon, A. M. (2008). Short-term memory loss over time without retroactive stimulus interference. *Psychonomic Bulletin & Review*, 15(1):230–235.

Cowan, N., Saults, J. S., and Nugent, L. D. (1997). The role of absolute and relative amounts of time in forgetting within immediate memory: The case of tone-pitch comparisons. *Psychonomic Bulletin & Review*, 4(3):393–397.

Cravo, A. M., Rohenkohl, G., Wyart, V., and Nobre, A. C. (2013). Temporal expectation enhances contrast sensitivity by phase entrainment of low-frequency oscillations in visual cortex. *Journal of Neuroscience*, 33(9):4002–10.

David, O. and Friston, K. J. (2003). A neural mass model for MEG/EEG:. *NeuroImage*, 20(3):1743–1755.

David, O., Kilner, J., and Friston, K. (2006). Mechanisms of evoked and induced responses in MEG/EEG. *NeuroImage*, 31(4):1580–91.

de Graaf, T. a., Gross, J., Paterson, G., Rusch, T., Sack, A. T., and Thut, G. (2013). Alpha-band rhythms in visual task performance: phase-locking by rhythmic sensory stimulation. *PloS one*, 8(3):e60035.

Ding, N. and Simon, J. (2013). Power and phase properties of oscillatory neural responses in the presence of background activity. *Journal of Computational Neuroscience*, 34(2):337–343.

Doherty, J. R., Rao, A., Mesulam, M. M., and Nobre, A. C. (2005). Synergistic effect of combined temporal and spatial expectations on visual attention. *Journal of Neuroscience*, 25(36):8259–66.

Dosenbach, N. U. F., Fair, D. A., Cohen, A. L., Schlaggar, B. L., and Petersen, S. E. (2008). A dual-networks architecture of top-down control. *Trends in Cognitive Sciences*, 12(3):99–105.

Dosenbach, N. U. F., Fair, D. A., Miezin, F. M., Cohen, A. L., Wenger, K. K., Dosenbach, R. A. T., Fox, M. D., Snyder, A. Z., Vincent, J. L., Raichle, M. E., Schlaggar, B. L., and Petersen, S. E. (2007). Distinct brain networks for adaptive and stable task control in humans. *Proceedings of the National Academy of Sciences of the United States of America*, 104(26):11073–8.

Dreher, J.-C., Koechlin, E., Ali, S. O., and Grafman, J. (2002). The Roles of Timing and Task Order during Task Switching. *NeuroImage*, 17(1):95–109.

Driver, J., Eimer, M., Macaluso, E., and Velzen, V. (2004). Neurobiology of human spatial attention: modulation, generation, and integration. In Kanwisher, N. and Duncan, J., editors, *Attention and Performance XX. Functional Imaging of Visual Cognition.*

Eckert, M. A., Menon, V., Walczak, A., Ahlstrom, J. B., Denslow, S., Horwitz, A., and Dubno, J. R. (2009). At the heart of the ventral attention system: the right anterior insula. *Human Brain Mappingrain mapping*, 30(8):2530–41.

Elbert, T., Junghöfer, M., Rockstroh, B., and Roth, W. T. (2001). Physiologische Grundlagen und Psychophysiologische Messmethoden der Hirnaktivität. In Rösler, F., editor, *Enzyklopädie der Psychologie*, volume 4, Grundla of *I, Biologische Psychologie*, pages 179–236. Hogrefe, Göttingen, fifth edition.

Erb, J., Henry, M. J., Eisner, F., and Obleser, J. (2013). The brain dynamics of rapid perceptual adaptation to adverse listening conditions. *Journal of Neuroscience*, 33(26):10688–97.

Ester, E. F., Anderson, D. E., Serences, J. T., and Awh, E. (2013). A neural measure of precision in visual working memory. *Journal of Cognitive Neuroscience*, 25(5):754–761.

Farrell, S. and Lewandowsky, S. (2002). An endogenous distributed model of ordering in serial recall. *Psychonomic Bulletin & Review*, 9(1):59–79.

Fisch, L., Privman, E., Ramot, M., Harel, M., Nir, Y., Kipervasser, S., Andelman, F., Neufeld, M. Y., Kramer, U., Fried, I., and Malach, R. (2009). Neural "ignition": enhanced activation linked to perceptual awareness in human ventral stream visual cortex. *Neuron*, 64(4):562–74.

Fischl, B., Sereno, M. I., Tootell, R. B., and Dale, A. M. (1999). High-resolution intersubject averaging and a coordinate system for the cortical surface. *Human Brain Mapping*, 8(4):272–84.

Fougnie, D., Suchow, J. W., and Alvarez, G. A. (2012). Variability in the quality of visual working memory. *Nature Communications*, 3:1229.

Foxe, J. J. and Snyder, A. C. (2011). The Role of Alpha-Band Brain Oscillations as a Sensory Suppression Mechanism during Selective Attention. *Frontiers in Psychology*, 2:154.

Fukuda, K., Awh, E., and Vogel, E. K. (2010). Discrete capacity limits in visual working memory. *Current Opinion in Neurobiology*, 20(2):177–82.

Fuster, J. M. (1999). *Memory in the cerebral cortex: An empirical approach to neural networks in the human and nonhuman primate*. MIT press.

Gaab, N., Gaser, C., Zaehle, T., Jancke, L., and Schlaug, G. (2003). Functional anatomy of pitch memory—an fMRI study with sparse temporal sampling. *NeuroImage*, 19(4):1417–1426.

Gazzaley, A. (2011). Influence of early attentional modulation on working memory. *Neuropsychologia*, 49(6):1410–24.

Gazzaley, A., Cooney, J. W., Rissman, J., and D'Esposito, M. (2005). Top-down suppression deficit underlies working memory impairment in normal aging. *Nature Neuroscience*, 8(10):1298–300.

Gazzaley, A. and Nobre, A. C. (2012). Top-down modulation: bridging selective attention and working memory. *Trends in Cognitive Sciences*, 16(2):128–134.

Glass, L. and Mackey, M. (1988). *From clocks to chaos: the rhythms of life*. Princeton University Press.

Goldman-Rakic, P. (1995). Cellular basis of working memory. *Neuron*, 14:477–485.

Gould, I. C., Rushworth, M. F., and Nobre, A. C. (2011). Indexing the graded allocation of visuospatial attention using anticipatory alpha oscillations. *Journal of Neurophysiology*, 105(3):1318–26.

Gross, J., Kujala, J., Hämäläinen, M., Timmermann, L., Schnitzler, A., and Salmelin, R. (2001). Dynamic imaging of coherent sources: Studying neural interactions in the human brain. *Proceedings of the National Academy of Sciences of the United States of America*, 98(2):694–9.

Haegens, S., Händel, B. F., and Jensen, O. (2011a). Top-down controlled alpha band activity in somatosensory areas determines behavioral performance in a discrimination task. *Journal of Neuroscience*, 31(14):5197–204.

Haegens, S., Nácher, V., Luna, R., Romo, R., and Jensen, O. (2011b). $\alpha$-Oscillations in the monkey sensorimotor network influence discrimination performance by rhythmical inhibition of neuronal spiking. *Proceedings of the National Academy of Sciences of the United States of America*, 108(48):19377–82.

Haegens, S., Osipova, D., Oostenveld, R., and Jensen, O. (2010). Somatosensory working memory performance in humans depends on both engagement and disengagement of regions in a distributed network. *Human Brain Mapping*, 31(1):26–35.

Hämäläinen, M., Hari, R., Ilmoniemi, R. J., Knuutila, J., and Lounasmaa, O. (1993). Magnetoencephalography–theory, instrumentation, and applications to noninvasive studies of the working human brain. *Reviews of Modern Physics*, 65(2):413–497.

Hanslmayr, S., Staudigl, T., and Fellner, M.-C. (2012). Oscillatory power decreases and long-term memory: the information via desynchronization hypothesis. *Frontiers in Human Neuroscience*, 6:74.

Hari, R., Levänen, S., and Raij, T. (2000). Timing of human cortical functions during cognition: role of MEG. *Trends in Cognitive Sciences*, 4(12):455–462.

Harris, J. D. (1952). The decline of pitch discrimination with time. *Journal of Experimental Psychology*, pages 3–6.

Helmholtz, H. (1853). Ueber einige Gesetze der Vertheilung elektrischer Ströme in körperlichen Leitern mit Anwendung auf die thierisch-elektrischen Versuche. *Annalen der Physik*, 165(6):211–233.

Henry, M. J. and Herrmann, B. (2014). Low-Frequency Neural Oscillations Support Dynamic Attending in Temporal Context. *Timing & Time Perception*, 2(1):62–86.

Henry, M. J., Herrmann, B., and Obleser, J. (2013). Selective attention to temporal features on nested time scales. *Cerebral Cortex*.

Henry, M. J. and McAuley, J. D. (2013). Failure to apply signal detection theory to the Montreal Battery of Evaluation of Amusia may misdiagnose amusia. *Music Perception: An Interdisciplinary Journal*, 30(5):480–496.

Henry, M. J. and Obleser, J. (2012). Frequency modulation entrains slow neural oscillations and optimizes human listening behavior. *Proceedings of the National Academy of Sciences of the United States of America*, 109(49):20095–20100.

Herman, L. and Gordon, J. (1974). Auditory delayed matching in the bottlenose dolphin. *Journal of the Experimental Analysis of Behavior*, 1(1):19–26.

Herremans, A. H. and Hijzen, T. H. (1997). The delayed-conditional-discrimination task improves measurement of working memory in rats. *Neuroscience and Biobehavioral Reviews*, 21(3):371–9.

Herrmann, B., Henry, M. J., Grigutsch, M., and Obleser, J. (2013). Oscillatory phase dynamics in neural entrainment underpin illusory percepts of time. *Journal of Neuroscience*, 33(40):15799–809.

Hesse, C. and Franz, V. H. (2010). Grasping remembered objects: exponential decay of the visual memory. *Vision Research*, 50(24):2642–50.

Hillyard, S. A., Vogel, E. K., and Luck, S. J. (1998). Sensory gain control (amplification) as a mechanism of selective attention: electrophysiological and neuroimaging evidence. *Philosophical Transactions of the Royal Society of London. Series B, Biological Sciences*, 353(1373):1257–70.

Hipp, J. F., Engel, A. K., and Siegel, M. (2011). Oscillatory synchronization in large-scale cortical networks predicts perception. *Neuron*, 69(2):387–96.

Hipp, J. F., Hawellek, D. J., Corbetta, M., Siegel, M., and Engel, A. K. (2012). Large-scale cortical correlation structure of spontaneous oscillatory activity. *Nature Neuroscience*, 15(6):884–90.

Howard, M. W., Rizzuto, D. S., Caplan, J. B., Madsen, J. R., Lisman, J. E., Aschenbrenner-Scheibe, R., Schulze-Bonhage, A., and Kahana, M. J. (2003). Gamma Oscillations Correlate with Working Memory Load in Humans. *Cerebral Cortex*, 13(12):1369–1374.

Hunter, W. S. (1913). The delayed reaction in animals and children. *Animal Behavior Monographs*.

Jacobs, J. and Kahana, M. J. (2010). Direct brain recordings fuel advances in cognitive electrophysiology. *Trends in Clisognitive Science*, 14(4):162–71.

Janssen, P. and Shadlen, M. N. (2005). A representation of the hazard rate of elapsed time in macaque area LIP. *Nature Neuroscience*, 8(2):234–241.

Jaramillo, S. and Zador, A. M. (2011). The auditory cortex mediates the perceptual effects of acoustic temporal expectation. *Nature Neuroscience*, 14(2):246–51.

Jensen, O. (2006). Maintenance of multiple working memory items by temporal segmentation. *Neuroscience*, 139(1):237–49.

Jensen, O., Bonnefond, M., and VanRullen, R. (2012). An oscillatory mechanism for prioritizing salient unattended stimuli. *Trends in Cognitive Science*, 16(4):200–206.

Jensen, O., Gelfand, J., Kounios, J., and Lisman, J. E. (2002). Oscillations in the alpha band (9-12 Hz) increase with memory load during retention in a short-term memory task. *Cerebral Cortex*, 12(8):877–82.

Jensen, O., Kaiser, J., and Lachaux, J.-P. (2007). Human gamma-frequency oscillations associated with attention and memory. *Trends in Neurosciences*, 30(7):317–24.

Jensen, O. and Mazaheri, A. (2010). Shaping Functional Architecture by Oscillatory Alpha Activity: Gating by Inhibition. *Frontiers in Human Neuroscience*, 4:1–8.

Jha, A. P. and McCarthy, G. (2000). The influence of memory load upon delay-interval activity in a working-memory task: an event-related functional MRI study. *Journal of Cognitive Neuroscience*, 12:90–105.

Jokisch, D. and Jensen, O. (2007). Modulation of gamma and alpha activity during a working memory task engaging the dorsal or ventral stream. *Journal of Neuroscience*, 27(12):3244–51.

Jones, M. R., Moynihan, H., MacKenzie, N., and Puente, J. (2002). Temporal Aspects of Stimulus-Driven Attending in Dynamic Arrays. *Psychological Science*, 13(4):313–319.

Jonides, J., Lewis, R. L., and Nee, D. E. (2008). The mind and brain of short-term memory. *Annual Review of Psychology*, 59:193–224.

Kaiser, J., Heidegger, T., Wibral, M., Altmann, C. F., and Lutzenberger, W. (2007a). Alpha synchronization during auditory spatial short-term memory. *Neuroreport*, 18(11):1129–32.

Kaiser, J., Leiberg, S., Rust, H., and Lutzenberger, W. (2007b). Prefrontal gamma-band activity distinguishes between sound durations. *Brain Research*, 1139:153–62.

Kaiser, J., Rahm, B., and Lutzenberger, W. (2009). Temporal dynamics of stimulus-specific gamma-band activity components during auditory short-term memory. *NeuroImage*, 44(1):257–64.

Kandel, E. R. (2000). Nerve Cells and Behavior. In Kandel, E. R., Schwartz, J. H., and Jessell, T. M., editors, *Principles of neural science*. McGraw-Hill, New York, 4 edition.

Keller, T. A., Cowan, N., and Saults, J. S. (1995). Can auditory memory for tone pitch be rehearsed? *Journal of Experimental Psychology. Learning, Memory, and Cognition*, 21(3):635–45.

Klimesch, W. (2012). Alpha-band oscillations, attention, and controlled access to stored information. *Trends in Cognitive Sciences*, 16(12):606–617.

Klimesch, W., Sauseng, P., and Hanslmayr, S. (2007). EEG alpha oscillations: the inhibition-timing hypothesis. *Brain Research Reviews*, 53:63–88.

Krause, C. M. (1996). Event-related. EEG desynchronization and synchronization during an auditory memory task. *Electroencephalography and Clinical Neurophysiology*, 98(4):319–326.

Kuo, B.-C., Rao, A., Lepsien, J., and Nobre, A. C. (2009). Searching for targets within the spatial layout of visual short-term memory. *Journal of Neuroscience*, 29(25):8032–8.

Lakatos, P., O'Connell, M. N., Barczak, A., Mills, A., Javitt, D. C., and Schroeder, C. E. (2009). The leading sense: supramodal control of neurophysiological context by attention. *Neuron*, 64(3):419–30.

Lakatos, P., Schroeder, C. E., Leitman, D. I., and Javitt, D. C. (2013). Predictive suppression of cortical excitability and its deficit in schizophrenia. *Journal of Neuroscience*, 33(28):11692–702.

Lakatos, P., Shah, A. S., Knuth, K. H., Ulbert, I., Karmos, G., and Schroeder, C. E. (2005). An oscillatory hierarchy controlling neuronal excitability and stimulus processing in the auditory cortex. *Journal of Neurophysiology*, 94(3):1904–11.

Lange, K. (2009). Brain correlates of early auditory processing are attenuated by expectations for time and pitch. *Brain and Cognition*, 69(1):127–37.

Lange, K. (2013). The ups and downs of temporal orienting: a review of auditory temporal orienting studies and a model associating the heterogeneous findings on the auditory N1 with opposite effects of attention and prediction. *Frontiers in Human Neuroscience*, 7:263.

Lange, K. and Röder, B. (2006). Orienting attention to points in time improves stimulus processing both within and across modalities. *Journal of Cognitive Neuroscience*, 18(5):715–29.

Lange, K. and Schnuerch, R. (2014). Challenging perceptual tasks require more attention: the influence of task difficulty on the N1 effect of temporal orienting. *Brain and cognition*, 84(1):153–63.

Large, E. W. and Jones, M. R. (1999). The dynamics of attending: How people track time-varying events. *Psychological Review*, 106(1):119–159.

Laufs, H., Holt, J. L., Elfont, R., Krams, M., Paul, J. S., Krakow, K., and Kleinschmidt, A. (2006). Where the BOLD signal goes when alpha EEG leaves. *NeuroImage*, 31(4):1408–18.

Lawrance, E. L. A., Harper, N. S., Cooke, J. E., and Schnupp, J. W. H. (2014). Temporal predictability enhances auditory detection. *The Journal of the Acoustical Society of America*, 135(6):EL357–EL363.

Leek, M. R. (2001). Adaptive procedures in psychophysical research. *Perception & Psychophysics*, 63(8):1279–92.

Leiberg, S., Kaiser, J., and Lutzenberger, W. (2006a). Gamma-band activity dissociates between matching and nonmatching stimulus pairs in an auditory delayed matching-to-sample task. *NeuroImage*, 30(4):1357–64.

Leiberg, S., Lutzenberger, W., and Kaiser, J. (2006b). Effects of memory load on cortical oscillatory activity during auditory pattern working memory. *Brain Research*, 1120(1):131–40.

Leung, A. W. S. and Alain, C. (2011). Working memory load modulates the auditory "What" and "Where" neural networks. *NeuroImage*, 55(3):1260–9.

Levitt, H. (1971). Transformed up-down methods in psychoacoustics. *The Journal of the Acoustical Society of America*, 49(2):467–77.

Lewandowsky, S., Geiger, S. M., Morrell, D. B., and Oberauer, K. (2010). Turning simple span into complex span: Time for decay or interference from distractors? *Journal of Experimental Psychology: Learning, Memory, and Cognition*, 36(4):958–78.

Lewandowsky, S., Oberauer, K., and Brown, G. D. a. (2009). No temporal decay in verbal short-term memory. *Trends in Cognitive Sciences*, 13(3):120–6.

Lima, B., Singer, W., and Neuenschwander, S. (2011). Gamma responses correlate with temporal expectation in monkey primary visual cortex. *The Journal of Neuropsychiatry and Clinical Neurosciences*, 31(44):15919–31.

Lisman, J. E. and Idiart, M. A. (1995). Storage of 7+- 2 short-term memories in oscillatory subcycles. *Science*, 267:1512–1515.

Lisman, J. E. and Jensen, O. (2013). The $\theta$-$\gamma$ neural code. *Neuron*, 77(6):1002–16.

Logothetis, N. K. (2008). What we can do and what we cannot do with fMRI. *Nature*, 453(7197):869–78.

Lopes da Silva, F. (2013). EEG and MEG: relevance to neuroscience. *Neuron*, 80(5):1112–28.

Luce, R. D. (1986). *Response Times: Their Role in Inferring Elementary Mental Organization*. Oxford University Press.

Luck, S. J. and Vogel, E. K. (1997). The capacity of visual working memory for features and conjunctions. *Nature*, 390(6657):279–81.

Lutzenberger, W., Ripper, B., Busse, L., Birbaumer, N., and Kaiser, J. (2002). Dynamics of gamma-band activity during an audiospatial working memory task in humans. *Journal of Neuroscience*, 22(13):5630–8.

Ma, W. J., Husain, M., and Bays, P. M. (2014). Changing concepts of working memory. *Nature Neuroscience*, 17(3):347–56.

Macmillan, N. A. and Creelman, C. D. (2004). *Detection theory: A user's guide*. Lawrence Erlbarun Associates, Inc., Mahwah, New Jersey, 2nd ed. edition.

Mäntysalo, S. and Näätänen, R. (1987). The duration of a neuronal trace of an auditory stimulus as indicated by event-related potentials. *Biological Psychology*, 24(3):183–95.

Maris, E. and Oostenveld, R. (2007). Nonparametric statistical testing of EEG- and MEG-data. *Journal of Neuroscience Methods*, 164(1):177–90.

Mathewson, K. E., Prudhomme, C., Fabiani, M., Beck, D. M., Lleras, A., and Gratton, G. (2012). Making waves in the stream of consciousness: entraining oscillations in EEG alpha and fluctuations in visual awareness with rhythmic visual stimulation. *Journal of Cognitive Neuroscience*, 24(12):2321–33.

McKeown, D. and Mercer, T. (2012). Short-term forgetting without interference. *Journal of Experimental Psychology: Learning,Memory, and Cognition*, 38(4):1057–68.

Medendorp, W. P., Kramer, G. F. I., Jensen, O., Oostenveld, R., Schoffelen, J.-M., and Fries, P. (2007). Oscillatory activity in human parietal and occipital cortex shows hemispheric lateralization and memory effects in a delayed double-step saccade task. *Cerebral Cortex*, 17(10):2364–74.

Mercer, T. and McKeown, D. (2014). Decay uncovered in nonverbal short-term memory. *Psychonomic Bulletin & Review*, 21(1):128–35.

Miller, E. K. and Cohen, J. D. (2001). An integrative theory of prefrontal cortex function. *Annual Review of Neuroscience*, 24:167–202.

Miller, G. A. (1956). The magical number seven, plus or minus two: some limits on our capacity for processing information. *Psychological Review*, 63(2):81–97.

Miller, K. J., Weaver, K. E., and Ojemann, J. G. (2009). Direct electrophysiological measurement of human default network areas. *Proceedings of the National Academy of Sciences of the United States of America*, 106(29):12174–7.

Miniussi, C., Wilding, E. L., Coull, J. T., and Nobre, A. C. (1999). Orienting attention in time. Modulation of brain potentials. *Brain*, 122:1507–18.

Mitra, P. P. and Pesaran, B. (1999). Analysis of dynamic brain imaging data. *Biophysical Journal*, 76(2):691–708.

Mora, G. and Camos, V. (2013). Two systems of maintenance in verbal working memory: evidence from the word length effect. *PloS ONE*, 8(7):e70026.

Moran, R. J., Campo, P., Maestu, F., Reilly, R. B., Dolan, R. J., and Strange, B. a. (2010). Peak frequency in the theta and alpha bands correlates with human working memory capacity. *Frontiers in Human Neuroscience*, 4:1–12.

Müller, N. and Weisz, N. (2012). Lateralized auditory cortical alpha band activity and interregional connectivity pattern reflect anticipation of target sounds. *Cerebral Cortex*, 22(7):1604–13.

Murray, A. M., Nobre, A. C., and Stokes, M. G. (2011). Markers of preparatory attention predict visual short-term memory performance. *Neuropsychologia*, 49(6):1458–65.

Näätänen, R. (2000). Mismatch negativity (MMN): perspectives for application. *International Journal of Psychophysiology*, 37(1):3–10.

Näätänen, R., Gaillard, A. W. K., and Mäntysalo, S. (1978). Early selective-attention effect on evoked potential reinterpreted. *Acta Psychologica*, 42:313–329.

Niemi, P. and Näätänen, R. (1981). Foreperiod and simple reaction time. *Psychological Bulletin*, 89(1):133–162.

Nobre, A. C. (2001). Orienting attention to instants in time. *Neuropsychologia*, 39(12):1317–28.

Nobre, A. C., Correa, A., and Coull, J. T. (2007). The hazards of time. *Current Opinion in Neurobiology*, 17(4):465–70.

Norman, D. A. and Bobrow, D. G. (1975). On data-limited and resource-limited processes. *Cognitive Psychology*, 64:44–64.

Nourski, K. V., Steinschneider, M., Oya, H., Kawasaki, H., and Howard, M. a. (2015). Modulation of response patterns in human auditory cortex during a target detection task: An intracranial electrophysiology study. *International Journal of Psychophysiology*, 95(2):191–201.

Oberauer, K. and Lewandowsky, S. (2013). Evidence against decay in verbal working memory. *Journal of Experimental Psychology. General*, 142(2):380–411.

Oberauer, K. and Lewandowsky, S. (2014). Further evidence against decay in working memory. *Journal of Memory and Language*, 73:15–30.

Oberauer, K., Lewandowsky, S., Farrell, S., Jarrold, C., and Greaves, M. (2012). Modeling working memory: an interference model of complex span. *Psychonomic Bulletin & Review*, 19(5):779–819.

Obleser, J. and Eisner, F. (2009). Pre-lexical abstraction of speech in the auditory cortex. *Trends in Cognitive Sciences*, 13(1):14–9.

Obleser, J., Lahiri, A., and Eulitz, C. (2003). Auditory-evoked magnetic field codes place of articulation in timing and topography around 100 milliseconds post syllable onset. *NeuroImage*, 20(3):1839–1847.

Obleser, J., Wöstmann, M., Hellbernd, N., Wilsch, A., and Maess, B. (2012). Adverse listening conditions and memory load drive a common alpha oscillatory network. *Journal of Neuroscience*, 32(36):12376–83.

Oostenveld, R., Fries, P., Maris, E., and Schoffelen, J.-M. (2011). FieldTrip: Open source software for advanced analysis of MEG, EEG, and invasive electrophysiological data. *Computational Intelligence and Neuroscience*, 2011:156869.

O'Reilly, J. X., Mesulam, M. M., and Nobre, A. C. (2008). The cerebellum predicts the timing of perceptual events. *Journal of Neuroscience*, 28(9):2252–60.

Owen, A. M., McMillan, K. M., Laird, A. R., and Bullmore, E. (2005). N-back working memory paradigm: a meta-analysis of normative functional neuroimaging studies. *Human Brain Mapping*, 25(1):46–59.

Palva, J. M., Monto, S., Kulashekhar, S., and Palva, S. (2010). Neuronal synchrony reveals working memory networks and predicts individual memory capacity. *Proceedings of the National Academy of Sciences of the United States of America*, 107(16):7580–5.

Palva, S. and Palva, J. M. (2007). New vistas for alpha-frequency band oscillations. *Trends in Neurosciences*, 30(4):150–8.

Pasternak, T. and Greenlee, M. W. (2005). Working memory in primate sensory systems. *Nature Reviews Neuroscience*, 6(2):97–107.

Paulesu, E., Frith, C., and Frackowiak, R. (1993). The neural correlates of the verbal component of working memory. *Nature*, 362:342–345.

Penttonen, M. (2003). Natural logarithmic relationship between brain oscillators. *Thalamus & Related Systems*, 2(2):145–152.

Percival, D. and Walden, A. (1993). *Spectral analysis for physical applications: multitaper and conventional univariate techniques*. University Press, Cambridge.

Peters, R. W., Moore, B. C., and Baer, T. (1998). Speech reception thresholds in noise with and without spectral and temporal dips for hearing-impaired and normally hearing people. *The Journal of the Acoustical Society of America*, 103(1):577–87.

Petersen, S. E. and Posner, M. I. (2012). The attention system of the human brain: 20 years after. *Annual Review of Neuroscience*, 35:73–89.

Peterson, L. R. and Peterson, M. J. (1959). Short-term retention of individual verbal items. *Journal of Experimental Psychology*, 58(3):193–198.

Pichora-Fuller, M. K. (2003). Cognitive aging and auditory information processing. *International Journal of Audiology*, 42(2):26–32.

Pichora-Fuller, M. K., Schneider, B. A., and Daneman, M. (1995). How young and old adults listen to and remember speech in noise. *The Journal of the Acoustical Society of America*, 97(1):593–608.

Pichora-Fuller, M. K. and Singh, G. (2006). Effects of Age on Auditory and Cognitive Processing: Implications for Hearing Aid Fitting and Audiologic Rehabilitation. *Trends in Amplification*, 10(1):29 – 59.

Pinal, D., Zurrón, M., and Díaz, F. (2014). Effects of load and maintenance duration on the time course of information encoding and retrieval in working memory: from perceptual analysis to post-categorization processes. *Frontiers in Human Neuroscience*, 8:165.

Posner, M. I. (1980). Orienting of attention. *The Quarterly Journal of Experimental Psychology*, 32(1):3–25.

Posner, M. I. and Keele, S. W. (1967). Decay of visual information from a single letter. *Science*, 158:137–139.

Postle, B. R. (2006). Working memory as an emergent property of the mind and brain. *Neuroscience*, 139(1):23–38.

Praamstra, P., Kourtis, D., Kwok, H. F., and Oostenveld, R. (2006). Neurophysiology of implicit timing in serial choice reaction-time performance. *Journal of Neuroscience*, 26(20):5448–55.

Priestley, M. B. (1981). *Spectral Analysis and Time Series*. Academic Press, London.

Raghavachari, S., Kahana, M. J., Rizzuto, D. S., Caplan, J. B., Kirschen, M. P., Bourgeois, B., Madsen, J. R., and Lisman, J. E. (2001). Gating of human theta oscillations by a working memory task. *Journal of Neuroscience*, 21(9):3175–83.

Ramirez, R. R., Wiof, D., and Baillet, S. (2010). Neuroelectromagnetic Source Imaging of Brain Dynamics. In Chaovalitwongse, W., Pardalos, P. M., and Xanthopoulos, P., editors, *Computational Neuroscience*, pages 127–155. Springer, Heidelberg.

Ray, W. J. and Cole, H. W. (1985). EEG alpha activity reflects attentional demands, and beta activity reflects emotional and cognitive processes. *Science*, 228(4700):750–2.

Ricker, T. J., Vergauwe, E., and Cowan, N. (2014). Decay theory of immediate memory: From Brown (1958) to today (2014). *The Quarterly Journal of Experimental Psychology*, pages 1–27.

Rimmele, J., Sussman, E., Keitel, C., Jacobsen, T., and Schröger, E. (2011). Electrophysiological evidence for age effects on sensory memory processing of tonal patterns. *Psychology and Aging*.

Rizzuto, D. S., Madsen, J. R., Bromfield, E. B., Schulze-Bonhage, a., Seelig, D., Aschenbrenner-Scheibe, R., and Kahana, M. J. (2003). Reset of human neocortical oscillations during a working memory task. *Proceedings of the National Academy of Sciences of the United States of America*, 100(13):7931–6.

Rohenkohl, G., Coull, J. T., and Nobre, A. C. (2011). Behavioural Dissociation between Exogenous and Endogenous Temporal Orienting of Attention. *PloS ONE*, 6(1):e14620.

Rohenkohl, G., Cravo, A. M., Wyart, V., and Nobre, A. C. (2012). Temporal Expectation Improves the Quality of Sensory Information. *Journal of Neuroscience*, 32(24):8424–8428.

Rohenkohl, G. and Nobre, A. C. (2011). Alpha Oscillations Related to Anticipatory Attention Follow Temporal Expectations. *Journal of Neuroscience*, 31(40):14076 –14084.

Roux, F. and Uhlhaas, P. J. (2013). Working memory and neural oscillations: alpha–gamma versus theta–gamma codes for distinct WM information? *Trends in Cognitive Sciences*, pages 1–10.

Roux, F., Wibral, M., Mohr, H. M., Singer, W., and Uhlhaas, P. J. (2012). Gamma-band activity in human prefrontal cortex codes for the number of relevant items maintained in working memory. *Journal of Neuroscience*, 32(36):12411–20.

Roux, F., Wibral, M., Singer, W., Aru, J., and Uhlhaas, P. J. (2013). The Phase of Thalamic Alpha Activity Modulates Cortical Gamma-Band Activity: Evidence from Resting-State MEG Recordings. *Journal of Neuroscience*, 33(45):17827–17835.

Rubin, D. and Wenzel, A. (1996). One hundred years of forgetting: A quantitative description of retention. *Psychological Review*, 103(4):734–760.

Rudner, M., Rönnberg, J., and Lunner, T. (2011). Working memory supports listening in noise for persons with hearing impairment. *Journal of the American Academy of Audiology*, 22(3):156–67.

Ruhnau, P., Herrmann, B., and Schröger, E. (2012). Finding the right control: the mismatch negativity under investigation. *Clinical Neurophysiology*, 123(3):507–12.

Sadaghiani, S., Hesselmann, G., and Kleinschmidt, A. (2009). Distributed and antagonistic contributions of ongoing activity fluctuations to auditory stimulus detection. *Journal of Neuroscience*, 29(42):13410–7.

Sadaghiani, S., Scheeringa, R., Lehongre, K., Morillon, B., Giraud, A.-L., D'Esposito, M., and Kleinschmidt, A. (2012). Alpha-Band Phase Synchrony Is Related to Activity in the Fronto-Parietal Adaptive Control Network. *Journal of Neuroscience*, 32(41):14305–14310.

Sadaghiani, S., Scheeringa, R., Lehongre, K., Morillon, B., Giraud, A.-L., and Kleinschmidt, A. (2010). Intrinsic connectivity networks, alpha oscillations, and tonic alertness: a simultaneous electroencephalography/functional magnetic resonance imaging study. *Journal of Neuroscience*, 30(30):10243–50.

Sanabria, D. and Correa, A. (2013). Electrophysiological evidence of temporal preparation driven by rhythms in audition. *Biological Psychology*, 92(2):98–105.

Sauseng, P., Klimesch, W., Heise, K. F., Gruber, W. R., Holz, E., Karim, A. a., Glennon, M., Gerloff, C., Birbaumer, N., and Hummel, F. C. (2009). Brain oscillatory substrates of visual short-term memory capacity. *Current Biology*, 19(21):1846–52.

Scheeringa, R., Fries, P., Petersson, K.-M., Oostenveld, R., Grothe, I., Norris, D. G., Hagoort, P., and Bastiaansen, M. C. M. (2011). Neuronal dynamics underlying high- and low-frequency EEG oscillations contribute independently to the human BOLD signal. *Neuron*, 69(3):572–83.

Schnitzler, A. and Gross, J. (2005). Normal and pathological oscillatory communication in the brain. *Nature Reviews Neuroscience*, 6(4):285–96.

Schoffelen, J.-M., Oostenveld, R., and Fries, P. (2008). Imaging the human motor system's beta-band synchronization during isometric contraction. *NeuroImage*, 41(2):437–47.

Schroeder, C. E. and Lakatos, P. (2009). Low-frequency neuronal oscillations as instruments of sensory selection. *Trends in Neurosciences*, 32(1):9–18.

Schröger, E. (2007). Mismatch Negativity. *Journal of Psychophysiology*, 21(3):138–146.

Schröger, E., Bendixen, A., Denham, S. L., Mill, R. W., Böhm, T. M., and Winkler, I. (2014). Predictive regularity representations in violation detection and auditory stream segregation: from conceptual to computational models. *Brain Topography*, 27(4):565–77.

Schubotz, R. I., von Cramon, D., and Lohmann, G. (2003). Auditory what, where, and when: a sensory somatotopy in lateral premotor cortex. *NeuroImage*, 20(1):173–185.

Schwarz, G. (1978). Estimating the dimension of a model. *The Annals of Statistics*, 6(2):461–464.

Shulman, G. L., Astafiev, S. V., Franke, D., Pope, D. L. W., Snyder, A. Z., McAvoy, M. P., and Corbetta, M. (2009). Interaction of stimulus-driven reorienting and expectation in ventral and dorsal frontoparietal and basal ganglia-cortical networks. *Journal of Neuroscience*, 29(14):4392–407.

Smith, E. E. and Jonides, J. (1998). Neuroimaging analyses of human working memory. *Proceedings of the National Academy of Sciences of the United States of America*, 95(20):12061–8.

Sohoglu, E., Peelle, J. E., Carlyon, R. P., and Davis, M. H. (2012). Predictive Top-Down Integration of Prior Knowledge during Speech Perception. *The Journal of Neuroscience*, 32(25):8443–53.

Sporns, O. (2013). The human connectome: origins and challenges. *NeuroImage*, 80:53–61.

Sreenivasan, K. K., Curtis, C. E., and D'Esposito, M. (2014). Revisiting the role of persistent neural activity during working memory. *Trends in Cognitive Sciences*, 18(2):82–9.

Stefanics, G., Hangya, B., Hernádi, I., Winkler, I., Lakatos, P., and Ulbert, I. (2010). Phase Entrainment of Human Delta Oscillations Can Mediate the Effects of Expectation on Reaction Speed. *Journal of Neuroscience*, 30(41):13578–13585.

Steriade, M., Nunez, A., and Amzica, F. (1993). A novel slow (< 1 Hz) oscillation of neocortical neurons in vivo: depolarizing and hyperpolarizing components. *Journal of Neuroscience*, 13:3252–3265.

Sternberg, S. (1966). High-speed scanning in human memory. *Science*, 153(3736):652–654.

Stokes, M. G. (2011). Top-down visual activity underlying VSTM and preparatory attention. *Neuropsychologia*, 49(6):1425–7.

Stokes, M. G., Kusunoki, M., Sigala, N., Nili, H., Gaffan, D., and Duncan, J. (2013). Dynamic coding for cognitive control in prefrontal cortex. *Neuron*, 78(2):364–75.

Surprenant, A. (1999). The Effect of Noise on Memory for Spoken Syllables. *International Journal of Psychology*, 34(5/6):328–333.

Tallon-Baudry, C. (2009). The roles of gamma-band oscillatory synchrony in human visual cognition. *Frontiers in Bioscience*, 14:321–332.

Tallon-Baudry, C., Bertrand, O., Peronnet, F., and Pernier, J. (1998). Induced gamma-band activity during the delay of a visual short-term memory task in humans. *Journal of Neuroscience*, 18(11):4244–54.

Taulu, S., Kajola, M., and Simola, J. (2004). Suppression of interference and artifacts by the Signal Space Separation Method. *Brain Topography*, 16(4):269–75.

Thorne, J. D., De Vos, M., Viola, F. C., and Debener, S. (2011). Cross-modal phase reset predicts auditory task performance in humans. *Journal of Neuroscience*, 31(10):3853–61.

Thorne, J. D. and Debener, S. (2013). Look now and hear what's coming: On the functional role of cross-modal phase reset. *Hearing Research*, 307:144–152.

Todorovic, A., van Ede, F., Maris, E., and de Lange, F. P. (2011). Prior expectation mediates neural adaptation to repeated sounds in the auditory cortex: an MEG study. *Journal of Neuroscience*, 31(25):9118–23.

Triviño, M., Correa, A., Arnedo, M., and Lupiáñez, J. (2010). Temporal orienting deficit after prefrontal damage. *Brain*, 133(Pt 4):1173–85.

Tuladhar, A. M., ter Huurne, N., Schoffelen, J.-M., Maris, E., Oostenveld, R., and Jensen, O. (2007). Parieto-occipital sources account for the increase in alpha activity with working memory load. *Human Brain Mapping*, 28(8):785–92.

Vaden, K. I., Kuchinsky, S. E., Cute, S. L., Ahlstrom, J. B., Dubno, J. R., and Eckert, M. A. (2013). The Cingulo-Opercular Network Provides Word-Recognition Benefit. *Journal of Neuroscience*, 33(48):18979–18986.

Vaden, R. J., Hutcheson, N. L., McCollum, L. a., Kentros, J., and Visscher, K. M. (2012). Older adults, unlike younger adults, do not modulate alpha power to suppress irrelevant information. *NeuroImage*, 63(3):1127–33.

Vallesi, A., Mussoni, A., Mondani, M., Budai, R., Skrap, M., and Shallice, T. (2007a). The neural basis of temporal preparation: Insights from brain tumor patients. *Neuropsychologia*, 45(12):2755–63.

Vallesi, A., Shallice, T., and Walsh, V. (2007b). Role of the prefrontal cortex in the foreperiod effect: TMS evidence for dual mechanisms in temporal preparation. *Cerebral Cortex*, 17(2):466–74.

van den Berg, R., Shin, H., Chou, W.-C., George, R., and Ma, W. J. (2012). Variability in encoding precision accounts for visual short-term memory limitations. *Proceedings of the National Academy of Sciences of the United States of America*, 109(22):8780–5.

van Dijk, H., Nieuwenhuis, I. L. C., and Jensen, O. (2010a). Left temporal alpha band activity increases during working memory retention of pitches. *The European Journal of Neuroscience*, 31(9):1701–7.

van Dijk, H., van der Werf, J., Mazaheri, A., Medendorp, W. P., and Jensen, O. (2010b). Modulations in oscillatory activity with amplitude asymmetry can produce cognitively relevant event-related responses. *Proceedings of the National Academy of Sciences of the United States of America*, 107(2):900–5.

van Ede, F., de Lange, F. P., Jensen, O., and Maris, E. (2011). Orienting attention to an upcoming tactile event involves a spatially and temporally specific modulation of sensorimotor alpha- and beta-band oscillations. *Journal of Neuroscience*, 31(6):2016–24.

van Ede, F., Köster, M., and Maris, E. (2012). Beyond establishing involvement: quantifying the contribution of anticipatory alpha- and beta-band suppression to perceptual improvement with attention. *Journal of Neurophysiology*, 108:2352–2362.

van Hest, A. and Steckler, T. (1996). Effects of procedural parameters on response accuracy: lessons from delayed (non-)matching procedures in animals. *Brain Research. Cognitive Brain Research*, 3(3-4):193–203.

van Vugt, M. K., Schulze-Bonhage, A., Litt, B., Brandt, A., and Kahana, M. J. (2010). Hippocampal gamma oscillations increase with memory load. *Journal of Neuroscience*, 30(7):2694–9.

Vangkilde, S., Coull, J. T., and Bundesen, C. (2012). Great expectations: temporal expectation modulates perceptual processing speed. *Journal of Experimental Psychology. Human Perception and Performance*, 38(5):1183–91.

Vergauwe, E., Camos, V., and Barrouillet, P. (2014). The impact of storage on processing: How is information maintained in working memory? *Journal of Experimental Psychology. Learning, Memory, and Cognition*, 40(4):1072–95.

Vrba, J. and Robinson, S. E. (2001). Signal processing in magnetoencephalography. *Methods*, 25(2):249–71.

Ward, L. M. (2003). Synchronous neural oscillations and cognitive processes. *Trends in Cognitive Sciences*, 7(12):553–559.

Watson, C. S., Wroton, H. W., Kelly, W. J., and Benbassat, C. a. (1975). Factors in the discrimination of tonal patterns. I. Component frequency, temporal position, and silent intervals. *The Journal of the Acoustical Society of America*, 57(5):1175–85.

Waugh, N. and Norman, D. (1965). Primary memory. *Psychological Review*, 72(2):89–104.

Weisz, N., Hartmann, T., Müller, N., Lorenz, I., and Obleser, J. (2011). Alpha rhythms in audition: cognitive and clinical perspectives. *Frontiers in Psychology*, 2(73):1–15.

Weisz, N. and Obleser, J. (2014). Synchronisation signatures in the listening brain: a perspective from non-invasive neuroelectrophysiology. *Hearing Research*, 307:16–28.

Weisz, N., Wühle, A., Monittola, G., Demarchi, G., Frey, J., Popov, T., and Braun, C. (2014). Prestimulus oscillatory power and connectivity patterns predispose conscious somatosensory perception. *Proceedings of the National Academy of Sciences of the United States of America*, 111(4):E417–E425.

Whitmarsh, S., Barendregt, H., Schoffelen, J.-M., and Jensen, O. (2014). Metacognitive awareness of covert somatosensory attention corresponds to contralateral alpha power. *NeuroImage*, 85:803–809.

Wichmann, F. A. and Hill, N. J. (2001). The psychometric function: I. Fitting, sampling, and goodness of fit. *Perception & Psychophysics*, 63(8):1293–313.

Wickelgren, W. A. (1969). Associative strength theory of recognition memory for pitch. *Journal of Mathematical Psychology*, 61:13–61.

Wilken, P. and Ma, W. J. (2004). A detection theory account of change detection. *Journal of Vision*, 4:1120–1135.

Wilsch, A., Henry, M. J., Herrmann, B., Maess, B., and Obleser, J. (2014). Alpha Oscillatory Dynamics Index Temporal Expectation Benefits in Working Memory. *Cerebral Cortex*, pages 1–9.

Wilson, F. A., Scalaidhe, S. P., and Goldman-Rakic, P. S. (1993). Dissociation of object and spatial processing domains in primate prefrontal cortex. *Science*, 260(5116):1955–1958.

Wolpert, D. M., Ghahramani, Z., and Jordan, M. I. (1995). An internal model for sensorimotor integration. *Science*, 263:1880–1882.

Woodrow, H. (1914). The measurement of attention. *Attention and Performance VIII*, 17(5):1–158.

Zanto, T. P., Chadick, J. Z., and Gazzaley, A. (2013). Anticipatory alpha phase influences visual working memory performance. *NeuroImage*, 245(1999):96861.

Zanto, T. P. and Gazzaley, A. (2009). Neural suppression of irrelevant information underlies optimal working memory performance. *Journal of Neuroscience*, 29(10):3059–66.

Zanto, T. P., Pan, P., Liu, H., Bollinger, J., Nobre, A. C., and Gazzaley, A. (2011). Age-related changes in orienting attention in time. *Journal of Neuroscience*, 31(35):12461–70.

Zanto, T. P., Toy, B., and Gazzaley, A. (2010). Delays in neural processing during working memory encoding in normal aging. *Neuropsychologia*, 48(1):13–25.

Zatorre, R. J., Evans, a. C., Meyer, E., and Gjedde, A. (1992). Lateralization of phonetic and pitch discrimination in speech processing. *Science*, 256(5058):846–9.

Zatorre, R. J. and Samson, S. (1991). Role of the right temporal neocortex in retention of pitch in auditory short-term memory. *Brain*, 114:2403–17.

Zhang, S., Bock, F., Si, A., Tautz, J., and Srinivasan, M. V. (2005). Visual working memory in decision making by honey bees. *Proceedings of the National Academy of Sciences of the United States of America*, 102(14):5250–5.

Zhang, W. and Luck, S. J. (2008). Discrete fixed-resolution representations in visual working memory. *Nature*, 453(7192):233–235.

Ziegler, P. and Wehner, R. (1997). Time-courses of memory decay in vector-based and landmark-based systems of navigation in desert ants, Cataglyphis fortis. *Journal of Comparative Physiology A*, 181:13–20.

# List of Figures

# Summary

## Introduction

The focus of the present thesis is on auditory working memory. The most striking characteristics of working memory are its limitations which are easily challenged by the amount of information to-be-maintained (memory load) and the duration of maintenance (memory decay). The underlying neural mechanisms such as top-down modulation of the sensory areas by the pre-frontal cortex (PFC; for review see Postle, 2006), as well as functional inhibition (for reviews see Jensen and Mazaheri, 2010; Klimesch et al., 2007) by means of neural oscillations in the alpha range, remain likely candidate mechanisms for an efficient way to handle these limitations.

Interestingly, most of the research conducted on working memory has been conducted in the visual domain. Therefore, to us it has been of major interest in how far memory limitations are challenged by auditory stimuli. Degraded speech has turned out to be a suitable domain because it has been shown to increase memory load (Pichora-Fuller and Singh, 2006). Moreover, in a study of Obleser et al. (2012), alpha power as a prominent marker for memory load increased parametrically with increasing speech degradation, showing that alpha power is also sensitive for memory load in the auditory domain.

Based on this finding, we here wanted to assess the potentially beneficial impact of temporal expectations on auditory working memory. In everyday life scenarios when processing (degraded) speech, one has prior knowledge about when the speech signal will be produced, based on the temporal structure of speech presentation, as in ongoing conversations. We therefore assumed that the a priori information on when to listen would facilitate the processing of degraded speech in working memory. Specifically, implications from previous findings on enhanced encoding precision (Rohenkohl et al., 2012; Cravo et al., 2013) due to temporal expectations allow to expect a load-reducing effect of temporal expectations for degraded speech. *In brief, the aim of the present thesis is to assess how temporal expectations modulate memory limitations as reflected by fluctuations of alpha power and behavioral performance with magnetoencephalography (see Figure S1).*

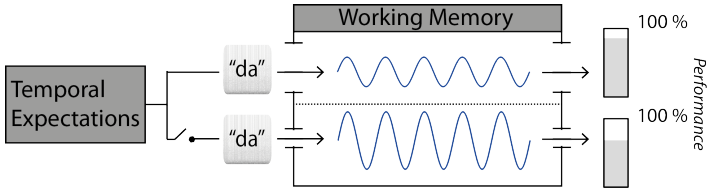


***Figure S1.*** **Expected impact of temporal expectations on working memory.** A syllable, "da", presented in noise enters working memory. Either, the syllable is temporally expected (upper stream) or temporally unexpected (lower stream). The amount of cognitive load is illustrated by means of a sinusoidal curve reflecting alpha power. Larger amplitude refers to high alpha power when there is no temporal expectations (lower stream). Lower amplitude refers to low alpha power when the syllable is expected (lower stream). But see Experiment III that presents the opposite effect for alpha power. Bars on the right illustrate expected behavioral performance modulated by temporal expectations: better performance with temporal expectations and lower performance without temporal expectations.

## Experiments and Results

*Experiment I* addressed the question whether temporal expectations reduce memory load of degraded speech. Two spoken syllables (S1, S2) were presented in a delayed matching-to-sample task separated by a two-second delay phase. Syllables were masked with noise in order to increase the memory load. Critically, temporal expectations for S1 was manipulated by means of three different a priori temporal cues that were either informative or not informative about S1-onset time with regard to cue-offset. We expected to observe reduced memory load in trials with temporal expectations reflected by decreased alpha power and increased memory performance. We could indeed demonstrate that due to temporal expectations alpha power was reduced during the delay phase and behavioral performance (percentage correct, $A_z$, response times) was improved. The effect of alpha power change was localized in the right insula, part of the cingulo-opercular network (Dosenbach et al., 2008) reflecting reduced need of top-down control during working memory maintenance. Moreover, we could show that the temporal expectations-effect in alpha power correlated positively with the effect of temporal expectations in memory performance. That in turn indicated that in the absence of temporal expectations, increased alpha power yielded improved memory performance.

A subset of participants of *Experiment I* took part in a subsequent study. The same experiment as in *Experiment I* was conducted with clear speech (without noise) in order to find out whether the previously observed reduction of memory load was specific to the noise masker. Could temporal expectations have similar effects in clear speech (*Experiment IIa*)? This comparably easy working memory task did not elicit

as much memory load as the noise experiment (significantly better task performance compared to noise) and did not present any modulation of delay-phase alpha power by temporal cues inducing expectations. Also on a statistical level we were able to show that the effect of temporal expectations on alpha power was significantly larger in noise compared to clear speech. Most likely, the explicit processing of the cues was too costly for this very easy task. Therefore, we also tested whether instead more implicit temporal expectations induced by the hazard rate function showed any effects. We wanted to assess whether this kind of temporal expectations first of all had an impact on processing of the target stimulus (S1) as well as on alpha power during the delay phase (*Experiment IIb*). Note that foreperiods between cue and S1 were jittered after each of the three different cues allowing for analyses across temporal cues. We expected to find increased phase coherence of slow neural oscillations in the frequency range of stimulus presentation with longer foreperiods. Here, increased phase coherence would be an indicator for a state of increased excitability due to temporal expectations (Lakatos et al., 2005). At the same time, we expected longer foreperiods to concomitantly reduce alpha power during the delay phase. That would show that temporal expectations based on the hazard function reduce cognitive load, similar to temporal cues. We were able to demonstrate that, in fact, longer foreperiods resulted in a decrease in alpha power during the delay phase, but also increased the phase coherence of neural oscillations in the slow-delta range during S1 presentation. Independent of foreperiod duration, we could show that increased delta phase coherence at S1 predicted decreased alpha power during the delay phase. This correlation provides the direct link of enhanced excitability (phase-coherence) and reduced memory load (alpha power) explained by temporal expectations.

In order to attain a complete picture on the limitations of auditory working memory and how they are reflected by modulations of alpha power, memory decay was examined in the next study (*Experiment III*). Here, auditory sensory memory (Cowan, 1984; Schröger, 2007) was assessed by presenting pure-tone sequences (S1, S2) instead of syllables which allowed for decay in memory. Memory decay is reflected by a decline in performance with longer delay phases. As before, S1 and S2 were embedded in noise to increase memory load and memory decay was manipulated parametrically by means of three different delay phase durations. Since there was no prior evidence on the modulations of alpha power by memory decay we could only assume whether a decline in performance after longer delay phases would be accompanied with a decline in alpha power. In addition, temporal expectations for S1 were manipulated again to investigate whether temporal expectations not just reduce memory load per se but also counteract memory decay. Here it was expected to observe less decline in behavioral performance

and potentially alpha power with temporal expectations. In addition to analyses on the sensor level, source localization of alpha power modulations were conducted for further insights on the brain regions modulated by the different experimental manipulations such as potential involvement of PFC.

Behaviorally, the data revealed that beyond the expected decline in performance over time, the decline, hence the memory decay, was less strong when the to-be-remembered stimulus had been temporally expected. It turned out that alpha power declined with memory decay, similarly to the decline in task performance. This effect emerged primarily from visual cortices (V1) and other posterior regions such as right inferior parietal lobe (IPL) and precuneus. Here, IPL and precuneus most likely reflected attentional modulations of maintenance processes. Increased alpha power in V1, on the other hand, is in line within the framework of functional inhibition. That is, decreased alpha power most probably signals less inhibition of task-irrelevant (visual) areas.

Moreover, temporal expectations exerted an effect on alpha power during early stages of the delay phase independent of memory decay. That is, when to-be-remembered stimuli were expected, alpha power was increased in the right hemisphere, specifically, in inferior frontal gyrus (IFG), anterior cingulate cortex (ACC) and superior temporal gyrus (STG). Comparable to the behavioral performance, temporal expectations prevented alpha power from declining as strongly as when stimuli were unexpected. This effect was localized in the left supramarginal gyrus (SMG).

Next, a correlation of alpha with $A_z$ presented a direct link between alpha modulations and behavioral performance. This effect partially emerged from different brain sites in early delay phase stages than in the end of the delay phase. At early stages, correlations of $A_z$ and alpha power emerged from the ventral attention network (STG and IFG), as well as from cingulo-opercular regions (ACC) and the fronto-parietal network (precuneus). At the end of the delay phase, the correlation of alpha power and $A_z$ emerged primarily from bilateral ACC, left SMG, right IFG, and bilateral V1. Interestingly, these brain regions overlap strongly with the brain regions found for temporal expectations ans memory decay. That in turn indicates that alpha power fluctuations following experimental manipulations are directly linked to the behavioral outcome in the memory task.

In the last experiment, we picked up on the interaction of temporal expectations and memory decay (*Experiment IV*). In principle,the same experiment as in the previous study was conducted. The aim of this experiment, however, was to fit a forgetting curve or exponential decay function onto the performance measure $A_z$, separately for trials with and without temporal expectations, in order to describe more precisely the effect of temporal expectations on memory decay. For that reason, memory decay was

operationalized by means of six different delay phase durations instead of three different delay phase durations as in the previous experiment. Two parameters of the function that was fitted were critical for decay. The first described the actual decay ($\gamma$) and the second described the degree to which "productive" memory processes, such as refreshing of the memory representation, were able to counteract the decay ($\lambda$). No significant differences between temporally expected and unexpected trails were found for the decay parameter. However, the production parameter was greater in trials with temporal expectations indicating stronger refreshing of the memory representation resulting in an overall less steep forgetting curve. The differences between the forgetting curves of temporally expected and unexpected stimuli replicates the effect of the previous study that temporal expectations counteract memory decay.

## Discussion

Altogether, the presented results indicate that top-down modulations via temporal expectations are beneficial for auditory working memory. Specifically, temporal expectations enhanced the encoding precision of auditory stimuli presented in noise. That in turn resulted in decreased memory load and concomitantly counteracted memory decay. The Time-Based Resource-Sharing model (TBRS; Barrouillet et al., 2004) accounts for these results in so far that it claims that stimulus processing or encoding and stimulus maintenance draw on the same cognitive resources and therefore, memory decay is modulated by memory load. Thus, enhanced encoding precision allowed for the recruitment of more attentional resources for enhanced stimulus maintenance. Specifically for auditory memory, this means that memory load and memory decay vary with the encoding precision of the to-be-remembered information.

In line with the TBRS are the findings on alpha power during stimulus maintenance. The maintenance of verbal (Experiment I) and the maintenance of non-verbal stimuli (Experiment III) elicited different alpha power effects, which can be explained by different maintenance strategies (rehearsal vs. attentional resources e.g., Vergauwe et al., 2014). Still, enhanced maintenance activity in terms of increased attentional resources was reflected by increased alpha power. This again explains this alpha power declined faster over time when stimuli were temporally unexpected because more resources were needed for stimulus encoding and less resources were available for stimulus maintenance.

Lastly, alpha power source localizations revealed that attention networks such as the cingulo-opercular, fronto-parietal, and the ventral network were involved in the maintenance of auditory information. The crucial role of these networks for working memory

(Postle, 2006) contradicts a direct inhibition of these areas in terms of functional inhibition. Therefore, we suggest that alpha power emerging from these regions rather modulates stimulus maintenance in a top-down fashion by inhibiting task-irrelevant brain regions such as primary visual cortex.

# Zusammenfassung

## Einführung

Der Schwerpunkt der vorliegenden Arbeit liegt auf dem auditiven Arbeitsgedächtnis. Das auffälligste Merkmal sind die Limitationen des Arbeitsgedächtnisses, die leicht durch die Menge der Informationen, die im Gedächtnis gespeichert werden sollen (Gedächtnislast), so wie durch die Dauer des Speicherns (Gedächtniszerfall), herausgefordert werden. Die zugrunde liegenden neuronalen Mechanismen, wie die Top-Down-Modulation sensorischer Areale durch den präfrontalen Cortex (PFC, Postle, 2006), sowie die funktionelle Inhibition durch neuronale Oszillationen im Alpha-Frequenzband (Jensen und Mazaheri, 2010; Klimesch et al, 2007), sind entscheidende Mechanismen für eine effiziente Art und Weise mit den Limitationen zurechtzukommen.

Interessanterweise wurden bisher die meisten Untersuchungen über das Arbeitsgedächtnis im visuellen Bereich durchgeführt. Deshalb war es in der vorliegenden Arbeit von großem Interesse, inwieweit die Limitationen des Arbeitsgedächtnisses durch auditive Signale herausgefordert werden. Gestörte Sprachsignale haben sich als ein geeignetes Untersuchungsobjekt erwiesen, weil es sich gezeigt hat, dass sie die Gedächtnislast erhöhen im Vergleich zu klarer Sprache (Pichora-Fuller und Singh, 2006).

Darüber hinaus wurde in einer Studie von Obleser et al. (2012) gezeigt, dass Alpha-Power, ein Marker für Gedächtnislast, sich parametrisch mit zunehmender Sprachdegradierung erhöhte. Das wiederum zeigte, dass Alpha-Power an sich auch sensitiv für Gedächtnislast im auditiven Arbeitsgedächtnis ist. Basierend auf diesen Ergebnissen, war das Ziel der vorliegenden Arbeit, die Auswirkungen zeitlicher Erwartungen auf das auditive Arbeitsgedächtnis zu untersuchen. In alltäglichen Situationen, z.B. bei fortlaufenden Konversationen, ist durch die zeitliche Struktur der Sprache in der Regel Vorwissen über den Auftretenszeitpunkt des bevorstehenden Sprachsignals vorhanden. Aus diesem Grund wird davon ausgegangen, dass zeitliche Erwartungen, d.h. a-priori-Informationen darüber, wann man hinhören sollte, die Verarbeitung von degradierter Sprache im Arbeitsgedächtnis erleichtern. Vor allem, weil, wie bereits gezeigt wurde, Erwartungen über den Auftretenszeitpunkt eines Stimulus die Präzision der Enkodierung dieses Stimulus verbessern (Rohenkohl et al.2012; Cravo et al., 2013). Diese Verbesse-

rung wiederum lässt davon ausgehen, dass zeitliche Erwartungen über den Auftretenszeitpunkt eines degradierten Sprachsignals die Gedächtnislast verringern.

Das Ziel der vorliegenden Arbeit ist es, zu beurteilen, inwiefern zeitliche Erwartungen Gedächtnislimitationen modulieren, reflektiert durch Fluktuationen der Alpha-Power, gemessen mit Magnetoencephalographie und der behavioralen Gedächtnisleistung.

## Experimente und Ergebnisse

*Experiment I* untersuchte die Fragestellung, ob zeitliche Erwartungen die Gedächtnislast von degradierte Sprachsignale reduzieren. Zwei gesprochenen Silben (S1, S2) wurden in einer sog. *delayed matching-to-sample* Aufgabe dargeboten, wobei S1 und S2 mit einem Abstand von zwei Sekunden präsentiert wurden. Die Silben wurden mit Rauschen maskiert, um die Gedächtnislast zu erhöhen. Entscheidend dabei war, dass die zeitlichen Erwartungen für S1 mit Hilfe von drei verschiedenen symbolischen Hinweisreizen manipuliert wurde. Die Hinweisreize wurden vor dem Auftreten von S1 gezeigt und variierten hinsichtlich ihres Informationsgehalts über den Auftretenszeitpunkt von S1. Wir erwarteten hier, dass zeitliche Erwartungen die Gedächtnislast reduzieren, was sich wiederum in verringerter Alpha-Power und verbesserter Gedächtnisleistung niederschlagen sollte. In der Tat konnte gezeigt werden, dass auf Grund der zeitlichen Erwartungen Alpha-Power während der Behaltensphase reduziert und die Gedächtnisleistung verbessert war. Dieser Effekt im Alpha Band wurde in der rechten Insula lokalisiert, welche ein Teil des cingulo-opercularen Aufmerksamkeitsnetzwerk ist (Dosenbach et al., 2008) und somit einen reduzierten Bedarf an Top-Down Kontrolle während der Behaltensphase darstellt. Darüber hinaus konnte gezeigt werden, dass die Effekte zeitlicher Erwartungen auf Alpha-Power positiv mit den Effekten zeitlicher Erwartungen auf die Gedächtnisleistung korrelierten. Diese Korrelation wiederum ist ein Indikator dafür, dass, wenn keine zeitliche Erwartungen aufgebaut wurde, erhöhte Alpha-Power die Gedächtnisleistung verbessert.

Eine Teilgruppe der Teilnehmer von *Experiments I* nahm an einer Folgestudie teil. Das gleiche Experiment wie *Experiment I* wurde mit klarer Sprache (d.h., ohne Rauschen) durchgeführt, um herauszufinden, ob die bisher beobachtete Reduktion der Gedächtnislast spezifisch für die Sprachverarbeitung im Rauschen zu finden war. Die Frage war also, ob zeitliche Erwartungen ähnliche Effekte auf klare Sprache haben könnten (*Experiment IIa*). Diese vergleichsweise einfache Arbeitsgedächtnisaufgabe rief weniger Gedächtnislast hervor als *Experiment I* (signifikant bessere Gedächtnisleistung) und Alpha-Power wurde nicht durch zeitliche Erwartungen moduliert. Auch statistisch konnte gezeigt werden, dass der Effekt der zeitlichen Erwartungen auf Alpha-Power im

Rauschen signifikant größer war als für klare Sprache. Höchstwahrscheinlich war die Verarbeitung der Hinweisreize im Verhältnis zu aufwendig für diese sehr einfache Aufgabe. Deshalb wurde im nächsten Schritt getestet, ob eher implizite zeitliche Erwartungen, die sich alleinig durch das Vergehen von Zeit aufbauen (die sog. Hazard-Function), Effekte zeigen.

Es wurde also untersucht, ob diese Art der zeitlichen Erwartungen einen Einfluss auf die Verarbeitung von S1 sowie auf Alpha-Power während der Behaltensphase hat (*Experiment IIb*). Der zeitliche Abstand zwischen Hinweisreiz und S1 (die Vorperiode) war über alle Durchgänge hinweg variabel. Dadurch konnten Analysen über Hinweisreize hinweg durchgeführt werden. Für diese Analysen wurde erwartet, dass sich die Phasenkohärenz im Bereich langsamer neuronaler Oszillationen sich mit längeren Vorperioden erhöht. Eine erhöhte Phasenkohärenz wäre hier ein Indikator für eine erhöhte neuronale Erregbarkeit durch zeitliche Erwartungen (Lakatos et al., 2005). Außerdem wurde erwartet, dass längere Vorperioden zu einer Reduktion der Alpha-Power während der Behaltensphase führen würde, was ein Indikator f r die Reduktion der Ged chtnislast w re. Tatsächlich konnte gezeigt werden, dass längere Vorperioden zu einer Reduktion der Alpha- Power während der Behaltensphase führte. Gleichermaßen erhöhte sich die Phasenkohärenz neuronaler Oszillationen im langsamen Delta-Bereich während der Präsentation von S1 mit längeren Vorperioden. Zusätzlich wurde eine negative Korrelation von Delta-Phasenkohärenz und Alpha-Power gefunden. Dieser Zusammenhang verdeutlicht die direkte Verbindung von erhöhter neuronaler Erregbarkeit während der Stimuluspräsentation (Phasenkohärenz) und reduzierter Gedächtnislast (Alpha-Power) durch zeitliche Erwartungen.

Um ein vollständiges Bild über die Limitationen des auditiven Arbeitsgedächtnis zu bekommen und darüber, wie Alpha-Power Gedächtnislimitationen reflektiert, wurde der Gedächtniszerfall direkt untersucht (*Experiment III*). Gedächtniszerfall ist durch Verschlechterung der Gedächtnisleistung über längere Behaltensphasen hinweg charakterisiert. Dafür wurde in diesem Experiment das auditive sensorische Gedächtnis untersucht, für das der Zerfall besser abgebildet wird als f r verbales Arbeiteged chtnis (Cowan, 1984; Schröger, 2007). Es wurden Tonmuster anstelle von Silben präsentiert. S1 und S2 wurden auch diesmal mit Rauschen maskiert, um die Gedächtnislast zu erhöhen. Gedächtniszerfall wurde durch drei verschieden lange Behaltensphasen manipuliert. Zusätzlich wurde wieder die zeitliche Erwartung für S1 manipuliert, um zu untersuchen, ob diese nicht nur Gedächtnislast reduziert, sondern auch dem Gedächtniszerfall entgegenwirkt. Zu den Analysen der Sensor-Daten wurden au erdem Quellanalysen berechnet, um die Ursprünge möglicher Alpha-Power-Fluktuationen zu lokalisieren und somit mögliche Einflüsse aus dem präfrontalen Cortex zu bestimmen.

Die Verhaltensdaten zeigen, dass zeitliche Erwartungen dem Gedächtniszerfall entgegenwirkten, d.h., dass für Stimuli, die zeitlich erwartet waren, die Gedächtnisleistung weniger stark über die Zeit hinweg abfiel, als wenn die Stimuli zeitlich nicht erwartet waren. Ähnliches wurde auch für Alpha-Power gefunden: Insgesamt nahm Alpha-Power im supramarginalen Gyrus (SMG) mit längeren Behaltensphasen ab, allerdings weniger stark bei zeitlich erwarteten Stimuli. Der Alpha-Power-Abfall über die Zeit wurde zudem im primären visuellen Cortex (V1), im rechten inferior-parietalen Lobulus (IPL) und im Precuneus lokalisiert. IPL und Precuneus reflektieren hier möglicherweise Modulationen der Behaltensprozesse durch Aufmerksamkeit. Erhöhte Alpha-Power in V1 passt zum Konzept der funktionellen Inhibiton insofern, als dass weniger Alpha-Power höchstwahrscheinlich die reduzierte Inhibition aufgabenirrelevanter (visueller) Hirnregionen signalisiert.

Die Manipulation der zeitlichen Erwartung hatte einen Effekt auf Alpha-Power zum Beginn der Behaltensphase: Wenn ein Stimulus zeitlich erwartet wurde, war die Alpha-Power im rechten inferior-frontalen Gyrus (IFG), im rechten anterior-cingulären Cortex (ACC) so wie im rechten superior-temporalen Gyrus erhöht. Als nächstes wurde durch eine Korrelation zwischen Alpha-Power und dem Verhaltensmaß $A_z$ die direkte Verbindung zwischen Alpha-Power Modulationen und Gedächtnisleistung aufgezeigt. Dieser Zusammenhang zeigt sich zu Beginn der Behaltensphase vor allem in ventralen und cingulo-opercularen Aufmerksamkeitsnetzwerken (STG, IFG, ACC). Zum Ende der Behaltensphase waren vor allem ACC, linker SMG, rechter IFG und bilateraler V1 involviert.

*In Experiment III* wurde der vorher gezeigt Effekt zeitlicher Erwartung auf Gedächtniszerfall aufgegriffen (*Experiment IV*). Im Prinzip wurde das gleiche Experiment erneut durchgeführt, allerdings wurden hier sechs, anstelle von drei, verschiedenen Behaltensphasen verwendet. Da das Ziel dieses Experiments war, eine Zerfalls- oder Vergessenskurve für das Verhaltensmaß $A_z$ zu schätzen, waren mehr Datenpunkte nötig. Die Zerfallskurven, die getrennt an Daten mit und ohne zeitlicher Erwartung angepasst wurden, sollten den Einfluss zeitlicher Erwartung auf den Zerfall noch präziser beschreiben. Die Zerfallskurven bestanden aus zwei Parametern, die den Daten angepasst werden mussten. Der erste Parameter beschreibt die Geschwindigkeit des Gedächtniszerfalls ($\gamma$) und der zweite Parameter ($\lambda$) beschreibt das Ausmaß "produktiver" Gedächtnisprozesse, die dem Gedächtniszerfall entgegenwirken wie z.B. die Aktualisierung der Gedächtnisreprä sentation. Die Geschwindigkeit des Gedächtniszerfalls zwischen zeitlich erwarteten und unerwarteten Stimuli zeigte keinen signifikanten Unterschied. Allerdings war der Produktionsparameter signifikant größer bei zeitlicher Erwartung. Dadurch war der Abfall der Zerfallskurve über die Zeit für diese Stimuli weniger steil als für zeitlich

weniger gut erwartet Stimuli. Dieser Unterschied pr zisiert die bereits gezeigten Effekte von zeitlicher Erwartung auf den Zerfall in *Experiment III*.

## Diskussion

Zusammengenommen zeigen die Ergebnisse der vorliegenden Doktorarbeit, dass Top-Down-Modulation durch zeitliche Erwartungen für das auditive Arbeitsgedächtnis vorteilhaft ist. Im Speziellen wurde gezeigt, dass zeitliche Erwartungen die Enkodierung auditiver Stimuli im Rauschen verbessern. Das führte zu reduzierter Gedächtnislast und wirkte dem Gedächtniszerfall entgegen. Die Daten lassen vermuten, dass durch das verbesserte Enkodieren mehr kognitive Ressourcen für den Behaltensprozess herangezogen werden konnte. Das bedeutet für das auditive Arbeitsgedächtnis, dass Gedächtnislast sowie Gedächtniszerfall von der Präzision des Enkodierens des zu behaltenden Stimulus abhängt.

Das Behalten von verbalen (*Experiment I*) und nicht-verbalen Stimuli (*Experiment III*) führte zu umgekehrten Alpha-Power Effekten, was durch unterschiedliche Behaltensstrategien ("rehearsal" vs. kognitive Ressourcen; e.g., Vergauwe et al., 2014) erklärt werden kann. Generell wurden verstärkte Behaltensprozesse, in der Form von vermehrten kognitive Ressourcen, durch erhöhte Alpha-Power reflektiert. Das wiederum erklärt, dass Alpha-Power schneller über die Zeit abnahm, wenn Stimuli zeitlich unerwartet waren: In diesem Falle wurden mehr Ressourcen für die Stimulusenkodierung benötigt und weniger Ressourcen standen für Behaltensprozesse zur Verfügung (Time-Based Resource-Sharing Model; Barrouillet et al., 2004).

Zu guter Letzt zeigten die Lokalisationen der Alpha-Power Effekte, dass Aufmerksamkeitsnetzwerke wie das cingulo-operculare, fronto-parietale und das ventrale Netzwerk für das Behalten auditiver Informationen eine große Rolle spielen. Da diese Netzwerke eine entscheidende Rolle für Arbeitsgedächtnisprozesse spielen (Postle, 2006), widerspricht dies einer unmittelbaren Inhibition dieser Areale im Sinne des Konzepts der funktionellen Inhibition (e.g., Jensen et al., 2010). Deshalb wird hier vorgeschlagen, dass Alpha-Power nicht diese Regionen unmittelbar inhibiert, sondern eher top-down die Behaltensprozesse über die Modulation sensorischer Areale kontrolliert.

# Curriculum Vitae

Anna Wilsch

Date of birth: 04 January, 1984

## Education

| | |
|---|---|
| 03/2011 | Diploma (MSc equivalent) in Psychology, University of Koblenz-Landau, Germany |
| 2006–2007 | Studies of Psychology, Free University of Brussels, Belgium |
| 2004–2011 | Studies of Psychology, University of Koblenz-Landau, Germany |

## Career

| | |
|---|---|
| 2011–2014 | PhD Student in the Max Planck Research Group Auditory Cognition at the Max Planck Institute for Human Cognitive and Brain Sciences, Germany |
| 2009 | Diploma Student at the Max Planck Institute for Human Cognitive and Brain Sciences, Germany |
| 2008 | Internship at the Max Planck Institute for Human Cognitive and Brain Sciences, Germany |
| 2008 | Internship and Student Assistant at the Sleep Laboratory of the Clinic for Psychiatry and Neurology, Pfalzklinikum, Germany |

## Publications

**Wilsch, A.**, Henry, M. J., Herrmann, B., Maess, B., and Obleser, J. (in revision). Slow-delta phase concentration marks improved temporal expectations based on the passage of time. *Psychophysiology.*

Wöstmann, M., Herrmann, B., **Wilsch, A.**, and Obleser, J. (in revision). Neural alpha dynamics reflect acoustic challenges and predictive benefits in adverse listening situations. *Journal of Neuroscience.*

**Wilsch, A.**, Henry, M. J., Herrmann, B., Maess, B., and Obleser, J. (2014). Alpha Oscillatory Dynamics Index Temporal Expectation Benefits in Working Memory. *Cerebral Cortex*, pages 1–9.

Obleser, J., Wöstmann, M., Hellbernd, N., **Wilsch, A.**, and Maess, B. (2012). Adverse listening conditions and memory load drive a common alpha oscillatory network. *Journal of Neuroscience, 32*(36), 12376–83.

## Talks

**Wilsch, A.**, Henry, M., Herrmann, B., and Obleser, J. (2014). Alpha power measured with magnetoencephalography reflects cognitive demands of noisy speech processing. Talk presented at Psychologie und Gehirn, L beck, Germany.

Selbständigkeitserklärung gemäß § 8(2) der Promotionsordnung

Hiermit versichere ich, dass die vorliegende Arbeit ohne unzulässige Hilfe und ohne Benutzung anderer als der angegebenen Hilfsmittel angefertigt wurde, und dass die aus fremden Quellen direkt oder indirekt übernommenen Gedanken in der Arbeit als solche kenntlich gemacht worden sind. Ich versichere, dass die vorliegende Arbeit in gleicher oder in ähnlicher Form keiner anderen wissenschaftlichen Einrichtung zum Zwecke einer Promotion oder eines anderen Prüfungsverfahrens vorgelegt und auch veröffentlicht wurde. Es haben keine früheren erfolglosen Promotionsversuche stattgefunden.

Leipzig, 4. Oktober 2014

Anna Wilsch

## MPI Series in Human Cognitive and Brain Sciences:

1 Anja Hahne
*Charakteristika syntaktischer und semantischer Prozesse bei der auditiven Sprachverarbeitung: Evidenz aus ereigniskorrelierten Potentialstudien*

2 Ricarda Schubotz
*Erinnern kurzer Zeitdauern: Behaviorale und neurophysiologische Korrelate einer Arbeitsgedächtnisfunktion*

3 Volker Bosch
*Das Halten von Information im Arbeitsgedächtnis: Dissoziationen langsamer corticaler Potentiale*

4 Jorge Jovicich
*An investigation of the use of Gradient- and Spin-Echo (GRASE) imaging for functional MRI of the human brain*

5 Rosemary C. Dymond
*Spatial Specificity and Temporal Accuracy in Functional Magnetic Resonance Investigations*

6 Stefan Zysset
*Eine experimentalpsychologische Studie zu Gedächtnisabrufprozessen unter Verwendung der funktionellen Magnetresonanztomographie*

7 Ulrich Hartmann
*Ein mechanisches Finite-Elemente-Modell des menschlichen Kopfes*

8 Bertram Opitz
*Funktionelle Neuroanatomie der Verarbeitung einfacher und komplexer akustischer Reize: Integration haemodynamischer und elektrophysiologischer Maße*

9 Gisela Müller-Plath
*Formale Modellierung visueller Suchstrategien mit Anwendungen bei der Lokalisation von Hirnfunktionen und in der Diagnostik von Aufmerksamkeitsstörungen*

10 Thomas Jacobsen
*Characteristics of processing morphological structural and inherent case in language comprehension*

11 Stefan Kölsch
*Brain and Music*
*A contribution to the investigation of central auditory processing with a new electrophysiological approach*

12 Stefan Frisch
*Verb-Argument-Struktur, Kasus und thematische Interpretation beim Sprachverstehen*

13 Markus Ullsperger
*The role of retrieval inhibition in directed forgetting – an event-related brain potential analysis*

14 Martin Koch
*Measurement of the Self-Diffusion Tensor of Water in the Human Brain*

15 Axel Hutt
*Methoden zur Untersuchung der Dynamik raumzeitlicher Signale*

16 Frithjof Kruggel
*Detektion und Quantifizierung von Hirnaktivität mit der funktionellen Magnetresonanztomographie*

17 Anja Dove
*Lokalisierung an internen Kontrollprozessen beteiligter Hirngebiete mithilfe des Aufgabenwechselparadigmas und der ereigniskorrelierten funktionellen Magnetresonanztomographie*

18 Karsten Steinhauer
*Hirnphysiologische Korrelate prosodischer Satzverarbeitung bei gesprochener und geschriebener Sprache*

19 Silke Urban
*Verbinformationen im Satzverstehen*

20 Katja Werheid
*Implizites Sequenzlernen bei Morbus Parkinson*

21 Doreen Nessler
*Is it Memory or Illusion? Electrophysiological Characteristics of True and False Recognition*

22 Christoph Herrmann
*Die Bedeutung von 40-Hz-Oszillationen für kognitive Prozesse*

23 Christian Fiebach
*Working Memory and Syntax during Sentence Processing.*
*A neurocognitive investigation with event-related brain potentials and functional magnetic resonance imaging*

24 Grit Hein
*Lokalisation von Doppelaufgabendefiziten bei gesunden älteren Personen und neurologischen Patienten*

25 Monica de Filippis
*Die visuelle Verarbeitung unbeachteter Wörter. Ein elektrophysiologischer Ansatz*

26 Ulrich Müller
*Die katecholaminerge Modulation präfrontaler kognitiver Funktionen beim Menschen*

27 Kristina Uhl
*Kontrollfunktion des Arbeitsgedächtnisses über interferierende Information*

28 Ina Bornkessel
*The Argument Dependency Model: A Neurocognitive Approach to Incremental Interpretation*

29 Sonja Lattner
*Neurophysiologische Untersuchungen zur auditorischen Verarbeitung von Stimminformationen*

30 Christin Grünewald
*Die Rolle motorischer Schemata bei der Objektrepräsentation: Untersuchungen mit funktioneller Magnetresonanztomographie*

31 Annett Schirmer
*Emotional Speech Perception: Electrophysiological Insights into the Processing of Emotional Prosody and Word Valence in Men and Women*

32 André J. Szameitat
*Die Funktionalität des lateral-präfrontalen Cortex für die Verarbeitung von Doppelaufgaben*

33 Susanne Wagner
*Verbales Arbeitsgedächtnis und die Verarbeitung ambiger Wörter in Wort- und Satzkontexten*

34 Sophie Manthey
*Hirn und Handlung: Untersuchung der Handlungsrepräsentation im ventralen prämotorischen Cortex mit Hilfe der funktionellen Magnet-Resonanz-Tomographie*

35 Stefan Heim
*Towards a Common Neural Network Model of Language Production and Comprehension: fMRI Evidence for the Processing of Phonological and Syntactic Information in Single Words*

36 Claudia Friedrich
*Prosody and spoken word recognition: Behavioral and ERP correlates*

37 Ulrike Lex
*Sprachlateralisierung bei Rechts- und Linkshändern mit funktioneller Magnetresonanztomographie*

38 Thomas Arnold
*Computergestützte Befundung klinischer Elektroenzephalogramme*

39 Carsten H. Wolters
*Influence of Tissue Conductivity Inhomogeneity and Anisotropy on EEG/MEG based Source Localization in the Human Brain*

40 Ansgar Hantsch
*Fisch oder Karpfen? Lexikale Aktivierung von Benennungsalternative bei der Objektbenennung*

41 Peggy Bungert
*Zentralnervöse Verarbeitung akustischer Informationen Signalidentifikation, Signallateralisation und zeitgebundene Informationsverarbeitung bei Patienten mit erworbenen Hirnschädigungen*

42 Daniel Senkowski
*Neuronal correlates of selective attention: An investigation of electrophysiological brain responses in the EEG and MEG*

43 Gert Wollny
*Analysis of Changes in Temporal Series of Medical Images*

44 Angelika Wolf
*Sprachverstehen mit Cochlea-Implantat: EKP-Studien mit postlingual ertaubten erwachsenen CI-Trägern*

45 Kirsten G. Volz
*Brain correlates of uncertain decisions: Types and degrees of uncertainty*

46 Hagen Huttner
*Magnetresonanztomographische Untersuchungen über die anatomische Variabilität des Frontallappens des menschlichen Großhirns*

47 Dirk Köster
*Morphology and Spoken Word Comprehension: Electrophysiological Investigations of Internal Compound Structure*

48 Claudia A. Hruska
*Einflüsse kontextueller und prosodischer Informationen in der auditorischen Satzverarbeitung: Untersuchungen mit ereigniskorrelierten Hirnpotentialen*

49 Hannes Ruge
*Eine Analyse des raum-zeitlichen Musters neuronaler Aktivierung im Aufgabenwechselparadigma zur Untersuchung handlungssteuernder Prozesse*

50 Ricarda I. Schubotz
*Human premotor cortex: Beyond motor performance*

51 Clemens von Zerssen
*Bewusstes Erinnern und falsches Wiedererkennen: Eine funktionelle MRT Studie neuroanatomischer Gedächtniskorrelate*

52 Christiane Weber
*Rhythm is gonna get you.*
*Electrophysiological markers of rhythmic processing in infants with and without risk for Specific Language Impairment (SLI)*

53 Marc Schönwiesner
*Functional Mapping of Basic Acoustic Parameters in the Human Central Auditory System*

54 Katja Fiehler
*Temporospatial characteristics of error correction*

55 Britta Stolterfoht
*Processing Word Order Variations and Ellipses: The Interplay of Syntax and Information Structure during Sentence Comprehension*

56 Claudia Danielmeier
*Neuronale Grundlagen der Interferenz zwischen Handlung und visueller Wahrnehmung*

57 Margret Hund-Georgiadis
*Die Organisation von Sprache und ihre Reorganisation bei ausgewählten, neurologischen Erkrankungen gemessen mit funktioneller Magnetresonanztomographie – Einflüsse von Händigkeit, Läsion, Performanz und Perfusion*

58 Jutta L. Mueller
*Mechanisms of auditory sentence comprehension in first and second language: An electrophysiological miniature grammar study*

59 Franziska Biedermann
*Auditorische Diskriminationsleistungen nach unilateralen Läsionen im Di- und Telenzephalon*

60 Shirley-Ann Rüschemeyer
*The Processing of Lexical Semantic and Syntactic Information in Spoken Sentences: Neuroimaging and Behavioral Studies of Native and Non-Native Speakers*

61 Kerstin Leuckefeld
*The Development of Argument Processing Mechanisms in German. An Electrophysiological Investigation with School-Aged Children and Adults*

62 Axel Christian Kühn
*Bestimmung der Lateralisierung von Sprachprozessen unter besondere Berücksichtigung des temporalen Cortex, gemessen mit fMRT*

63 Ann Pannekamp
*Prosodische Informationsverarbeitung bei normalsprachlichem und deviantem Satzmaterial: Untersuchungen mit ereigniskorrelierten Hirnpotentialen*

64 Jan Derrfuß
*Functional specialization in the lateral frontal cortex: The role of the inferior frontal junction in cognitive control*

65 Andrea Mona Philipp
*The cognitive representation of tasks – Exploring the role of response modalities using the task-switching paradigm*

66 Ulrike Toepel
*Contrastive Topic and Focus Information in Discourse – Prosodic Realisation and Electrophysiological Brain Correlates*

67 Karsten Müller
*Die Anwendung von Spektral- und Waveletanalyse zur Untersuchung der Dynamik von BOLD-Zeitreihen verschiedener Hirnareale*

68 Sonja A.Kotz
*The role of the basal ganglia in auditory language processing: Evidence from ERP lesion studies and functional neuroimaging*

69 Sonja Rossi
*The role of proficiency in syntactic second language processing: Evidence from event-related brain potentials in German and Italian*

70 Birte U. Forstmann
*Behavioral and neural correlates of endogenous control processes in task switching*

71 Silke Paulmann
*Electrophysiological Evidence on the Processing of Emotional Prosody: Insights from Healthy and Patient Populations*

72 Matthias L. Schroeter
*Enlightening the Brain – Optical Imaging in Cognitive Neuroscience*

73 Julia Reinholz
*Interhemispheric interaction in object- and word-related visual areas*

74 Evelyn C. Ferstl
*The Functional Neuroanatomy of Text Comprehension*

75 Miriam Gade
*Aufgabeninhibition als Mechanismus der Konfliktreduktion zwischen Aufgabenrepräsentationen*

76 Juliane Hofmann
*Phonological, Morphological, and Semantic Aspects of Grammatical Gender Processing in German*

77 Petra Augurzky
*Attaching Relative Clauses in German – The Role of Implicit and Explicit Prosody in Sentence Processing*

78 Uta Wolfensteller
*Habituelle und arbiträre sensomotorische Verknüpfungen im lateralen prämotorischen Kortex des Menschen*

79 Päivi Sivonen
*Event-related brain activation in speech perception: From sensory to cognitive processes*

80 Yun Nan
*Music phrase structure perception: the neural basis, the effects of acculturation and musical training*

81 Katrin Schulze
*Neural Correlates of Working Memory for Verbal and Tonal Stimuli in Nonmusicians and Musicians With and Without Absolute Pitch*

82 Korinna Eckstein
*Interaktion von Syntax und Prosodie beim Sprachverstehen: Untersuchungen anhand ereigniskorrelierter Hirnpotentiale*

83 Florian Th. Siebörger
*Funktionelle Neuroanatomie des Textverstehens: Kohärenzbildung bei Witzen und anderen ungewöhnlichen Texten*

84 Diana Böttger
*Aktivität im Gamma-Frequenzbereich des EEG: Einfluss demographischer Faktoren und kognitiver Korrelate*

85 Jörg Bahlmann
*Neural correlates of the processing of linear and hierarchical artificial grammar rules: Electrophysiological and neuroimaging studies*

86 Jan Zwickel
*Specific Interference Effects Between Temporally Overlapping Action and Perception*

87 Markus Ullsperger
*Functional Neuroanatomy of Performance Monitoring: fMRI, ERP, and Patient Studies*

88 Susanne Dietrich
*Vom Brüllen zum Wort – MRT-Studien zur kognitiven Verarbeitung emotionaler Vokalisationen*

89 Maren Schmidt-Kassow
*What's Beat got to do with ist? The Influence of Meter on Syntactic Processing: ERP Evidence from Healthy and Patient populations*

90 Monika Lück
*Die Verarbeitung morphologisch komplexer Wörter bei Kindern im Schulalter: Neurophysiologische Korrelate der Entwicklung*

91 Diana P. Szameitat
*Perzeption und akustische Eigenschaften von Emotionen in menschlichem Lachen*

92 Beate Sabisch
*Mechanisms of auditory sentence comprehension in children with specific language impairment and children with developmental dyslexia: A neurophysiological investigation*

93 Regine Oberecker
*Grammatikverarbeitung im Kindesalter: EKP-Studien zum auditorischen Satzverstehen*

94 Şükrü Barış Demiral
*Incremental Argument Interpretation in Turkish Sentence Comprehension*

95 Henning Holle
*The Comprehension of Co-Speech Iconic Gestures: Behavioral, Electrophysiological and Neuroimaging Studies*

96 Marcel Braß
*Das inferior frontale Kreuzungsareal und seine Rolle bei der kognitiven Kontrolle unseres Verhaltens*

97 Anna S. Hasting
*Syntax in a blink: Early and automatic processing of syntactic rules as revealed by event-related brain potentials*

98 Sebastian Jentschke
*Neural Correlates of Processing Syntax in Music and Language – Influences of Development, Musical Training and Language Impairment*

99 Amelie Mahlstedt
*The Acquisition of Case marking Information as a Cue to Argument Interpretation in German*
*An Electrophysiological Investigation with Pre-school Children*

100 Nikolaus Steinbeis
*Investigating the meaning of music using EEG and fMRI*

101 Tilmann A. Klein
*Learning from errors: Genetic evidence for a central role of dopamine in human performance monitoring*

102 Franziska Maria Korb
*Die funktionelle Spezialisierung des lateralen präfrontalen Cortex: Untersuchungen mittels funktioneller Magnetresonanztomographie*

103 Sonja Fleischhauer
*Neuronale Verarbeitung emotionaler Prosodie und Syntax: die Rolle des verbalen Arbeitsgedächtnisses*

104 Friederike Sophie Haupt
*The component mapping problem: An investigation of grammatical function reanalysis in differing experimental contexts using eventrelated brain potentials*

105 Jens Brauer
*Functional development and structural maturation in the brain's neural network underlying language comprehension*

106 Philipp Kanske
*Exploring executive attention in emotion: ERP and fMRI evidence*

107 Julia Grieser Painter
*Music, meaning, and a semantic space for musical sounds*

108 Daniela Sammler
*The Neuroanatomical Overlap of Syntax Processing in Music and Language - Evidence from Lesion and Intracranial ERP Studies*

109 Norbert Zmyj
*Selective Imitation in One-Year-Olds: How a Model's Characteristics Influence Imitation*

110 Thomas Fritz
*Emotion investigated with music of variable valence – neurophysiology and cultural influence*

111 Stefanie Regel
*The comprehension of figurative language: Electrophysiological evidence on the processing of irony*

112 Miriam Beisert
*Transformation Rules in Tool Use*

113 Veronika Krieghoff
*Neural correlates of Intentional Actions*

114 Andreja Bubić
*Violation of expectations in sequence processing*

115 Claudia Männel
*Prosodic processing during language acquisition: Electrophysiological studies on intonational phrase processing*

116 Konstanze Albrecht
*Brain correlates of cognitive processes underlying intertemporal choice for self and other*

117 Katrin Sakreida
*Nicht-motorische Funktionen des prämotorischen Kortex: Patientenstudien und funktionelle Bildgebung*

118 Susann Wolff
*The interplay of free word order and pro-drop in incremental sentence processing: Neurophysiological evidence from Japanese*

119 Tim Raettig
*The Cortical Infrastructure of Language Processing: Evidence from Functional and Anatomical Neuroimaging*

120 Maria Golde
*Premotor cortex contributions to abstract and action-related relational processing*

121 Daniel S. Margulies
*Resting-State Functional Connectivity fMRI: A new approach for assessing functional neuroanatomy in humans with applications to neuroanatomical, developmental and clinical questions*

122 Franziska Süß
*The interplay between attention and syntactic processes in the adult and developing brain: ERP evidences*

123 Stefan Bode
*From stimuli to motor responses: Decoding rules and decision mechanisms in the human brain*

124 Christiane Diefenbach
*Interactions between sentence comprehension and concurrent action: The role of movement effects and timing*

125 Moritz M. Daum
*Mechanismen der frühkindlichen Entwicklung des Handlungsverständnisses*

126 Jürgen Dukart
*Contribution of FDG-PET and MRI to improve Understanding, Detection and Differentiation of Dementia*

127 Kamal Kumar Choudhary
*Incremental Argument Interpretation in a Split Ergative Language: Neurophysiological Evidence from Hindi*

128 Peggy Sparenberg
*Filling the Gap: Temporal and Motor Aspects of the Mental Simulation of Occluded Actions*

129 Luming Wang
*The Influence of Animacy and Context on Word Order Processing: Neurophysiological Evidence from Mandarin Chinese*

130 Barbara Ettrich
*Beeinträchtigung frontomedianer Funktionen bei Schädel-Hirn-Trauma*

131 Sandra Dietrich
*Coordination of Unimanual Continuous Movements with External Events*

132 R. Muralikrishnan
*An Electrophysiological Investigation Of Tamil Dative-Subject Constructions*

133 Christian Obermeier
*Exploring the significance of task, timing and background noise on gesture-speech integration*

134 Björn Herrmann
*Grammar and perception: Dissociation of early auditory processes in the brain*

135 Eugenia Solano-Castiella
*In vivo anatomical segmentation of the human amygdala and parcellation of emotional processing*

136 Marco Taubert
*Plastizität im sensomotorischen System – Lerninduzierte Veränderungen in der Struktur und Funktion des menschlichen Gehirns*

137 Patricia Garrido Vásquez
*Emotion Processing in Parkinson's Disease: The Role of Motor Symptom Asymmetry*

138 Michael Schwartze
*Adaptation to temporal structure*

139 Christine S. Schipke
*Processing Mechanisms of Argument Structure and Case-marking in Child Development: Neural Correlates and Behavioral Evidence*

140 Sarah Jessen
*Emotion Perception in the Multisensory Brain*

141 Jane Neumann
*Beyond activation detection: Advancing computational techniques for the analysis of functional MRI data*

142 Franziska Knolle
*Knowing what's next: The role of the cerebellum in generating predictions*

143 Michael Skeide
*Syntax and semantics networks in the developing brain*

144 Sarah M. E. Gierhan
*Brain networks for language*
*Anatomy and functional roles of neural pathways supporting language comprehension and repetition*

145 Lars Meyer
*The Working Memory of Argument-Verb Dependencies*
*Spatiotemporal Brain Dynamics during Sentence Processing*

146 Benjamin Stahl
*Treatment of Non-Fluent Aphasia through Melody, Rhythm and Formulaic Language*

147 Kathrin Rothermich
*The rhythm's gonna get you: ERP and fMRI evidence on the interaction of metric and semantic processing*

148 Julia Merrill
*Song and Speech Perception – Evidence from fMRI, Lesion Studies and Musical Disorder*

149 Klaus-Martin Krönke
*Learning by Doing?*
*Gesture-Based Word-Learning and its Neural Correlates in Healthy Volunteers and Patients with Residual Aphasia*

150 Lisa Joana Knoll
*When the hedgehog kisses the frog*
*A functional and structural investigation of syntactic processing in the developing brain*

151 Nadine Diersch
*Action prediction in the aging mind*

152 Thomas Dolk
*A Referential Coding Account for the Social Simon Effect*

153 Mareike Bacha-Trams
*Neurotransmitter receptor distribution in Broca's area and the posterior superior temporal gyrus*

154 Andrea Michaela Walter
*The role of goal representations in action control*